

**FUNCTIONAL AND MOLECULAR EFFECTS OF
HYPERCHOLESTEROLEMIA ON THE MYOCARDIUM:
THE ROLE OF CONNEXIN-43 AND MICRORNA-25**

Zoltán Varga

PhD Thesis

**SZEGED
2013**

**FUNCTIONAL AND MOLECULAR EFFECTS OF
HYPERCHOLESTEROLEMIA ON THE MYOCARDIUM:
THE ROLE OF CONNEXIN-43 AND MICRORNA-25**

PhD. thesis

Zoltán Varga

Supervisor: Tamás Csont

**Cardiovascular Research Group
Department of Biochemistry
Faculty of Medicine
University of Szeged**

www.cardiovasc.com

2013

1. Table of contents

1. Table of contents	1
2. List of publications	4
2.1 List of full papers directly related to the subject of the thesis.....	4
2.2 Other full papers	4
3. List of abbreviations	5
4. Introduction	7
4.1 Epidemiological importance of hypercholesterolemia.....	7
4.2 Biological effects of hypercholesterolemia on the heart	7
4.2.1 Coronary atherosclerosis	7
4.2.2 Direct myocardial effects on the regulation of gene expression	8
4.2.2.1 Transcriptional regulation	8
4.2.2.2 Posttranscriptional regulation: role of microRNAs.....	9
4.2.3 Myocardial oxidative stress in hypercholesterolemia	9
4.2.3.1 ROS sources and defense mechanisms	9
4.2.3.2 Oxidative stress and hypercholesterolemia	10
4.2.4 Direct myocardial effects on contractile function	11
4.2.4.1 Impaired contractility due to hypercholesterolemia.....	11
4.2.4.2 Role of oxidative stress in impaired contractility.....	12
4.2.5 Direct myocardial effects on endogenous ischemic adaptation	12
4.2.5.1 Cardioprotective mechanisms: pre- and postconditioning	12
4.2.5.2 Blunted cardioprotection in co-morbidities.....	13
4.2.5.3 Mechanisms of cardioprotection	13
5. Aims	15
6. Materials and Methods	16

6.1 Experimental design	16
6.2 Measurement of lipid parameters	18
6.3 Immunohistochemistry and determination of infarct size	18
6.4 Isolation of mitochondria and analysis of mitochondrial Cx43 content	19
6.5 Characterization of oxidative/nitrative stress	20
6.5.1 Cardiac superoxide production by lucigenin-enhanced chemiluminescence	20
6.5.2 Cardiac free 3-nitrotyrosine ELISA	20
6.5.3 In situ detection of superoxide	21
6.5.4 Measurement of protein carbonylation	21
6.5.5 Quantitative analysis of NOX mRNAs by QRT-PCR	21
6.5.6 Measurement of NOX proteins by western immunoblotting	22
6.6 Primary neonatal rat cardiomyocyte cell culture transfection	23
6.7 Measurement of oxidative stress in microRNA-25 inhibitor or mimic transfected cells by fluorescent microplate reader	24
6.8 Measurement of oxidative stress in microRNA-25 inhibitor or mimic transfected cells by fluorescent microscopy	24
6.9 Luciferase reporter assay	24
6.10 MicroRNA isolation, microarray, stem-loop QRT-PCR, and microRNA target prediction ..	25
6.11 Statistical analysis	26
7. Results	27
7.1 Cholesterol diet results in elevation of serum cholesterol level	27
7.2 Hypercholesterolemia leads to mild diastolic dysfunction	27
7.3 Hypercholesterolemia leads to increased myocardial oxidative and nitrative stress	28
7.4 Hypercholesterolemia leads to global microRNA expression changes	31
7.5 Potential targets of microRNA-25	32

7.6 MicroRNA-25 down-regulation results in increased NOX4 expression, thereby causing oxidative/nitrative stress in the hypercholesterolemic heart	34
7.7 Hypercholesterolemia attenuates the anti-ischemic effect of ischemic preconditioning	38
7.8 Hypercholesterolemia leads to redistribution of sarcolemmal and mitochondrial Cx43	38
8. Discussion	42
8.1 New findings	42
8.1 The effect of hypercholesterolemia on myocardial microRNA expression	43
8.2 MicroRNA-25 regulates NOX4 expression in the heart	43
8.3 Cardiac NOX4 is up-regulated due to hypercholesterolemia.....	44
8.4 Cx43 plays a role in the impaired cardioprotective effect of preconditioning in hypercholesterolemia	45
8.4.1 Connexin43 re-distribution	45
8.4.2 Role of Cx43 in the blunted cardioprotective effect of preconditioning due to hypercholesterolemia	46
9. Conclusions	47
10. Acknowledgements	49
11. References	51
12. Annex	58

2. List of publications

2.1 List of full papers directly related to the subject of the thesis

I. **Varga ZV**, Kupai K, Szűcs G, Gáspár R, Pálóczi J, Faragó N, Zvara A, Puskás LG, Rázga Z, Tizslavicz L, Bencsik P, Görbe A, Csonka C, Ferdinandy P, Csont T.: MicroRNA-25-dependent up-regulation of NADPH oxidase 4 (NOX4) mediates hypercholesterolemia-induced oxidative/nitrative stress and subsequent dysfunction in the heart. *J Mol Cell Cardiol.* (2013) 62:111-21. [IF: 5.148]

II. Görbe A, **Varga ZV**, Kupai K, Bencsik P, Kocsis GF, Csont T, Boengler K, Schulz R, Ferdinandy P.: Cholesterol diet leads to attenuation of ischemic preconditioning-induced cardiac protection: the role of connexin 43. *Am J Physiol Heart Circ Physiol.* (2011) 300:H1907-13. [IF: 3.708]

Cumulative impact factor of the papers directly related to the thesis: **8.856**

2.2 Other full papers

I. A. Görbe, **Z.V. Varga**, N. Klincumhom, T. Eschenhagen, J. Pálóczi, M. K. Purity, A. Dinnyés, S. Rungarunlert, R. Madonna, T. Csont, P. Ferdinandy: Cytoprotection by the NO-donor SNAP against ischemia/reoxygenation injury in mouse embryonic stem cell-derived cardiomyocytes. *Mol Biotechnol.* (2013) (in press accepted manuscript). [IF:2.262]

II. Kocsis GF, Sárközy M, Bencsik P, Pipicz M, **Varga ZV**, Pálóczi J, Csonka C, Ferdinandy P, Csont T.: Preconditioning protects the heart in a prolonged uremic condition. *Am J Physiol Heart Circ Physiol.* (2012) 303:H1229-36. [IF:3.629]

III. Faragó N, Zvara A, **Varga Z**, Ferdinandy P, Puskás LG.: Purification of high-quality micro RNA from the heart tissue. *Acta Biol Hung.* (2011) 62:413-25. [IF: 0.593]

IV. Csont T, Görbe A, Bereczki E, Szunyog A, Aypar E, Tóth ME, **Varga ZV**, Csonka C, Fülöp F, Sántha M, Ferdinandy P.: Biglycan protects cardiomyocytes against hypoxia/reoxygenation injury: role of nitric oxide. *J Mol Cell Cardiol.* (2010) 48:649-52. [IF: 5.499]

Total impact factor: **20.839**

3. List of abbreviations

BSA = bovine serum albumin

CF = coronary flow

CO = cardiac output

Cx = connexin

DCF-DA = 2',7'-dichlorofluorescein-diacetate

DHE = dihydroethidium

DMSO = dimethyl sulfoxide

DPI = diphenyleneiodonium

+dP/dt_{max} = maximal rate of ventricular pressure rise

-dP/dt_{max} = maximal rate of ventricular pressure decline

DPI = diphenyleneiodonium

ELISA = enzyme-linked immunosorbent assay

FITC = fluorescein isothiocyanate

GAPDH = glyceraldehyde 3-phosphate dehydrogenase

GSH and GSSG – reduced and oxidized glutathione

GSK3 β = glycogen synthase kinase 3 beta

H₂O₂ = hydrogen peroxide

HbA1c = hemoglobin A1c

HDL = high density lipoprotein

HPRT = hypoxanthine guanine phosphoribosyl transferase

HRP = horse radish peroxidase

HW = heart weight

HW/BW = heart weight/body weight ratio

I_{Pre} = ischemic preconditioning

I_{Post} = ischemic postconditioning

LDL = low density lipoprotein

LV = left ventricle

LVDP = left ventricular developed pressure

LVEDP = left ventricular end-diastolic pressure

LXR = liver X receptor

MMP = matrix metalloprotease

MPTP = mitochondrial permeability transition pore

NOX1 = NADPH oxidase isoenzyme 1

NOX2 = NADPH oxidase isoenzyme 2

NOX4 = NADPH oxidase isoenzyme 4

ONOO = peroxynitrite

oxLDL = oxidized low density lipoprotein

p38 MAPK = mitogen activated protein kinase

PBS = phosphate buffered saline

PKC ϵ = protein kinase C epsilon

QRT-PCR = quantitative reverse transcription polymerase chain reaction

rno-miR = Rattus Norvegicus microRNA

ROS = reactive oxygen species

SDS-PAGE = SDS-poly acryl-amide gel electrophoresis

SREBP = sterol-regulatory element binding protein

STAT = signal transducer and activator – protein kinase

TBS = Tris-buffered saline

3' UTR = three prime untranslated region

VLDL = very low density lipoprotein

4. Introduction

4.1 Epidemiological importance of hypercholesterolemia

Incidence of metabolic diseases (including obesity, type II diabetes, high blood pressure, and hypercholesterolemia-dyslipidemia) leading to severe cardiovascular complications (e.g. acute myocardial infarction, post-infarction heart failure, stroke, vascular dementia, peripheral artery disease) is growing worldwide. The cost of this both in human lives and in dollars is overwhelming. According to the American Heart Association 2012 Heart Disease and Stroke Statistics, elevated cholesterol level is still the leading risk factor for heart diseases. Almost 34 million people in the US have markedly elevated total cholesterol level (above 240 mg/dl – equal to 6.2 mmol/l) [1]. Recently it has been shown also that the relative contribution of hypercholesterolemia to cardiovascular diseases is more significant than insulin resistance (reduction in HbA1c level results in only modest disease prevention) [2]. Although complications caused by hypercholesterolemia may affect several organs (brain, kidney, heart, etc.), cardiac effects are responsible for the majority of hypercholesterolemia-related morbidity and mortality. The pathoetiology of metabolic diseases and especially that of hypercholesterolemia have been studied extensively for many years, nevertheless, alterations in molecular signaling pathways leading to cardiac complications are not entirely known.

4.2 Biological effects of hypercholesterolemia on the heart

4.2.1 *Coronary atherosclerosis*

It is well known, that hypercholesterolemic patients have a much higher morbidity and mortality from cardiovascular diseases, considering the central role of elevated cholesterol levels in the development of atherosclerosis. Coronary atherosclerosis directly leads to development of ischemic heart disease.

The main pathophysiological hypothesis of atherosclerosis highlights the central role of low-density lipoprotein (LDL) and its oxidized derivatives (oxLDL and other oxysterols) in the initiation of the atherosclerotic process [3]. Oxidized LDL is present in large amount in atherosclerotic plaques, where it facilitates inflammatory cell migration, and oxidative stress [4]. However, it is now well-accepted that atherosclerosis is not solely a lipid disorder, but also characterized by chronic inflammation. Migration of monocytes and T-cells from the circulation

into the intima of the arterial wall is a key step. These cells then differentiate into macrophages, which then take up modified lipoproteins thereby transforming into foam cells. In addition, these activated leukocytes start to produce a variety of cytokines that can exert several pro-inflammatory effects, maintaining chronic vascular inflammation that is typical for atherosclerosis [5].

However, the molecular communication, between cholesterol or its oxy-derivatives, cytokines and cells within the arterial wall, and also gene expression alterations responsible for atherogenesis are still far from clear.

4.2.2 Direct myocardial effects on the regulation of gene expression

Cholesterol may exert several direct effects on the myocardium that seems to be independent of the development of atherosclerosis. It is obvious now that cellular cholesterol homeostasis is regulated by feedback mechanisms involving the cholesterol molecule itself, as an end product repressor. Since cholesterol has a lipophilic characteristic it may regulate gene expression, similarly to steroid hormones. Cholesterol-induced gene regulation is still an enigmatic research area. Cholesterol may regulate gene expression at both transcriptional and posttranscriptional levels.

4.2.2.1 Transcriptional regulation

Two key transcription factors have been implicated so far in cholesterol-dependent transcriptional gene expression regulation: sterol-regulatory element binding protein (SREBP) and the liver X receptor (LXR) [6,7]. Sterol regulatory element (SRE)/SRE-like sequence has been identified in the promoter region of many genes encoding for several enzymes in the cholesterol biosynthetic pathway (such as HMGCoA synthase, and reductase); LDL receptor (apoB-specific); and Bcl-2 (a repressor of apoptosis) implicating the importance of cholesterol-dependent gene regulation [8]. Indeed, our research group also identified several interesting gene targets in the hearts of cholesterol-fed rats [9]. In this early microarray study (with “only” 3200 templates) we have found an up-regulation of several cellular stress related transcripts (Hsp86, methallothionein II) and cell adhesion markers (tensin, catenin), while down-regulation of the members of cholesterol synthetic pathways (farnesyl transferase) and importantly enzymes of cellular energy homeostasis (ATP synthase subunits, NADH-ubiquinone oxidoreductase, enolase) was detectable. Nevertheless, the factors (epigenetic, transcriptional, posttranscriptional,

and posttranslational) that may regulate these cholesterol-induced gene expression changes are not entirely known.

4.2.2.2 Posttranscriptional regulation: role of microRNAs

Recently, microRNAs have emerged as powerful posttranscriptional regulators of gene expression [10], having pivotal role in essential cardiovascular functions.

MicroRNAs are small RNA molecules, approximately 22 nucleotides in length, encoded within the genomes of eukaryotes. MicroRNAs regulate eukaryotic gene expression at the post-transcriptional level by binding to canonical sites on the mRNA that are located in mRNA 3'UTRs. Specificity of microRNA function is controlled through the direct base pairing on the targeted mRNAs [11]. MicroRNA-regulated mRNAs often have multiple microRNA target sites within their 3'UTRs, and these sites are often evolutionary conserved between species [12]. MicroRNAs have roughly the same size as small-interfering RNAs (siRNAs) but their biogenesis and mechanism of action is different.

MicroRNAs are known to play important roles in many physiological and pathological processes in the heart, including myocyte contractility, cardiac development, myocardial infarction, cardiac fibrosis, hypertrophic response, and arrhythmogenesis [13]. However, the role of cardiac microRNAs in metabolic disease states, especially in the myocardium in hypercholesterolemia is not known.

4.2.3 Myocardial oxidative stress in hypercholesterolemia

Despite the high prevalence and significance of metabolic diseases, the mechanisms of impaired cardiovascular function are not fully understood. Some molecular mechanisms were described, however, increasing evidence suggests that many of these alterations are highly associated with elevated reactive oxygen species (ROS) levels. ROS, also called reactive oxygen intermediers are a group of reactive substances, including superoxide, hydrogen peroxide, hydroxyl radicals and peroxynitrite.

4.2.3.1 ROS sources and defense mechanisms

Although ROS are generally considered as harmful molecules, trace amounts of ROS may also serve as signaling molecules (as triggers) in physiological conditions. ROS can be formed by several enzymes (Figure 1.). These include NADPH oxidases, xanthine oxidases, cyclooxygenases, mitochondrial respiratory chain, the uncoupled nitric oxide synthase, and

peroxidases [14]. However, NADPH oxidases emerge from this list, as an origin of ROS since these enzymes are the only known enzymes that are solely responsible for ROS generation as

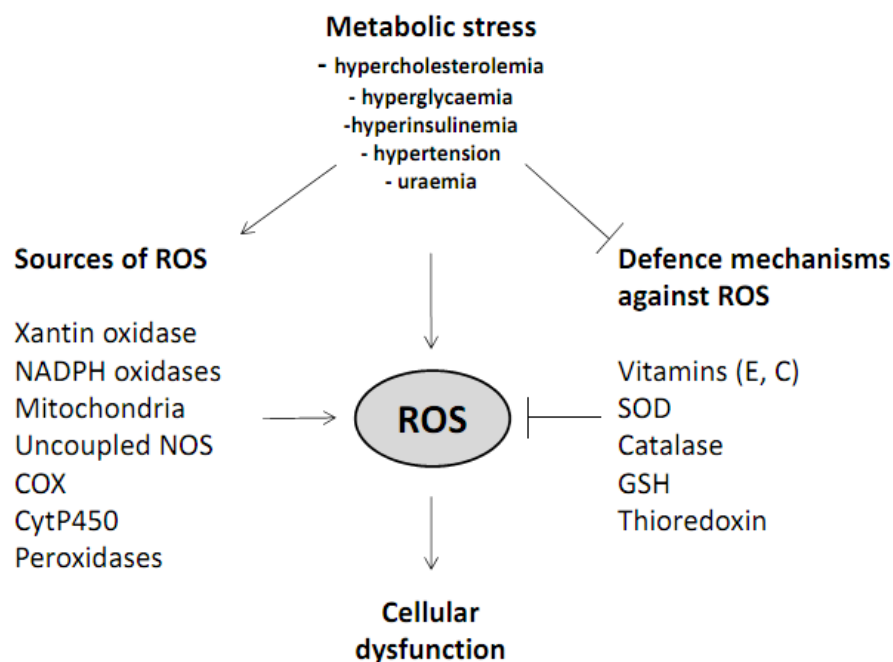


Figure 1. Oxidative stress in metabolic stress situations

their main function. An increasing amount of data has also confirmed that NADPH oxidase expression and activity positively correlate with the development and progression of several cardiovascular diseases [15]. In order to protect cellular functions from ROS, cells possess various defense mechanisms, involving enzymatic and non-enzymatic reactions (Figure 1.). The enzymatic antioxidant pathway involves superoxide dismutases, catalase, and glutathione peroxidase. The dismutation of superoxide by superoxide dismutase results in the generation of H_2O_2 , a species that is further converted by catalase to water and oxygen. In the non-enzymatic pathways, there are a variety of redox-based defense systems including anti-oxidant scavengers, such as vitamins E and C, the ratio of reduced glutathione (GSH) to oxidized glutathione (GSSG), and the thioredoxin system.

4.2.3.2 Oxidative stress and hypercholesterolemia

ROS are highly reactive and unstable molecules causing irreversible and deleterious reactions with biological macromolecules. Therefore, excessive production of ROS may lead to

pathologic cellular alterations. Cardiac conditions such as hypertension [16], diabetes mellitus [17], coronary artery disease [18], cardiomyopathies, heart failure [19], and hypercholesterolemia [20] are associated with altered metabolism of ROS, resulting in chronically increased oxidative stress (Figure 1.).

Previously, we have shown that in different animal models of hypercholesterolemia (2% cholesterol-fed rats [21] and apoB100 transgenic mice [22]) there is apparent cardiac oxidative/nitrative stress. We also implicated in our studies that increased expression of NADPH oxidases are the major source of ROS in hypercholesterolemia [22].

4.2.4 Direct myocardial effects on contractile function

Recent studies have shown that hypercholesterolemia exerts direct myocardial effects independent of the development of atherosclerosis both in humans [23,24] and in animal models [25]. Observations in human clinical trials and animal models suggest a direct effect of cholesterol on myocardial contractile function. Several clinical trials have shown e.g. that statins, drugs that are used to reduce serum cholesterol levels, improve the symptoms of heart failure [26]. Although these observations in humans suggest a non-coronary role of statins in improving cardiac performance, they did not directly link dyslipidemia and hypercholesterolemia to impaired myocardial function.

4.2.4.1 Impaired contractility due to hypercholesterolemia

Direct effects of cholesterol exposure on cardiomyocyte function have been shown by Bastiaanse et al. showing decreased cytosolic calcium levels and impaired cardiac myocyte contractility after elevation of membrane cholesterol content in ventricular cardiomyocytes in a cell culture model [27]. This has been further confirmed in vivo in cholesterol-fed rabbits and rats, showing apparent contractile changes (decrease in maximum rate of shortening, decrease in the rate of relaxation, increase of left ventricular end-diastolic pressure [25,28]). These contractile alterations are similar to those seen in models of myocardial hypertrophy but without the accompanying hypertrophy (normal histology) or hemodynamic overloading (normal morphology). Whether these alterations occur in humans during hypercholesterolemia is not entirely clear at this time. However, there are reports, showing a positive correlation between serum HDL levels and LV ejection fractions in patients with hypercholesterolemia even in the absence of angiographic evidence of coronary atherosclerosis [29,30].

4.2.4.2 Role of oxidative stress in impaired contractility

In metabolic stress situations (such as diabetes mellitus) cardiac dysfunction and oxidative stress are well correlated [31], suggesting the role of oxidative stress as a culprit in metabolic stress induced myocardial dysfunction. Our research group has previously published that hypercholesterolemia-induced myocardial oxidative/nitrative stress significantly contributes to the development of cardiac dysfunction, since contractile alterations can be diminished by pharmacologic attenuation of cardiac nitrative stress (e.g. with a peroxynitrite decomposition catalyst) [21,22]. However, the exact underlying molecular mechanisms in relation to hypercholesterolemia and oxidative stress are still not entirely clear. One possible mechanism might be the oxidation of contractile proteins that was described by Canton et al. [32]. In human failing heart samples there is an obvious oxidation and nitrosylation of tropomyosin and actin, showing a positive correlation with diminished contractile function (as indicated by a decrease in ejection fraction).

4.2.5 Direct myocardial effects on endogenous ischemic adaptation

In addition to the observed contractile changes, hypercholesterolemia may influence ischemia/reperfusion injury and cardioprotective mechanisms in hearts exposed to ischemia/reperfusion. To date, a few studies have demonstrated aggravated ischemia/reperfusion injury in hypercholesterolemic models as well as in humans [33-36]. Hypercholesterolemia may also adversely influence the evolution of infarction (i.e. the remodeling process) even after successful reopening of the occluded coronary artery [37]. After myocardial infarction, the surviving myocardium undergoes a complex sequence of cardiac remodeling, which may have some beneficial effect on cardiovascular performance, but later may become detrimental and may contribute to the development of heart failure. In experimental studies, the degree of deleterious remodeling is highly affected by the size of the infarct [38].

4.2.5.1 Cardioprotective mechanisms: pre- and postconditioning

The heart is known to have a remarkable adaptive ability to withstand myocardial ischemia/reperfusion injury. The phenomenon in which brief periods of ischemic episodes protect the heart against the subsequent lethal ischemia/reperfusion injury was termed ischemic preconditioning (IPre) [39]. The protection afforded by IPre involves the reduction of myocardial infarct size, decrease the incidence of ventricular arrhythmias, and improvement of functional

contractile recovery during reperfusion. This powerful cardioprotective effect appears to be ubiquitous having been reproduced in all species tested including humans and in different organs other than the heart [40]. Later it was described, that the ischemia/reperfusion-induced myocardial injury could be further reduced, if the myocardial reperfusion process was delayed or modified to a staged or gradual form of myocardial reperfusion. This phenomenon is known as ischemic postconditioning (IPost) [41].

4.2.5.2 Blunted cardioprotection in co-morbidities

Although, IPre and IPost has a marked cytoprotective effect in a variety of species, including humans; several studies described (including studies from our research group) that the effectiveness of cardioprotection may be attenuated or blunted in some co-morbid disease states such as high blood pressure, diabetes, heart failure, hyperlipidemia, renal failure, etc. [see for extensive review: 40]. This has to be considered as a major limitation of the clinical applicability of cardioprotective interventions, since almost every patient with an acute myocardial infarction has at least one of these comorbidities. Indeed, our research group has shown previously the attenuation of cardioprotection by Ipre and Ipost in experimental hypercholesterolemia [28,42] and in patients undergoing percutaneous coronary intervention [43]. Although several mechanisms has been proposed to be involved in the attenuated cardioprotective effect in these disease states (nitric oxide, heat shock response, etc.), the role of Cx43 has not been examined in this context.

4.2.5.3 Mechanisms of cardioprotection

In the last decades, an enormous amount of information has been generated on the molecular mechanisms involved in Ipre and Ipost (Figure 2.). A large number of stimuli (ROS, NO, adenosine, cardiac pacing) are capable to trigger a state of increased resistance to ischemia/reperfusion, and several interrelated signal transduction pathways (Erk and Akt signaling, cGMP-PKG pathway, etc.) have been identified. However, the end-effectors of cardioprotective interventions remained largely unknown so far, although they may represent promising therapeutic targets against ischemia/reperfusion injury. The end-effectors have also central role in necrotic cell death due to ischemia/reperfusion injury (Figure 2.). Calpains and matrix metalloproteinases, the mitochondrial permeability transition pore, the sodium/calcium

exchanger of the cardiomyocytes and gap junctions formed by connexin43 (Cx43) hemi-channels have been considered so far as potential end-effectors [44].

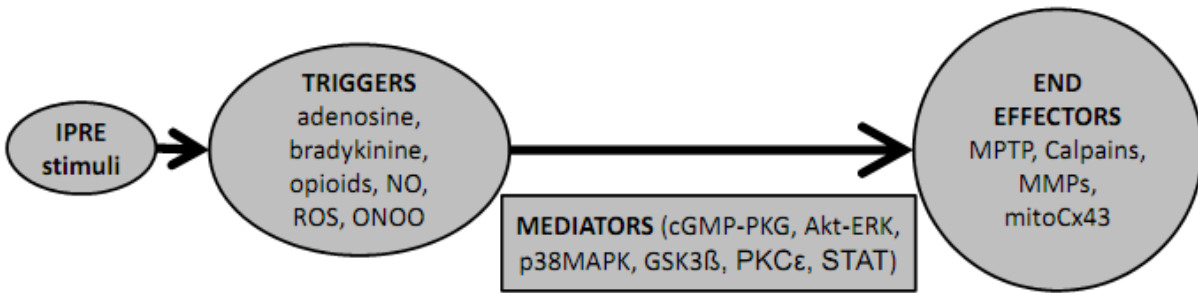


Figure 2. Proposed molecular mechanisms of ischemic preconditioning

Gap junctions form channels between adjacent cells that are composed of connexin (Cx) protein subunits that may allow direct intercellular communication. To date, 21 proteins are classified into the connexin gene family in humans, among them Cx43 is the most abundant form in ventricular cardiomyocytes. Several studies implicated the role of Cx43 formed gap junction mediated cell coupling and/or uncoupling in the mechanisms of cardioprotective interventions, but these early studies were mainly inconclusive and controversial [45,46]. Straightforward studies showed that cardioprotection is blunted in Cx43 knockout mice [47], and later Boengler et. al described the presence of Cx43 hemi-channels in the mitochondria of cardiomyocytes (mouse, rat, pig, and human) showing that Cx43 is present at the inner membrane of sub-sarcolemmal mitochondria [48], and that mitochondrial Cx43 increases potassium influx into the mitochondrial matrix [49]. Furthermore, decreased mitochondrial import of Cx43 to below 50% of normal attenuates the infarct size reduction by ischemic or diazoxide-induced preconditioning in mice and rat hearts [50], showing its pivotal role in cardioprotection. However, the role of mitochondrial Cx43 in the attenuation of cardioprotection in cardiac co-morbidities is still unclear.

5. Aims

Here in this thesis our objective was to obtain a deeper insight into the functional and molecular effects of hypercholesterolemia on the myocardium.

Our first aim was to investigate the possible causes of hypercholesterolemia-induced oxidative/nitrative stress and subsequent myocardial dysfunction.

Therefore we have assessed:

- whether cardiac microRNAs are affected by experimental hypercholesterolemia.
- if microRNAs participate in the regulation of myocardial oxidative/nitrative stress in hearts of hypercholesterolemic rats
- potential protein targets of microRNAs affected by hypercholesterolemia

Our second aim was to analyze the direct molecular effects of hypercholesterolemia on the end-effectors of cardioprotective mechanisms. Although, mitochondrial Cx43 plays an essential role in cardioprotection, changes in cardiac mitochondrial Cx43 in hypercholesterolemia have not yet been analyzed. Therefore, we aimed to determine total and mitochondrial Cx43 levels in rats fed a cholesterol-rich diet. Furthermore, ischemic and preconditioned rat hearts were examined whether changes in mitochondrial Cx43 might be involved in attenuated cardioprotection in hypercholesterolemia.

6. Materials and Methods

The investigation conforms with the Guide for the Care and Use of Laboratory Animals published by the U.S. National Institutes of Health (National Institutes of Health publication 85-23, revised 1996), and it was approved by a local animal ethics committee of the University of Szeged (ethical approval No.: I-74-5/20010).

6.1 Experimental design

In order to investigate the possible molecular mechanism of hypercholesterolemia-induced oxidative/nitrative stress and consequent myocardial dysfunction, male Wistar rats (250 g) were fed normal or 2% cholesterol- and 0.25% cholate-enriched rat chow for 12 weeks (Figure 3. Protocol A). At the end of the diet period, venous blood was taken for determination of serum lipids. Hearts of anesthetized (sodium pentobarbital; 60 mg/kg i.p.) and heparinized (sodium heparin; 500 U/kg i.v.) rats were then isolated and perfused according to Langendorff with an oxygenated Krebs-Henseleit buffer at 37°C for 10 minutes. Tissue samples of the ventricular myocardium (n=10-12 in each group) were rapidly frozen in liquid nitrogen for further biochemical analysis (microRNA assays, NADPH oxidase (NOX1,2, and 4) Western blots, nitro-tyrosine ELISA). Some of the hearts were fixed in 4% formaldehyde and were used for

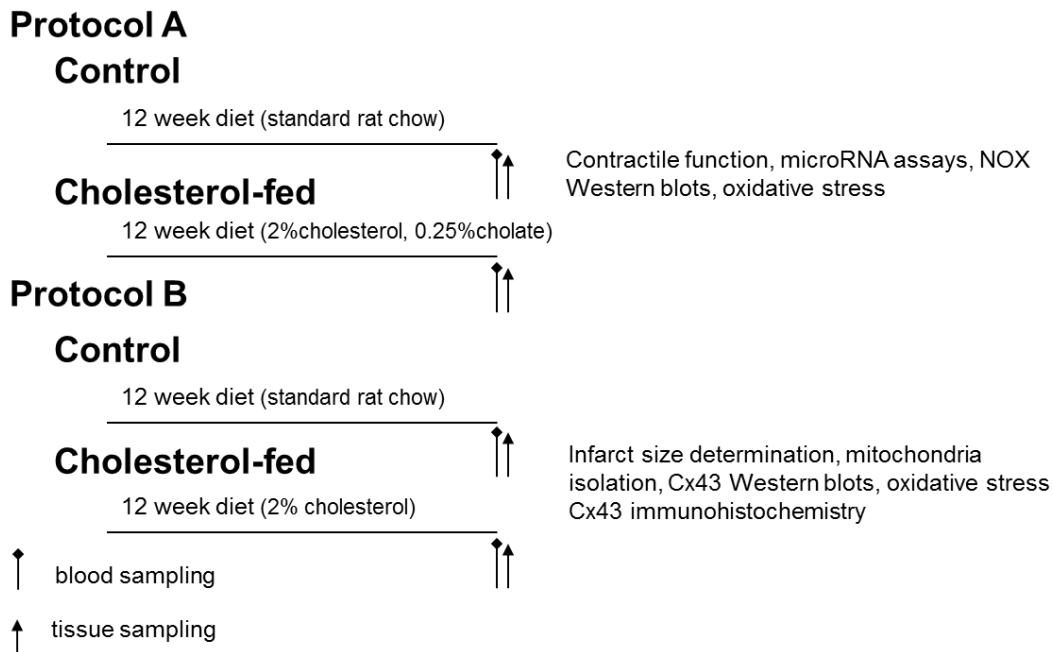


Figure 3. Experimental protocol

histological analysis. In a separate set of experiments, isolated hearts were perfused in a “working” mode according to Neely for 30 minutes following the 10-min Langendorff perfusion. Hemodynamic parameters including heart rate, coronary flow, aortic flow were measured at the end of “working” perfusion. To record ventricular pressure parameters, we inserted a polyethylen catheter attached to a pressure transducer into the left ventricle through the left atrial cannula.

Another set of animals were used for heart catheterization to record ventricular pressure in vivo. Rats were anesthetized with an intraperitoneal injection of pentobarbital sodium (60 mg/kg) and placed on a heated pad to maintain body temperature. To record left ventricular pressure curve, the right carotid artery was exposed, and a 1.6-Fr pressure catheter (Transonic Scisense Inc., London, ON, Canada) was inserted into the left ventricle. Left ventricular pressure curves were evaluated using the Labscribe2 software.

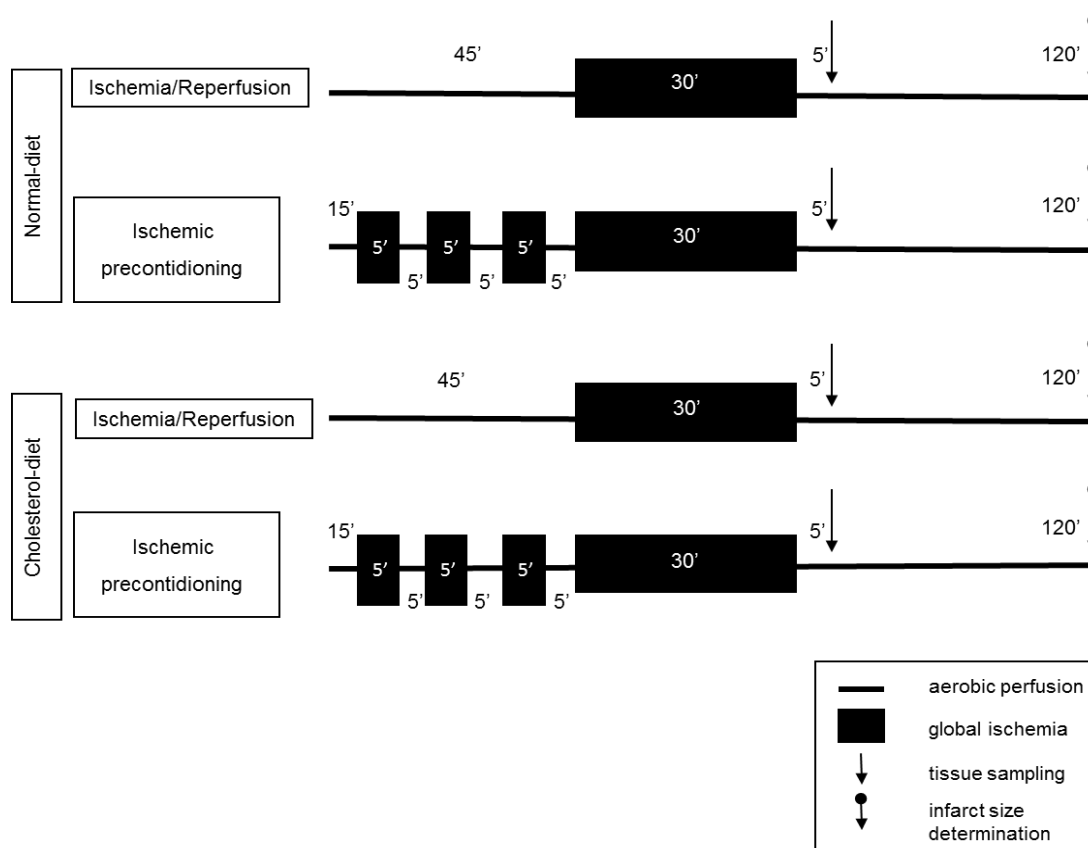


Figure 4. Isolated heart perfusion protocol

In order to investigate the possible role of mitochondrial Cx43 in impaired cardioprotection due to hypercholesterolemia, male Wistar rats (250-300 g) were fed normal (n=18) or 2% cholesterol-enriched rat chow (n=18) for 12 weeks (Figure 3. Protocol B). At the

end of the diet, animals were anesthetized with diethylether and given 500 U/kg heparin. Hearts were then isolated and perfused according to Langendorff with Krebs-Henseleit buffer. Hearts from normal (n=6) and cholesterol-fed rats (n=6) were perfused aerobically for 10 min, these hearts were rapidly frozen in liquid nitrogen for further biochemical experiments (Western blots, immunohistochemistry). Then hearts in both diet-groups were subjected to a no-flow ischemia-induced preconditioning protocol (3 x 5-min ischemia and 5-min reperfusion) or a time-matched non-preconditioning protocol each followed by test ischemia/reperfusion (30-min global normothermic ischemia followed by 5-min or 120 min reperfusion, respectively n=6 in each group) (Figure 4.). Tissue samples from these perfusion groups were used for mitochondria isolation and Western blots, and in separate experiments myocardial infarct size was determined.

6.2 Measurement of lipid parameters

To validate the development of hypercholesterolemia in our cholesterol-fed rat models, at the end of the diet period, serum cholesterol and triacylglycerol levels were determined by colorimetric enzymatic assays in triplicates (Diagnosticum, Budapest, Hungary). To analyze α (HDL), pre- β (VLDL), and β -lipoproteins (LDL) in the serum of rats fed cholesterol-enriched or normal diet, lipoproteins were separated on agarose gels, using Paragon Electrophoresis System Lipoprotein Electrophoresis Kit (Beckman Coulter, Fullerton, CA) according to the manufacturer's instructions.

6.3 Immunohistochemistry and determination of infarct size

Formaldehyde-fixed myocardial samples were embedded in paraffin, 4- μ m sections were placed on silanized slides and, after conventional methods of dewaxing and rehydration, the samples were subjected to immunohistochemical analysis for NOX4 protein. Rabbit polyclonal anti-NOX4 antibody (Novus Biologicals, Cambridge, UK) was used as primary antibody (1:100; 30 min). The Envision Flex System (DAKO, Denmark) with High pH was used as visualization system. The sections were counterstained with hematoxylin (for 1 min) and examined by two independent histologists by means of light microscopy at 40 \times magnification.

Cx43 level of intercalated discs were detected also by immunohistochemistry. Fresh frozen sections (10 μ m) of hearts were fixed in fresh acetone for 5 min. After allowing them to dry at room temperature for 30 min they were blocked with 5% BSA (Sigma) in TBS for 15 min. Incubation with the primary antibody (monoclonal mouse anti-Cx43 (GAP1, 1:100, (3, 41)) were

carried out at room temperature for 1.5 h in a humidified chamber. The sections were washed 3 x 5 min in TBS and incubated in secondary antibody (FITC-conjugated anti-mouse) (Dako) diluted in TBS (1:300) for 40 min. Sections were mounted on a slide in Faramount mounting medium (Dako). Images of immunostained sections were captured using fluorescent microscope (Nikon, Labophot 2). At least eight random images were collected on each heart muscle sample stained for Cx43. Digital single channel images were transformed into 8-bit black-and-white format and were analyzed using the ImageJ 1.29x software (Wayne Rasband, NIH, USA). At standard threshold settings, which ensured that only specific signals were considered and the background was excluded, the area fraction of Cx43 immunofluorescent dots and plaques was measured on each image. Then immunofluorescent plaques (size ≥ 50 pixels) were measured separately representing the intercalated disc fraction. The ratio of intercalated disc intensity and total intensity in each group was summarized in graphs.

At the end of the perfusion protocols, hearts were frozen, sliced, and incubated at 37°C in 1% triphenyltetrazolium chloride to delineate infarcted tissue. Slices were then fixed and quantified by planimetry using our own software, Infarctsize 2.4.

6.4 Isolation of mitochondria and analysis of mitochondrial Cx43 content

In order to assess mitochondrial Cx43 content, mitochondria were isolated from hearts of hypercholesterolemic and control animals following 10 min aerobic perfusion, or from preconditioned and ischemic control hearts (Figure 3. Protocol B). Mitochondrial isolation procedure was performed according to Boengler et al.[48]. Briefly, fresh heart tissue were minced with scissors in ice-cold isolation buffer (250 mM sucrose, 10 mM HEPES, 1 mM EGTA; pH 7,4). Heart tissue samples were homogenised by ultrasonic homogenisator for 3 x 5 seconds. The homogenate was centrifuged at 480 g for 10 min and the supernatant was filtered through a nylon filter (250 μ m pore size) and then centrifuged again at 10780x g for 10 min. The pellet containing mitochondria was re-suspended in isolation buffer and then centrifuged again at 7650 g for 20 min. Then the pellet was re-suspended in 50 μ l isolation buffer and layered onto 30% Percoll solution and ultracentrifuged at 35000 g for 30 min. The lower band reflecting intact mitochondria was collected and washed in isolation buffer by centrifugation at 8000 g for 5 min.

Cx43 level in isolated mitochondria and in total heart homogenates was determined by Western blotting. Heart powder samples were homogenised by ultrasonic homogenisator at maximum power, 90% sonication time for 2 x 20 seconds. The protein concentrations of total

heart and mitochondria fractions were determined by the bicinchoninic acid assay (Pierce). 20 ug samples were loaded on SDS-PAGE (10%) followed by the transfer of proteins onto a nitrocellulose membrane (400 mA, 1 h). Membranes were then blocked overnight at 4 °C in TBS-T (0.1% Tween-20) and 5% skimmed milk powder. Membranes were incubated either with rabbit polyclonal anti-rat Cx43 (Zymed), or mouse monoclonal anti-succinate dehydrogenase (Molecular Probes), rabbit polyclonal anti Na/K ATP-ase α -1 (Upstate) and mouse monoclonal anti Actin (BD Biosciences) antibodies for 1.5 h at room temperature and horseradish peroxidase-conjugated rabbit anti-mouse or goat anti-rabbit secondary antibody (Dako) for 40 min. Membranes were then developed with an enhanced chemiluminescence kit (GE HealthCare), exposed to X-ray (Kodak) film and scanned. Band density was calculated by integrating the area (in pixels \times intensity, expressed in arbitrary units).

6.5 Characterization of oxidative/nitrative stress

6.5.1 Cardiac superoxide production by lucigenin-enhanced chemiluminescence

Cardiac superoxide production in freshly minced ventricles was assessed by lucigenin-enhanced chemiluminescence in normal and cholesterol-fed groups (Figure 3 Protocol B). Approximately 100 mg of the apex of the heart was placed in 1 ml air-equilibrated Krebs–Henseleit solution containing 10 mmol/l HEPES (pH 7.4) and 5 μ mol/l lucigenin. Chemiluminescence was measured at room temperature in a liquid scintillation counter using a single active photomultiplier positioned in out-of-coincidence mode in the presence or absence of the superoxide scavenger nitroblue tetrazolium (NBT, 200 μ mol/l). NBT-inhibitable chemiluminescence was considered an index of myocardial superoxide generation.

6.5.2 Cardiac free 3-nitrotyrosine ELISA

Cardiac free 3-nitrotyrosine level was measured by enzyme-linked immunosorbent assay (ELISA; Cayman Chemical) from normal and cholesterol-fed heart tissue samples. Briefly, supernatants of ventricular tissue homogenate was incubated overnight with anti-nitrotyrosine rabbit IgG specific to free 3-nitrotyrosine and nitrotyrosine acetylcholine esterase tracer in precoated (mouse anti-rabbit IgG) microplates followed by development with Ellman's reagent. Free nitrotyrosine content was normalized to protein content of cardiac homogenate and expressed as nanograms per milligram protein.

6.5.3 In situ detection of superoxide

In situ detection of superoxide was performed by fluorescent microscopy using the oxidative fluorescent dye dihydroethidium (DHE). DHE is freely permeable to cell membranes and reacts with superoxide anions forming a red fluorescent product which intercalates with DNA. Fresh frozen heart sections (30 μm) were incubated with 10^{-6} mol/l DHE (Sigma) in PBS (pH 7.4; 37°C; 30 min) in a dark humidified container. Fluorescence in heart sections was then detected by a fluorescent microscope (Nikon, Japan) with a 590-nm long-pass filter. Images of sections treated with saline (negative control) were measured first. The fluorescence intensity was evaluated with ImageJ 1.44.

6.5.4 Measurement of protein carbonylation

In order to confirm the effect of oxidative stress on cardiac proteins, total myocardial protein carbonylation was measured using the Oxyblot protein oxidation detection kit (Merck-Millipore, Billerica, USA) according to the manufacturer's protocol. Briefly, carbonyl groups were derivatized with 2,4-dinitrophenylhydrazine for 15 min. Dinitrophenyl-derivatized proteins were resolved by sodium dodecylsulphate–polyacrylamide gel electrophoresis and transferred to nitrocellulose membrane. Membranes were incubated overnight with anti-dinitrophenyl primary antibodies and then with goat anti-rabbit/horseradish peroxidase antibodies. Signals were visualized by chemiluminescence detection using X-ray films.

6.5.5 Quantitative analysis of NOX mRNAs by QRT-PCR

To investigate the expression of NOX enzymes at the transcript level, QRT-PCR was performed on a RotorGene 3000 instrument (Corbett Research, Sydney, Australia) with gene-specific primers and SybrGreen protocol. 2 μg of total RNA was reverse transcribed using the High-Capacity cDNA Archive Kit (Applied Biosystems Foster City, CA, USA) according to the manufacturer's instructions in final volume of 30 μL . The temperature profile of the reverse transcription was the following: 10 min at room temperature, 2 hours at 37 °C, 5 min on ice and finally 10 min at 75 °C for enzyme inactivation. These steps were carried out in a Thermal Cycler machine (MJ Research Waltham, MA, USA). After dilution with 30 μL of water, 1 μL of the diluted reaction mix was used as template in the QRT- PCR. Reactions were done with FastStart SYBR Green Master mix (Roche Applied Science, Mannheim, Germany) according to the manufacturer's instructions at a final primer (sequences are shown in Table 2.) concentration of

250 nM under the following conditions: 15 min at 95°C, 45 cycles of 95°C for 15 sec, 60°C for 25 sec and 72°C for 25 sec. The fluorescence intensity of SybrGreen dye was detected after each amplification step. Relative expressions were calculated as normalized ratios to the average Ct value of rat HPRT and Cyclophyllin genes. The final relative gene expression ratios were calculated as delta-delta Ct values.

6.5.6 Measurement of NOX proteins by western immunoblotting

In order to investigate whether hypercholesterolemia leads to an increased expression of NOX4 at the protein level in the heart, western blot analysis was performed. Frozen heart samples were homogenized with NP-40 lysis buffer (150 mM NaCl, 50 mM Tris, 1% NP-40) or cultured cardiomyocytes were harvested by scraping and then homogenized and concentrated by centrifugation (7500 g, 20 min). Protein concentrations were determined by means of bicinchoninic acid method using bovine serum albumin as standard (Pierce, Rockford, USA). Forty (heart) or twenty (cells) µg of protein was loaded from each sample onto 10% SDS-polyacrylamide gel. After separation by electrophoresis, proteins were transferred (wet transfer, 2.5 hours) onto nitrocellulose membrane (Amersham Biosciences, Piscataway, USA). Transfer was controlled by using Ponceau dye. The membrane was blocked with 5% non-fat dry milk in 0.1% TBS-T overnight at 4°C. After the blocking step, the membrane was cut horizontally and the upper part was incubated with a primary antibody (dissolved in 1% non-fat dry milk - TBS-T, 1:1000 dilution) against either NOX4 (Novus Biologicals, Cambridge, United Kingdom) - reported to specifically recognize NOX4 protein [51,52] -, NOX2 (Merck-Millipore, Darmstadt, Germany), or NOX1 (Novus Biologicals, Cambridge, United Kingdom) for 2 hours at room temperature, followed by washing with TBS-T (3 x 10 min). After washing, the membrane was incubated with a secondary antibody (horseradish peroxidase-conjugated affinity purified goat anti-rabbit, 1:5000 dilution) in 1% non-fat dry milk in TBS-T for 1 hour at room temperature. Then the membrane was washed again 3 times for 10 min. For detection of the bands, the membrane was incubated with ECL-plus reagent (Amersham Biosciences, Piscataway, USA) for 5 min and then visualized on X-ray films. Band densities were evaluated by using Quantity One software (Bio-Rad Imaging System, Hercules, USA). Loading control was done by determining GAPDH content of each sample. Briefly, bottom of the membrane was probed with a primary antibody that recognizes GAPDH (1:10000 dilution) for 2 hours at room temperature, followed by washing with TBS-T. Then the membrane was incubated with horseradish peroxidase-

conjugated affinity purified goat anti-rabbit antibody (1:20000 dilution) for 1 hour at room temperature. The membrane was washed again and band visualization and evaluation of band densities were done as describe above. There was no significant difference in GAPDH between the groups.

6.6 Primary neonatal rat cardiomyocyte cell culture transfection

To investigate the mechanisms by which microRNA-25 down-regulation affects NOX4 expression, neonatal rat cardiomyocyte cultures were prepared from newborn Wistar rats by triptic digestion. Cardiomyocytes were plated at a density of 3×10^4 cells/well onto 96-well plates and 5×10^5 cells/well onto 6-well plates. The culture was grown for 3 days before experimentation. Culture medium was changed the day after preparation. The cells were maintained at 37°C (humidified atmosphere; 5% CO₂) in a standard CO₂ incubator (Sanyo, Japan). To knock-down endogenous expression of microRNA-25, a microRNA-25 inhibitor was used, while to up-regulate microRNA-25, a synthetic microRNA-25 mimic was used (both from Dharmacon, Lafayette, USA). As a negative control, a corresponding microRNA inhibitor or mimic control (Dharmacon, Lafayette, USA) was transfected into rat neonatal cardiomyocytes, as recommended by the manufacturer. The transfection was carried out according to the recommendations of the manufacturer. Briefly, the microRNA-25 inhibitor or the inhibitor control was diluted in the medium at a final concentration of 100 nM. To confirm the efficiency of transfection, the same amount of Dy547-labelled positive control (Dharmacon, Lafayette, USA) was transfected in separate experiments. The 100 nM concentration of Dy547-labelled microRNA-inhibitor did not decrease cell viability as compared to 25 and 50 nM, however, it considerably increased efficacy of transfection (data not shown). The morphology and contractile ability of the transfected primary cardiomyocytes was not affected significantly by the transfection process as indicated by spontaneous beating 24 h after transfection. Cells were incubated with microRNA-25 inhibitor or with the negative control microRNA inhibitor for 24 h and then used for NOX4 western blot analysis or for fluorescent oxidative stress measurement. Expression level of microRNA-25 following microRNA-25 mimic and inhibitor transfection was assessed by QRT-PCR.

6.7 Measurement of oxidative stress in microRNA-25 inhibitor or mimic transfected cells by fluorescent microplate reader

Transfected neonatal cardiomyocytes were loaded either with 2',7'-dichlorofluorescein-diacetate (DCF-DA) or dihydroethidium (DHE). Briefly, the cells were washed twice with Dulbecco's PBS (D-PBS) and loaded with DCF-DA (10 μ M) or DHE (10 μ M) for 30 minutes in dark at room temperature. After loading the dyes were removed, and the cells were covered with D-PBS and each well was scanned in a fluorescent microplate reader (FluoStar Optima, BMG Labtech, Ortenberg, Germany) using 495 nm excitation/520 nm emission filter combination for DCF-DA, and 505 nm excitation/620 nm emission filter combination for DHE. To test the NADPH oxidase inhibitor diphenyleneiodonium (DPI), the cells were pre-incubated with DPI for 4 hours, before fluorescent staining.

6.8 Measurement of oxidative stress in microRNA-25 inhibitor or mimic transfected cells by fluorescent microscopy

To further mechanistically prove our hypothesis in vitro, neonatal cardiomyocytes were plated on glass coverslips, and transfected with a microRNA-25 mimic or inhibitor, or with their corresponding controls. The transfected cells were loaded with dihydroethidium (DHE), as described above. The coverslips were mounted on glass microscope slides covered with a fluorescent mounting medium (Dako, Glostrup, Denmark), to reduce fading of the fluorescent dye. Fluorescence in the transfected cells was detected by a fluorescent microscope (Nikon, Japan) with a standard rhodamine filter, using the same settings (exposition time, ISO sensitivity, etc) on each sample.

6.9 Luciferase reporter assay

To investigate whether microRNA-25 directly regulates NOX4 expression, human NOX4 3'-UTR sequence was inserted downstream of a Renilla luciferase open reading frame (GoClone System, SwitchGear Genomics, Menlo Park, CA). The luciferase construct was transfected into HEK293 reporter cells together with either a mimic of microRNA-25 or with an inhibitor of microRNA-25 or with a non-targeting sequence (mimic/inhibitor control), respectively, by using the Dharmafect Duo transfection reagent. In each case, 10 ng plasmid DNA and 100 nM microRNA were used. HEK293 cells were chosen for their high efficiency of transfection. Cells were cultured for 24 hours and assayed with the Luciferase Assay Reagent of the manufacturer (SwitchGear Genomics, Menlo Park, CA).

6.10 MicroRNA isolation, microarray, stem-loop QRT-PCR, and microRNA target prediction

In order to investigate the role of microRNAs in the development of myocardial dysfunction due to hypercholesterolemia, heart samples (n=6) from both diet groups were powdered in liquid nitrogen. Steps of microRNA isolation were done according to the protocol of the microRNA isolation kit (Roche, Germany) with modifications [53]. The quality and quantity was assessed spectrophotometrically (Nanodrop, USA) and with 2100 Bioanalyzer (Agilent, CA, USA). Random pairs of the RNA extracted from the 6 different samples in each group were pooled, and the obtained 3 samples/group were assayed on the microarrays. A total of 50 ng purified microRNA was labeled using Agilent's microRNA Complete Labeling and Hyb kit system (Agilent Technologies Palo Alto, CA, USA). The protocol was briefly the following: 25-25 ng of two parallel samples were pooled together in a final volume of 2 μ l and subjected to a dephosphorylation reaction using Calf Intestinal Alkaline Phosphatase (CIP) at 37°C for 30 minutes in the final volume of 4 μ l. In the second step, 2.8 μ l of DMSO was added to each sample for denaturation at 100°C for 5 minutes and placed on ice immediately. Following this step, a ligation reaction was carried out using T4 RNA Ligase and Cyanine3-pCp in a total volume of 11.3 μ l for 2 hours at 16°C to label the RNA samples. The labeled samples were completely vacuum dried on medium-high (45°C) heat setting and hybridized onto the surface of Agilent 8x15k Rat microRNA Microarray (Agilent Technologies, Palo Alto, CA, USA). The microarray contained probes for 350 microRNAs from the Sanger database v 10.1. Dried and labeled samples were re-suspended in 18 μ l of nuclease-free water and denatured at 100°C for 5 minutes in the presence of 1x Blocking Agent and 1x Hi-RPM Hybridization Buffer in a final volume of 45 μ l and immediately placed on ice. These mixes were used for the hybridization, which was done in microarray hybridization chambers (Agilent Technologies, Palo Alto, CA). After hybridization the slides were washed in Gene Expression Wash buffer 1 containing Triton X-100 from Agilent Technologies at room temperature for 1 minute, then in Gene Expression Wash buffer 2 containing Triton X-100 at 37°C for another 1 minute before scanning. Each array was scanned as described earlier with an Agilent Scanner with 5 μ m resolution. Output image analysis and feature extraction was done using Feature Extraction software of Agilent Technologies.

To confirm microarray results, quantitative real-time PCR (QRT-PCR) was used. The reverse transcription reaction was performed with the TaqMan® MicroRNA Reverse

Transcription Kit (Applied Biosystems, CA, USA). 350 ng from each sample was reverse transcribed in the presence of 5x RT TaqMan® MicroRNA Assays (Applied Biosystems, CA, USA). 8 µL reaction mixture contained 0.2 µl dNTPs, 1.5 µl MultiScribe™ Reverse Transcriptase (50 U/µL), 0.8 µl 10x RT Buffer, 0.9 µl MgCl₂, 0.1 µl RNase Inhibitor (20 U/µL), 1.5 µl 5x RT primer and the template in a total volume of 3 µl. Reverse Transcription was carried out with the following cycling parameters in a thermocycler (Bioneer, Daedong, Korea): 16°C for 2 minutes, 42°C for 1 minutes, 50°C for 1 second, 45 cycles, then hold the samples on 85°C for 5 minutes. After dilution with 64 µl of water, 9 µl of the diluted reaction mix was used as template in QRT-PCR. Reactions were performed on a RotorGene 3000 instrument (Corbett Research, Sydney, Australia) with the TaqMan protocol. 20 µl reaction mixture contained 10 µl TaqMan® Universal PCR Master Mix (Applied Biosystems), 1 µl of the TaqMan® MicroRNA Assays and 9 µl of the diluted cDNA. The microRNA databases and target prediction tools TargetScan (www.targetscan.org) [54] and microRNA.org (www.microrna.org) [55] were used to identify potential microRNA-25 targets.

6.11 Statistical analysis

Values are expressed as mean±SEM. One- or two-way analysis of variance (ANOVA) was used to evaluate differences in between treatment groups. Otherwise Student's t-test was used. Statistical analysis of microRNA microarrays were by using the Feature Extraction software of Agilent Technologies. All the individual microRNAs were represented by 20 different probes on the array. Total gene signal is equal to the sum of the signals of the individual probes. Expressions of all the 350 microRNAs found in the Sanger miRBase (version 10.1) were checked. Six heart samples from each diet groups were analyzed by microRNA microarray. Two-two samples were pooled together and a total of 6 hybridization experiments were carried out to gain raw data for statistical analysis. Altogether 9 individual parallel gene activity comparisons were done to determine the average changes, standard deviations and p-values. Using two tailed two sample unequal variance Student t-test, the p-value was determined and used to find the significant gene expression changes. Gene expression ratio with p-value < 0.05 and log₂ ratio < -0.6 or log₂ ratio > 0.6 (~1.5 fold change) are considered as repression or overexpression, respectively. Changes in gene expression were plotted as log₂ ratios of signal intensity values. MicroRNAs having less than 4 individual parallel gene activity comparisons were excluded.

7. Results

7.1 Cholesterol diet results in elevation of serum cholesterol level

Cholesterol-enriched diet for 12 weeks caused a significant increase in cholesterol level in the serum (Figure 5. A) which was accompanied by an altered lipoprotein pattern (Figure 5. B). The 12-week long diet induced a decrease in HDL-fraction. Cholesterol-enriched diet had no influence on serum triacylglycerol level (Figure 5. C).

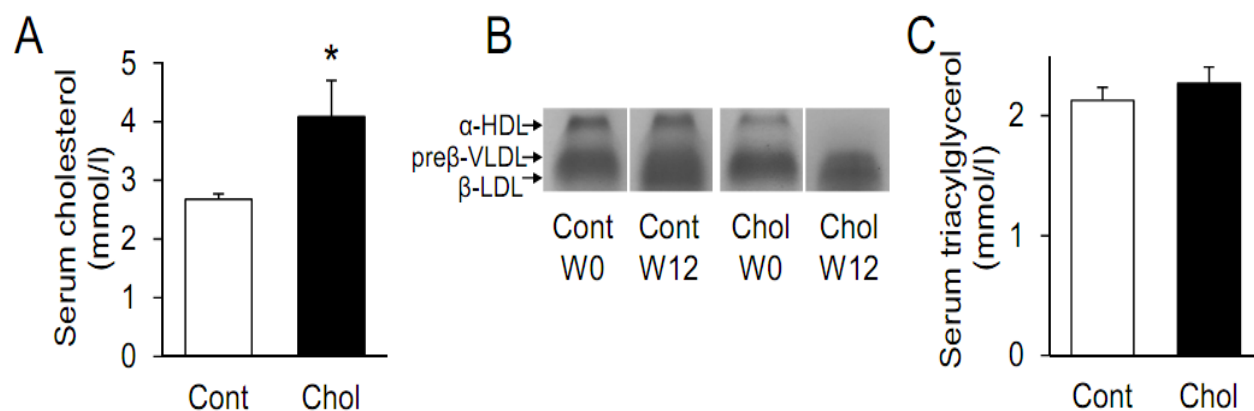


Figure 5. Serum lipid parameters

*Effect of 12-week cholesterol-enriched diet on serum cholesterol (A), serum lipoprotein distribution (B), and serum triacylglycerol (C). The cholesterol-fed group (Chol) displayed a decrease in HDL concentration as compared to the standard chow-fed group (Cont). Results are expressed as mean \pm SEM; n=8 10. * p <0.05 vs. control.*

7.2 Hypercholesterolemia leads to mild diastolic dysfunction

Parameters of myocardial contractile function measured both *in vivo* and in isolated perfused hearts are shown in Table 1. Left ventricular end-diastolic pressure (LVEDP) showed a significant increase in the cholesterol-fed group as assessed both *in vivo* and *ex vivo*, indicating impaired relaxation and diastolic dysfunction. In addition, there was a non-significant ($p=0.096$) decrease in $+dP/dt_{\max}$ in the *ex vivo* perfused hearts of cholesterol-fed rats. Other examined parameters (heart weight, heart weight/body weight ratio, coronary flow, cardiac output, left ventricular developed pressure, $-dP/dt_{\max}$) did not change significantly due to the diet.

	Control	Cholesterol-fed
HW (mg)	1753±52	1687±25
HW/BW (‰)	3.29±0.08	3.32±0.07
Ex vivo parameters:		
CF (ml/min)	34.4±2.4	34.5±3.1
CO (ml/min)	93.7±5.6	93.2±5.1
LVDP (kPa)	19.9±1.25	19.6±1.18
LVEDP (kPa)	1.41±0.30	2.41±0.35*
+dP/dt _{max} (kPa/sec)	742.6±43.6	624.6±50.4
-dP/dt _{max} (kPa/sec)	437.6±12.4	417.2±14.3
In vivo parameters:		
LVDP (mmHg)	104.6±8.0	104.1±8.0
LVEDP (mmHg)	2.93±0.20	3.50±0.14*
+dP/dt _{max} (mmHg/sec)	7958 ±615	8233±648
-dP/dt _{max} (mmHg/sec)	7740±632	8712±726

Table 1. Hemodynamic parameters at the end of 12-week diet

Data are presented as means ± SEM, * $p < 0.05$ vs. control, $n = 8$.

HW: heart weight; HW/BW: heart weight/body weight ratio; CF: coronary flow; CO: cardiac output; LVDP: left ventricular developed pressure; LVEDP: left ventricular end-diastolic pressure; +dP/dt_{max}: maximal rate of ventricular pressure rise; -dP/dt_{max}: maximal rate of ventricular pressure decline.

7.3 Hypercholesterolemia leads to increased myocardial oxidative and nitrative stress

Myocardial oxidative stress was estimated by staining frozen myocardial sections with dihydroethidium. Increased nuclear red fluorescence was detectable in the hearts of cholesterol-fed rats as compared to control rats, indicating enhanced superoxide formation (Figure 6.).

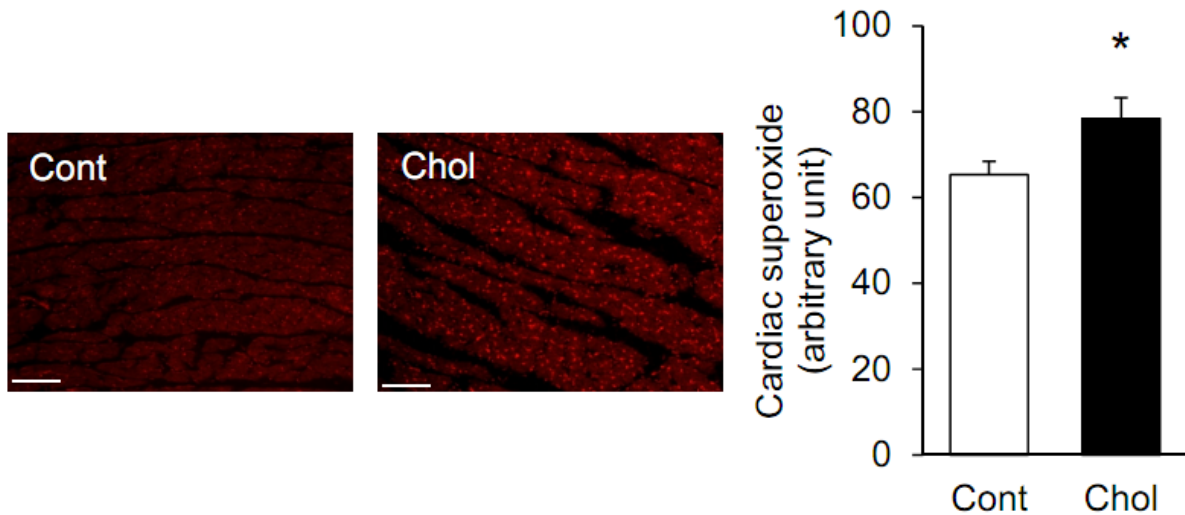


Figure 6. In situ detection of superoxide

Representative ventricular sections from control (Cont) and cholesterol-fed rats (Chol) stained for superoxide by dihydroethidium histochemistry. The representative images show the localization and intensity (red fluorescence) of superoxide in the nucleus (scale bar represents 100 μ m). Bar chart shows quantification of dihydroethidium fluorescence of hearts from control and cholesterol-fed rats, representing myocardial oxidative stress. Values are mean \pm SEM; n=10 in each group. * p <0.05 vs. control group.

The amount of oxidatively modified myocardial proteins was elevated in the cholesterol-fed group as assessed by dinitrophenylhydrazine assay (Oxyblot; Figure 7.). The intensity of the

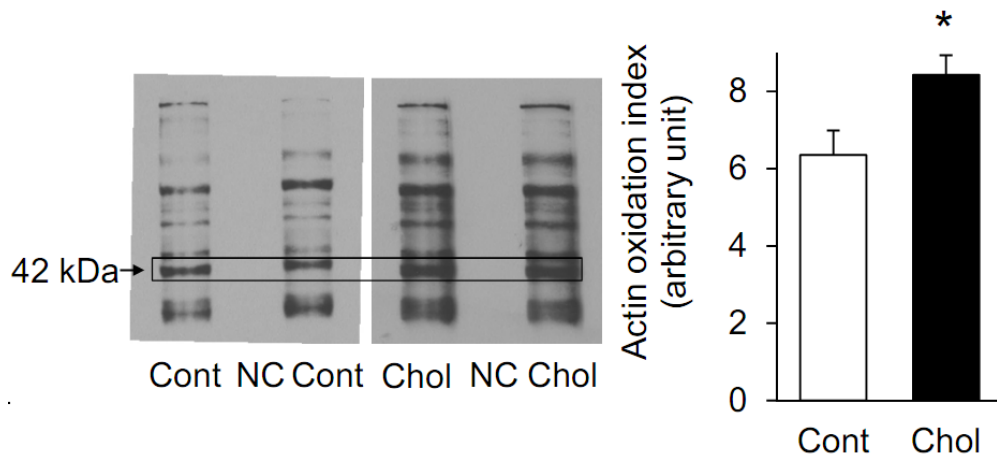


Figure 7. Oxidative protein carbonylation

Representative western blot of carbonylated myocardial proteins from cardiac homogenates from cholesterol-fed (Chol) and control (Cont) animals (NC represents negative control lane). The 42 kDa band corresponds to actin. Quantification of the intensity of the carbonylated 42kDa bands from cholesterol-fed (Chol) and control (Cont) animals. Values are mean \pm SEM; n=5 in each group. * p <0.05 vs. control group.

band with a molecular weight corresponding to actin (42 kDa) was significantly increased (Figure 7.), suggesting that oxidation of contractile proteins are likely involved in hypercholesterolemia-induced myocardial dysfunction.

The nitrative stress marker nitrotyrosine was also elevated in the heart due to cholesterol-enriched diet (Figure 8.).

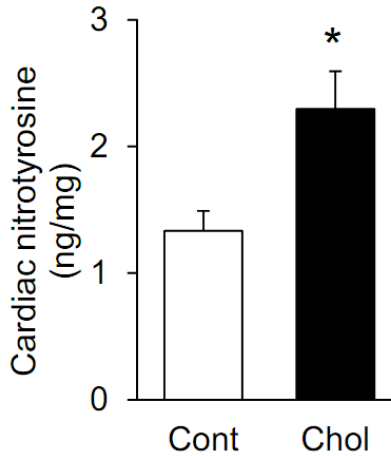


Figure 8. Nitrative stress as assessed by 3-nitrotyrosine ELISA

*Quantification of cardiac 3-nitrotyrosine content, a marker of endogenous peroxynitrite-induced nitrative stress. Free 3-nitrotyrosine was assayed by enzyme-linked immunosorbent assay. Values are mean \pm SEM; n=10–12. *p<0.05 vs. control.*

Moreover we have found elevated superoxide level in the hearts of cholesterol-fed rats according to Protocol B on Figure 1.(for data see annex 2)

As we have previously proposed in our studies that NADPH oxidases might be involved in hypercholesterolemia-induced oxidative stress [22], in the present study we have examined, whether hypercholesterolemia leads to modulation of expression of the cardiac NOX enzymes. QRT-PCR analysis of myocardial samples obtained from cholesterol-fed and control animals showed no alterations in transcript levels of any of the NOX isoforms (NOX1, 2, and 4; Table 2.).

Gene	NM number	Forward primer	Reverse primer	Log ₂	SEM	Fold
NOX1	NM_053683	ggcatcccttactctgacct	tgctgctcgaatatgaatgg	-0.25	0.33	-1,19
NOX2	NM_023965	gctgggattggagtcacg	gcacagccagtagaagtagatcttt	-0,001	0.24	-1,001
NOX4	NM_053524	gaaccaagtccaagctca	gcacaaaggtccagaaatcc	-0,123	0,16	-1,09

Table 2. QRT-PCR analysis of NOX isoenzyme (NOX1, NOX2, and NOX4) transcript levels

To determine whether hypercholesterolemia induces protein expression alteration in abundant cardiac NOX isoforms, we also examined the protein expression of NOX1, NOX2, and NOX4. Although, there were no alterations in the protein level of cardiac NOX1 or NOX2 due to cholesterol-enriched diet, our analysis revealed the up-regulation of NOX4 after 12 weeks of cholesterol-enriched diet, suggesting its role in hypercholesterolemia-induced oxidative stress (Figure 9.).

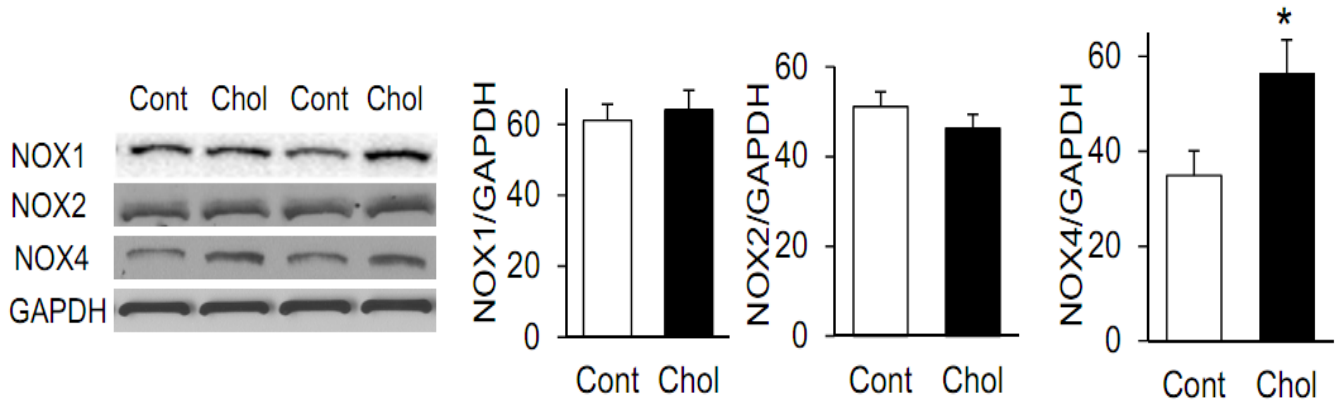


Figure 9. Western blot analysis of cardiac NOX isoenzyme expression

Representative western blots of NOX1, NOX2, NOX4, and GAPDH from cardiac homogenates from cholesterol-fed (Chol) and control (Cont) animals. Quantification of western blot analysis of NOX1, NOX2, and NOX4 proteins in hearts of normal and cholesterol-fed rats normalized to the GAPDH control. Data are mean ± SEM; n=8-10 in each group. *p<0.05 vs. control rats.

Immunostaining for NOX4 showed a diffuse positive staining in cardiomyocytes in both diet groups (Figure 10.) on FFPE sections.

7.4 Hypercholesterolemia leads to global microRNA expression changes

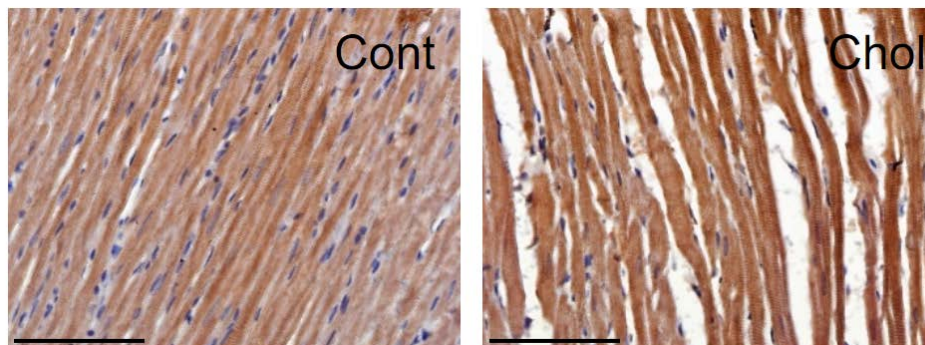


Figure 10. Immunohistochemistry of NOX4 in the rat heart

Representative ventricular sections from control and cholesterol-fed rats immunostained for NOX4 (scale bar represents 100 μm).

In order to analyze the role of microRNAs in the direct myocardial effects of hypercholesterolemia, myocardial microRNAs were isolated from the left ventricles of

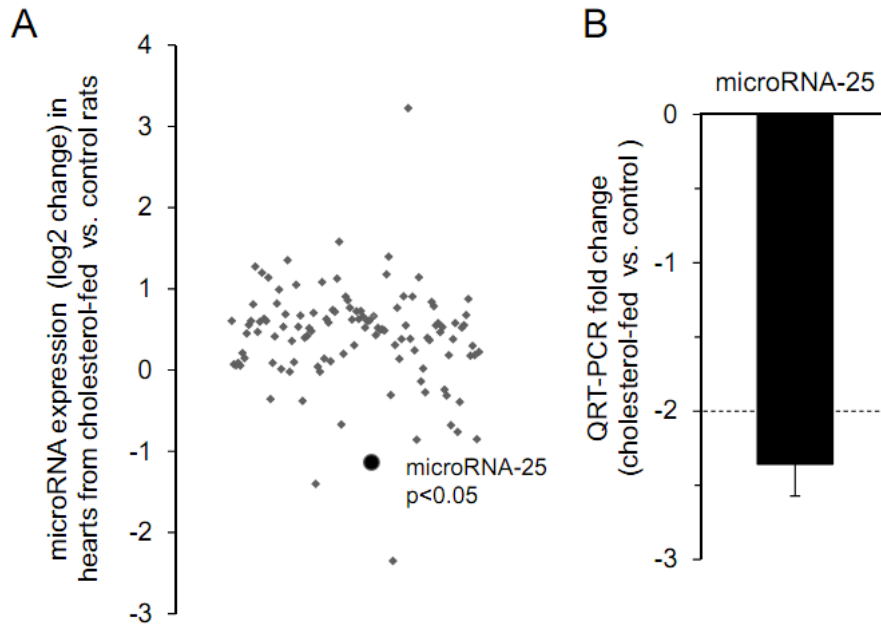


Figure 11. Global cardiac microRNA expression after 12-week cholesterol-enriched diet

Effects of 12-week cholesterol-enriched diet on global cardiac microRNA expression as assessed by microarray analysis (A), each data point represent a log₂ ratio of signal intensity values of a certain microRNA, showing myocardial expression alteration in response to cholesterol-enriched diet. The black circle represents, microRNA-25 showing a pronounced and significant down-regulation in the heart of cholesterol-fed rats. MicroRNA-25 expression was further validated by using QRT-PCR.

cholesterol-fed and control rats and were analyzed on a microRNA microarray. Among the assessed 350 microRNAs 120 showed detectable expression in both groups (Figure 11.A). One of the most pronounced and significant alteration with reasonable inter-sample variation was seen in the case of microRNA-25 (-1.13 log₂ down-regulation). MicroRNA-29c* also showed a significant down-regulation (-2.35 log₂ down-regulation), however, a marked inter-sample variation was seen in the case of this microRNA. The cholesterol-enriched diet-induced down-regulation of microRNA-25 was further confirmed by QRT-PCR (Figure 11.B).

7.5 Potential targets of microRNA-25

To identify putative microRNA-25 targets, we have performed a bioinformatic analysis by searching for potential 3' UTR binding sites in two different databases (Table 3.).

Gene Symbol	Gene Name	Seed Match
NOX4	NADPH oxidase 4	8mer
BGN	biglycan	8mer
SMAD7	SMAD family member 7	7mer
GATA2	GATA binding protein 2	8mer
PRKCE	protein kinase C, epsilon	7mer
AQP2	Aquaporin 2	7mer
COL1A2	collagen, type I, alpha 2	8mer
MEF2D	myocyte-specific enhancer factor 2D	8mer
IDH1	isocitrate dehydrogenase	8mer

Table 3. Predicted microRNA-25 target messenger RNAs selected on their relation to cardiovascular diseases

Several proteins were listed, which were previously shown to be involved in myocardial physiology and/or pathophysiology. Out of these hypothetical targets, NADPH oxidase 4 (NOX4) seemed to be a promising one, as it has 3 conserved and 1 poorly conserved 3' UTR

Conserved sites

position 35-45

```

NOX4 3' UTR 5' CUAAAAAGGGAACAAGUGCAAUU
rno-miR-25 3' AGUCUGGCUCUGGUUCACGUUAC

```

position 1367-1374

```

NOX4 3' UTR 5' CCUCCUACGGGCAACGUGCAAUG
rno-miR-25 3' AGUCUGGCUCUGGUUCACGUUAC

```

position 1508-1514

```

NOX4 3' UTR 5' UGGUCCAAGCUUAAUGGCAAUA
rno-miR-25 3' AGUCUGGCUCUGGUUCACGUUAC

```

Poorly conserved site

position 1419-1424

```

NOX4 3' UTR 5' AAACUACCGACAUCUUUGCAAUAC
rno-miR-25 3' AGUCUGGCUCUGGUUCACGUUAC

```

Figure 12. MicroRNA-25 binding sites in the NOX4 3'UTR

Sequences of microRNA-25 binding sites in NOX4 3' UTR. Complementary nucleotide sequences are indicated by bold letters.

sites (Figure 12.). To exclude the role of other cardiac NOX isoforms, we also screened

microRNA-25 binding sites for NOX1, NOX2, and p22 phox, however, neither of these were predicted to be a potential target of microRNA-25.

7.6 MicroRNA-25 down-regulation results in increased NOX4 expression, thereby causing oxidative/nitrative stress in the hypercholesterolemic heart

Luciferase reporter assay was carried out, in order to prove the direct binding of microRNA-25 to NOX4 3'UTR (Figure 13.). Co-transfection of a mimic of microRNA-25 and

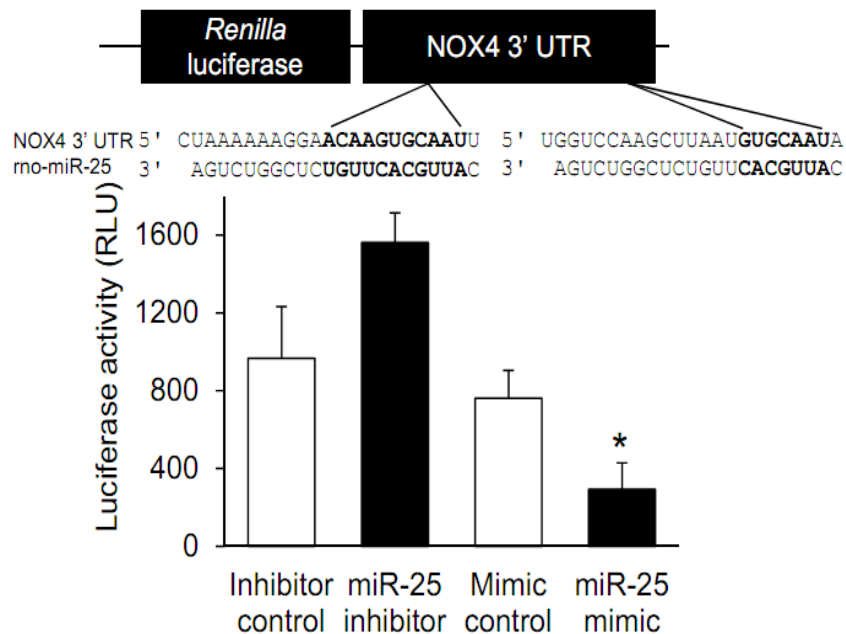


Figure 13. Luciferase reporter assay

*Demonstration of the direct binding of rat microRNA-25 to human NOX4 3'UTR using HEK293 cells. Values are mean±SEM; n=3. *p<0.05 vs. corresponding control.*

the luciferase construct (consisting of the 3'UTR region of the NOX4 mRNA) resulted in a decrease in the luciferase signal, indicating direct binding of microRNA-25 to NOX4 3'UTR. In addition, when the inhibitor of microRNA-25 was co-transfected with the luciferase construct, there was a non-significant increase in the luciferase signal (p=0.062).

To further investigate, whether binding of microRNA-25 to NOX4 3'UTR affects oxidative stress, cardiomyocytes were transfected with a mimic of microRNA-25 resulting in an up-regulation of microRNA-25 (4.14±1.22 log₂ expression alteration). Dihydroethidium staining showed a decrease in superoxide level (Figure 14.), suggesting that the direct binding of microRNA-25 to NOX4 3' UTR likely results in decreased NOX4 activity.

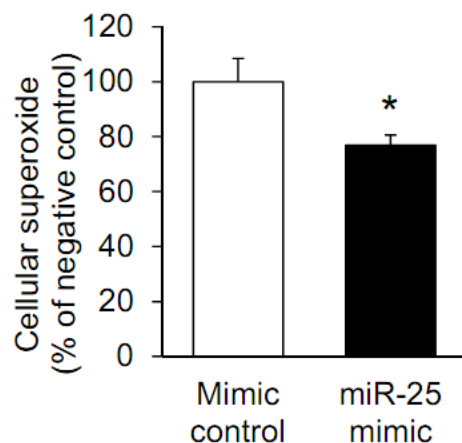


Figure 14. Superoxide level in microRNA-25 mimic transfected cells

*Quantification of cellular oxidative stress by the superoxide-specific dihydroethidium in microRNA-25 mimic transfected primary rat cardiomyocytes. Values are mean±SEM; n=4. *p<0.05 vs. control.*

To prove that the down-regulation of microRNA-25 - as seen in hypercholesterolemic hearts - is responsible for increased oxidative stress by modulation of NOX4, we have transfected neonatal rat cardiomyocytes with a synthetic microRNA-25 inhibitor which induces knock-down of endogenous microRNA-25 level (-6.96 ± 3.07 log₂ expression alteration). As a negative control, a non-targeting microRNA inhibitor control was used. Transfection efficiency was analyzed by transfecting Dy547-labeled positive control microRNA yielding in an efficient transfection (Figure 15.).

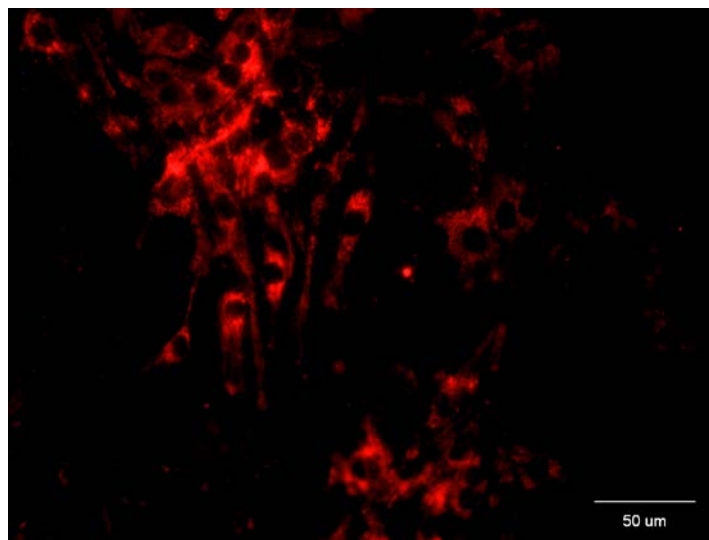


Figure 15. Transfection of the Dy547-conjugated positive control microRNA into cardiomyocytes

We have found that microRNA-25 knock-down significantly increased the fluorescence intensity of the hydrogen peroxide-sensitive dye dichlorofluorescein-diacetate (DCF-DA) (Figure 16. A) in cultured cardiomyocytes. Similarly, the fluorescence signal of the superoxide-specific dihydroethidium (DHE) was also increased significantly in cells transfected with microRNA-25 inhibitor (Figure 16. B). The non-selective NADPH oxidase inhibitor, diphenyleneiodonium (DPI), dose-dependently attenuated the microRNA-25 inhibitor-induced oxidative stress.

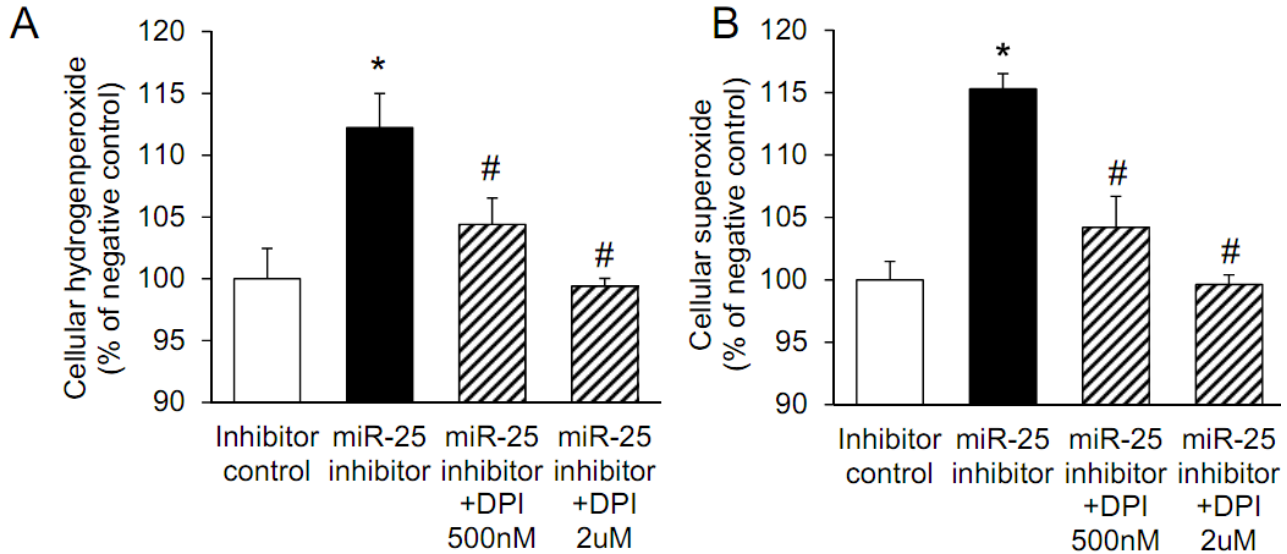


Figure 16. Oxidative stress in microRNA-25-inhibitor transfected cells

*Quantification of cellular oxidative stress by the hydrogen peroxide-sensitive dye dichlorofluorescein-diacetate (DCF-DA) and by the superoxide-specific dihydroethidium (DHE), analyzed by a fluorescent microplate reader. Neonatal cardiac myocytes were treated with a microRNA-25 inhibitor or a non-targeting microRNA inhibitor control in the presence or absence of 500 nM or 2 μ M diphenyleneiodonium (DPI), a non-specific NOX inhibitor. MicroRNA-25 inhibitor significantly increased the amount of ROS level while DPI abolished both hydrogen peroxide (A) and superoxide (B) generation in a dose-dependent manner. Values are mean \pm SEM; n=5-6. * p <0.05 vs. control.*

Transfection of cardiomyocytes with microRNA-25 inhibitor showed an increased fluorescent signal as assessed by DHE histochemistry, whereas, a reduced signal was detected in the microRNA-25 mimic transfected cells, as shown on representative images (Figure 17.).

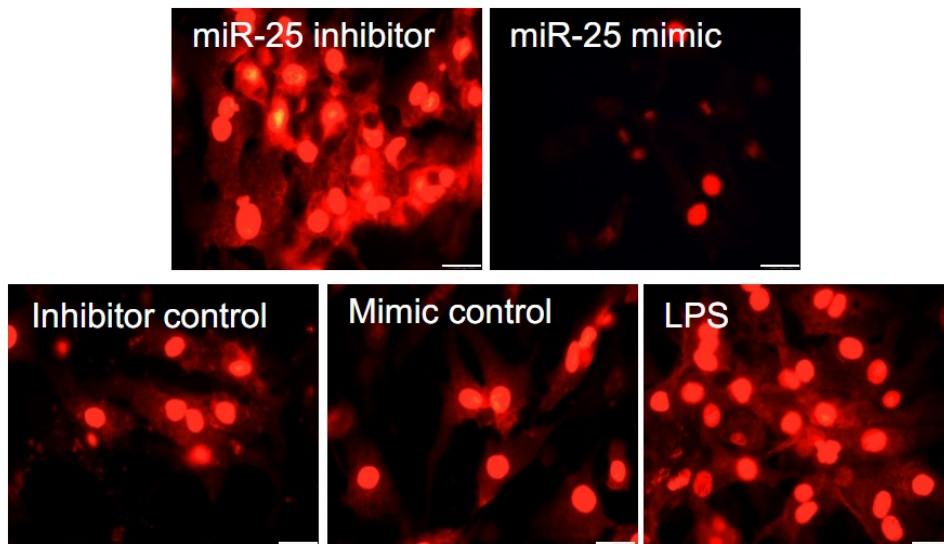


Figure 17. In situ detection of superoxide in transfected cardiomyocytes

Representative microscopic images showing the relative amount of superoxide in primary cardiomyocytes transfected with the inhibitor control, mimic control, and inhibitor control treated with LPS (10 $\mu\text{g}/\text{ml}$) or with microRNA-25 inhibitor, and microRNA-25 mimic. Scale bar represents 20 μm .

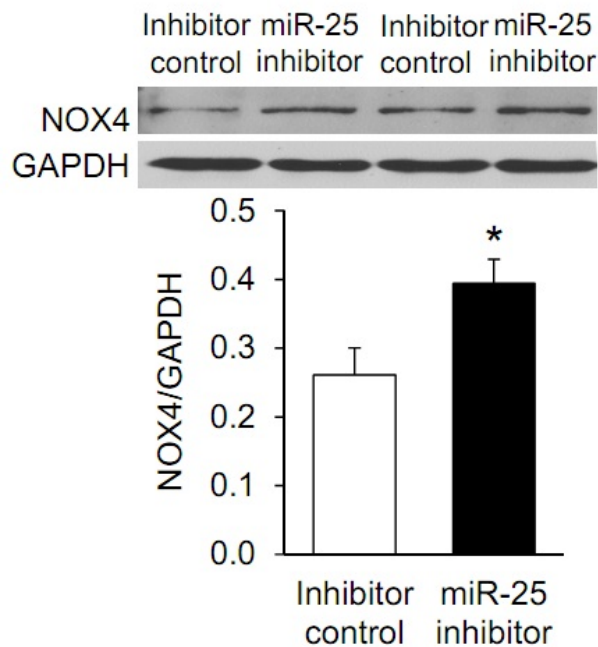


Figure 18. NOX4 protein expression in transfected cardiomyocytes

Regulation of NOX4 protein expression by microRNA-25 in neonatal cardiac myocytes transfected with microRNA-25 inhibitor or microRNA inhibitor control. Representative NOX4 and GAPDH western blots as well as quantified NOX4/GAPDH ratios show increased NOX4 expression in neonatal cardiac myocytes transfected with microRNA-25 inhibitor. Values are mean \pm SEM; $n=5-6$. * $p<0.05$ vs. control.

To confirm that the knock-down of microRNA-25 results in increased oxidative stress as

a result of NOX4 up-regulation, NOX4 protein level was determined in transfected cells. MicroRNA-25 inhibitor significantly increased NOX4 protein level in primary cardiomyocytes (Figure 18.).

7.7 Hypercholesterolemia attenuates the anti-ischemic effect of ischemic preconditioning

To investigate the role of Cx43 in the attenuation of cardioprotection in hypercholesterolemia, we determined infarct size in normal and cholesterol-fed rats subjected to ischemia/reperfusion and preconditioning protocols (Figure 4.). Infarct size was $29 \pm 2\%$ in normal

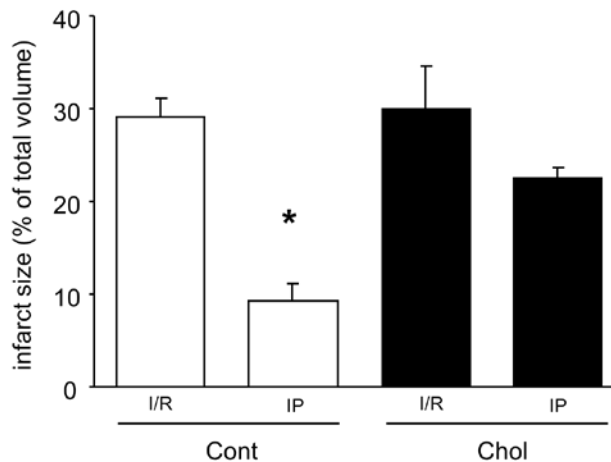


Figure 19. Infarct size in control and cholesterol-fed rats subjected to ischemia/reperfusion and preconditioning

*Ratio of infarcted zone/total left ventricle in normal and cholesterol-fed ischemic/reperfused (I/R) and ischemic preconditioned (IP) rat hearts. Data are mean \pm SEM; * $p < 0.05$ vs ischemia/reperfusion ($n = 5$ each group).*

ischemic/reperfused heart, whereas it was significantly reduced to $9 \pm 2\%$ following ischemic preconditioning. The protective effect of ischemic preconditioning was abolished in cholesterol-fed rats (Figure 3. Protocol B, Figure 4. and Figure 19.).

7.8 Hypercholesterolemia leads to redistribution of sarcolemmal and mitochondrial Cx43

To determine the role of Cx43 in the hypercholesterolemia-induced attenuated cardioprotection, protein expression of Cx43 was determined in whole tissue homogenates from control and cholesterol-fed groups subjected to preconditioning and ischemia/reperfusion perfusion protocols. Total myocardial Cx43 content (sum of Po, P1, P2 signal intensities)

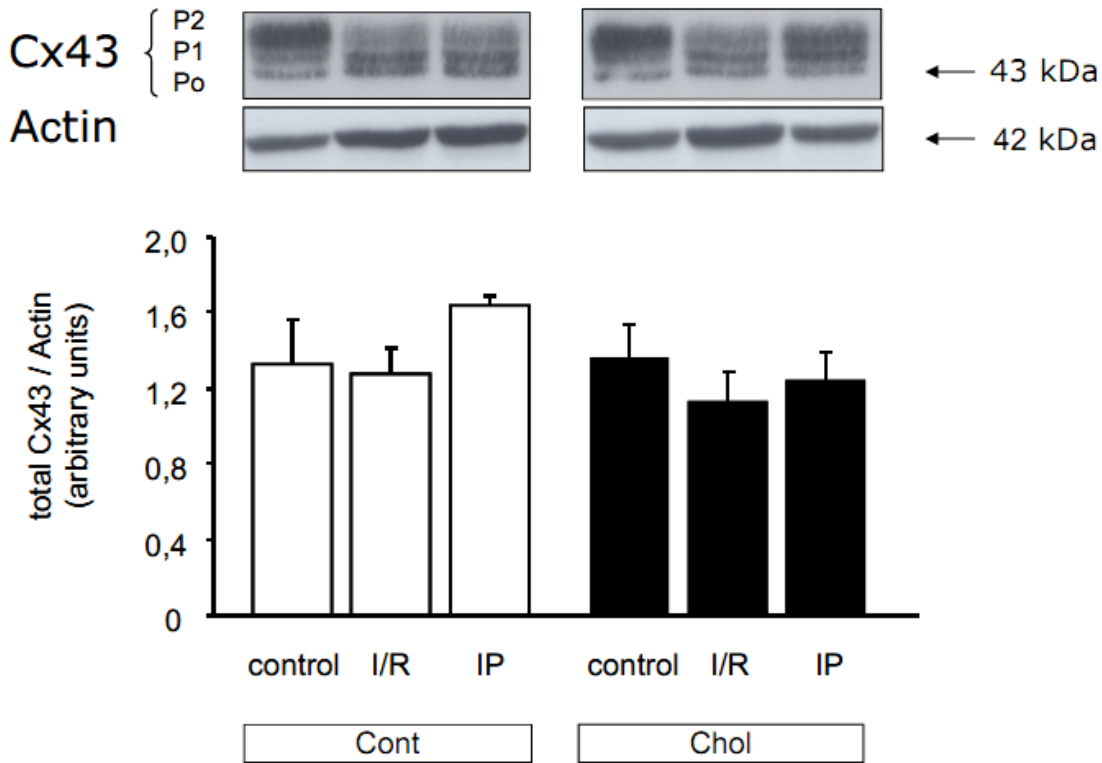


Figure 20. Total Cx43/actin in control, ischemic/reperfused (I/R) and ischemic preconditioned (IP) rat hearts

Western blot analysis of the Cx43 (Po, P1, P2) and actin protein level in hearts of normal(Cont) and cholesterol-fed rats (Chol). Representative images for normal and cholesterol-fed groups were spliced from 2 different regions of the same blot. Bar graphs are representing the total Cx43/actin ratio in all groups. Data are mean \pm SEM ($n=6$ in each group).

remained unchanged following 12-weeks of cholesterol-rich diet, and neither ischemia/reperfusion, nor preconditioning altered total Cx43 level (Western blot, Figure 20.). However, there was an increase in Po with ischemia which was partially reversed by preconditioning in both cholesterol and normal-fed rats.

However, Cx43 localized at the intercalated discs was significantly decreased by hypercholesterolemia (Figure 21.), as revealed by our immunohistochemical analysis.

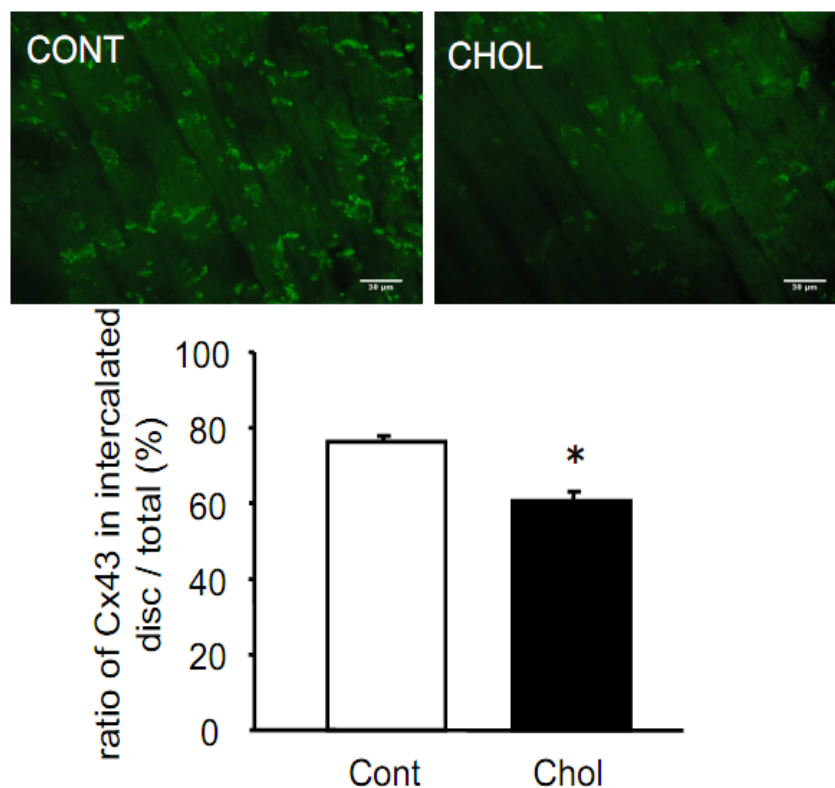


Figure 21. Morphometric analysis of Cx43 in intercalated discs of rat hearts

*Immunofluorescent staining of Cx43 in longitudinal sections of myocardium in normal and cholesterol-fed control hearts. Quantification in a bar diagram shows the ratio of intercalated disc and total Cx43 content in those groups. Data are mean \pm SEM; * $p < 0.05$ (Student's *t*-test, $n=6$ in both groups).*

To further investigate intracellular redistribution of Cx43 due to preconditioning and hypercholesterolemia, Cx43 protein levels were determined in mitochondrial fractions (succinate dehydrogenase-enriched) not contaminated with sarcolemma (no signal for Na/K-ATP-ase, Figure 22. A). Mitochondrial total Cx43 content was decreased approximately by 50% in cholesterol-fed as compared to normal-fed rats (Figure 22. B). At 5 min reperfusion following 30 min global ischemia the total and dephosphorylated mitochondrial Cx43 content was increased which was significantly decreased by ischemic preconditioning in case of both normal and high-cholesterol diet.

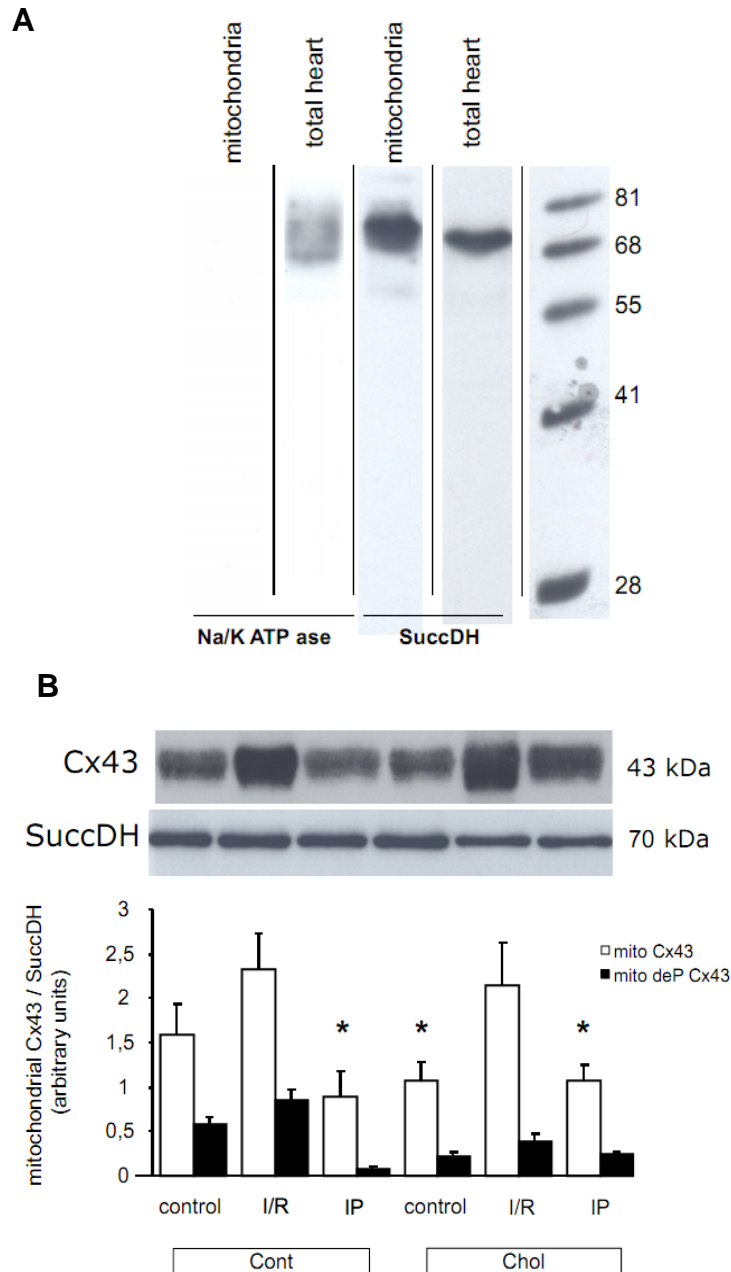


Figure 22. Mitochondrial Cx43 in control, ischemic/reperfused (I/R) and ischemic preconditioned (IP) rat hearts

Western blot analysis of the isolated mitochondria and total heart samples for anti Na/K ATP-ase (specific for plasma membrane) and anti-succinate-dehydrogenase (specific for mitochondria) (A). Cx43 and succinate-dehydrogenase protein level in mitochondria isolated from all groups. Bar graphs are representing the mitochondrial Cx43/Succinate-dehydrogenase level in all groups (B). Data are mean \pm SEM; * $p < 0.05$ vs normal-diet control ($n=6$ in each group).

8. Discussion

8.1 New findings

1. Cardiac microRNA expression is altered in the heart

Here we report for the first time in the literature that diet-induced hypercholesterolemia affects myocardial microRNA expression pattern, suggesting the involvement of microRNAs in the posttranscriptional regulation of cardiac gene expression in hypercholesterolemic rats.

2. MicroRNA-25 regulates NOX4 expression in the heart

We have identified and validated with several experimental approaches that NOX4 is a major microRNA-25 target that is responsible for oxidative/nitrative stress in hearts of hypercholesterolemic rats.

3. Cardiac NOX4 is up-regulated due to hypercholesterolemia

We have shown here for the first time that NOX4 is up-regulated in the heart due to hypercholesterolemia. Our present results show, that the microRNA-25 dependent up-regulation of NOX4 is likely a major contributor of increased oxidative/nitrative stress due to hypercholesterolemia.

4. Cx43 plays a role in the impaired cardioprotective effect of preconditioning in hypercholesterolemia

We demonstrated for the first time the intracellular redistribution of Cx43 in hypercholesterolemia. Here we showed that cholesterol feeding did not affect the total expression of Cx43, while the mitochondrial total and dephosphorylated Cx43 content as well as gap junctional Cx43 were decreased concomitantly with a significant increase in cardiac superoxide levels. This was further associated with the loss of the protective effect of preconditioning in hypercholesterolemia.

8.1 The effect of hypercholesterolemia on myocardial microRNA expression

Here we reported, for the first time in the literature, that myocardial microRNA expression pattern is affected by hypercholesterolemia. However, it is now obvious, that microRNAs are central molecular determinants of cardiovascular physiology and pathology [13], their role in the hypercholesterolemic myocardium has not been investigated yet.

The importance of microRNAs in cardiac pathologies further suggests their promising therapeutic potential [56,57]. Modulation of microRNA expression in vivo with specific synthetic oligonucleotides is a feasible approach, as application of both microRNA inhibitors (antagomiRs) and microRNA mimics offer a potential of therapeutic intervention.

The role of microRNAs in the regulation of cholesterol metabolism has been studied extensively in the hope of identifying new microRNA based therapeutics to treat hypercholesterolemia. Indeed microRNA-33 has been explored as a central regulator of pathways involved in cholesterol synthesis [58], moreover antagomiRs of microRNA-33 has been reported to positively affect cholesterol homeostasis (HDL level, reverse cholesterol transport, cholesterol efflux, macrophage cholesterol content) in mouse [59].

However, the opposite way of regulation, i.e. the regulation of microRNAs by cholesterol itself is not really known. There are only a few reports showing that cholesterol affects microRNA expression, however, these studies were carried out on the liver in cholesterol fed pigs [60] and baboons [61]. Interestingly, a recent report showed an epigenetic regulation of microRNA-29b expression by oxidized-LDL [62], raising a new possible level of cholesterol-dependent gene regulation.

8.2 MicroRNA-25 regulates NOX4 expression in the heart

In our present study, cardiac microRNA-25 showed a pronounced down-regulation due to cholesterol-enriched diet. MicroRNA-25 is encoded in an intronic region of the minichromosome maintenance helixase 7. Interestingly, this region has been previously associated with a serum cholesterol QTL (quantitative trait locus) in rats [63]. To date, mainly cancer related reports were published showing the involvement of microRNA-25 in apoptotic signaling [64] and in cell invasion and migration [65]. Here we used bioinformatic analyses to characterize microRNA-25 mRNA targets (targetome) and a luciferase reporter assay to validate the direct binding of microRNA-25 to the 3'UTR region of the most putative target, NOX4. We have identified and validated NOX4 as a major microRNA-25 target that is responsible for

oxidative/nitrative stress in hearts of hypercholesterolemic rats. However, several additional targets may be involved in the action of microRNA-25, especially in other cardiovascular disease conditions, considering the relevance of the identified hypothetical targets in cardiovascular diseases (Table 2.).

8.3 Cardiac NOX4 is up-regulated due to hypercholesterolemia

One of the most interesting findings in this study was to show that hypercholesterolemia-induced myocardial dysfunction is mediated by a microRNA-dependent regulation of NADPH oxidase activity. The NADPH oxidase 4 isoenzyme (NOX4, first described as Renox [66]) is highly expressed in the heart [67] including cardiomyocytes (Figure 10.) and localized in different intracellular organelles (e.g. mitochondria [67], ER [68], nucleus [69,70]). In addition, its increased expression has been shown to be involved in myocardial dysfunction in heart failure after transverse aortic constriction [71]. Nevertheless, some reports showed opposite results, i.e. NOX4 may be protective against pressure overload-induced heart failure [72]. This discrepancy may be due to the use of different knock-out animal models, allowing the expression of active splice variants [73]. However, there is increasing evidence showing that NOX4 is involved in many pathological cardiac and vascular processes, including diabetic cardiomyopathy [52], TNF alpha-induced endothelial cell apoptosis [51], and stroke associated neurodegeneration by increasing the production of reactive oxygen species [74]. Our present study also suggests that the reactive oxygen species produced by NOX4 may contribute to myocardial dysfunction induced by cholesterol-feeding.

Despite its definite role in the myocardium, the molecular mechanisms, which mediate up-regulation of cardiac NOX4 were not identified so far. It has been previously hypothesized, that increased cellular cholesterol level increases NADPH oxidase activity by acting on membrane microdomain assembly to recruit and organize the cytosolic NADPH oxidase subunits to form the active NADPH oxidase [75]. This can be true especially for the NOX2 isoenzyme, having several cytosolic and membrane-associated subunits. However, in case of NOX4, cytosolic regulatory subunits are not required for its activation [76]. Moreover, the NOX4 mRNA and protein has a very rapid turnover (1-2 h is needed for induction and 4-8 h for degradation) in stark contrast to NOX2 (persists for several days) suggesting that NOX4 is likely regulated at the posttranscriptional level [76]. In a recent report, Fu et al. analyzed the potential role of

microRNAs in the regulation of NOX4 in renal mesangial cells. They found, that at least five different microRNAs (microRNA-363, -92-a, 92-b, -32 and -25) have a predicted binding site to the rat NOX4 3' UTR [77]. This further suggests that microRNA-25 may act as an endogenous regulator of NOX4 by fine-tuning its expression in physiologic and pathologic conditions as well, which was now confirmed in our present study in the hearts of hypercholesterolemic rats as well as in primary cardiomyocyte cultures.

Our present results show, that the microRNA-25 dependent up-regulation of NOX4 is likely a major contributor of increased oxidative/nitrative stress. Oxidative as well as nitrative stress has been shown to play a central role in several cardiovascular diseases, including hyperlipidemia-induced cardiovascular pathologies [78]. Previous studies from our research group showed that diet-induced hyperlipidemia increases cardiac oxidative and nitrative stress and contributes to myocardial dysfunction [21,22]. In addition, recently Canton et al. has reported that oxidation of myocardial contractile proteins (e.g. actin, tropomyosin) in human samples correlate with decreased ejection fraction in heart failure [32]. In line with these reports we have confirmed in our current model that oxidation of myocardial proteins may contribute to hypercholesterolemia-induced cardiac dysfunction. The present study confirms our previous reports, and reveals a previously unknown molecular regulatory pathway (i.e. hypercholesterolemia - microRNA-25 - NOX4 – oxidative stress – oxidized contractile protein - dysfunction axis, see. Figure 23.), providing more insight into the mechanism of hypercholesterolemia-induced myocardial dysfunction.

8.4 Cx43 plays a role in the impaired cardioprotective effect of preconditioning in hypercholesterolemia

8.4.1 Connexin43 re-distribution

In the present study by investigating the role of Cx43 in the impairment of preconditioning in hypercholesterolemia, we have found that, hypercholesterolemia did not alter total myocardial Cx43 protein expression. In contrast, marked hyperlipidemia, which can be induced by 12-weeks cholesterol-enriched diet in rabbits caused down-regulation of total myocardial Cx43 protein and also its redistribution [79]. In the present study, intracellular Cx43 distribution was altered as the gap junctional Cx43 content was decreased in cholesterol-fed rats. Altered Cx43 protein levels, Cx43 phosphorylation and/or Cx43 lateralization were already

detected under a variety of pathophysiological conditions of the heart [80,81]. The mechanism by which hypercholesterolemia may influence Cx43 localization and content is not known in detail. Increased cholesterol level could have an indirect effect on Cx43 expression and Cx43-formed channel activity. In endothelial cells, Cx43 trafficking was altered by oxidative stress [82]. Accordingly, in the present study enhanced superoxide levels were detected in cholesterol-fed rat hearts, offering explanation why Cx43 content was reduced in myocardial intercalated discs and mitochondria of cholesterol-fed rats.

8.4.2 Role of Cx43 in the blunted cardioprotective effect of preconditioning due to hypercholesterolemia

Our hypothesis was based on the observations of our collaborators, i.e. Cx43 is present at the inner membrane of subsarcolemmal mitochondria [48], increasing potassium influx into the mitochondrial matrix [49].

In the present study, mitochondrial Cx43 content in hypercholesterolemic rat hearts was reduced to approximately 50% of the content measured in mitochondria obtained from rats fed a normal diet, and this decrease in mitochondrial Cx43 content was associated with the loss of ischemic preconditioning's cardioprotection. A similar association between a reduced mitochondrial Cx43 content and a loss of infarct size reduction by ischemic preconditioning was seen in aged hearts [83]. Mitochondrial Cx43 content was slightly higher following the prolonged ischemic period in pig myocardium [48], which is in accordance with our present results, showing an increase in mitochondrial Cx43 at 5 min reperfusion following the prolonged ischemic period.

Ischemic preconditioning increased mitochondrial Cx43 content before [50] and at the end of the sustained ischemic period [48]; however, in contrast to the previous studies, ischemic preconditioning reduced mitochondrial Cx43 content at 5 min reperfusion following the prolonged ischemic period in normal and hypercholesterolemic rats. Similarly, ischemic postconditioning limited the migration of phospho-Cx43 to mitochondria following the prolonged ischemic period in isolated rat hearts [84]. Such decrease in mitochondrial Cx43 following ischemia/reperfusion in pre- and postconditioned hearts could contribute to protection, since mitochondrial Cx43 was proposed as regulator of apoptosis in neonatal myocytes after simulated ischemia and reoxygenation [85].

9. Conclusions

Increased oxidative stress plays a central role in the development of cardiac functional disturbances caused by hypercholesterolemia. Our results clearly show that NADPH oxidases (especially NOX4) are major sources of ROS in the hypercholesterolemic myocardium, and that the expression of NOX4 is regulated and fine-tuned by a microRNA-dependent posttranscriptional mechanism. Furthermore we have shown here that intracellular Cx43 redistributions and mitochondrial Cx43 alterations might play a role in the attenuation of the

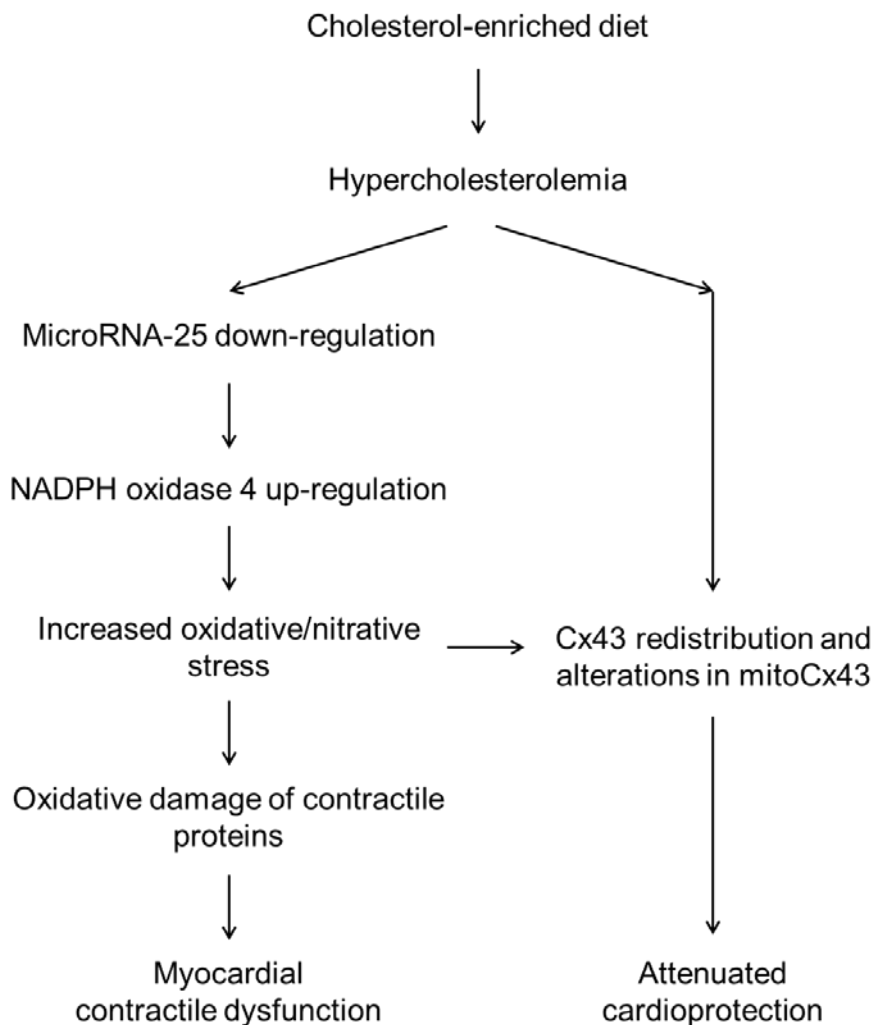


Figure 23. Proposed mechanisms in hypercholesterolemia-induced myocardial dysfunction and attenuated cardioprotection

cardioprotective effect of ischemic preconditioning in hypercholesterolemia (Figure 23.).

These results provided information on the source of oxidative stress (microRNA25-NOX4) and on the mechanisms by which oxidative stress may interfere with cardioprotective interventions (Cx43). We hope that these results enhanced our knowledge on the myocardial effects of hypercholesterolemia and may open new perspectives in the treatment of hypercholesterolemic patients.

10. Acknowledgements

These studies were supported by the following grants: National Development Agency (BAROSS-DA07-DA-TECH-07-2008-0041; MED_FOOD) – New Hungary Development Plan (TÁMOP-4.2.2-08/1/2008-0013, TÁMOP-4.2.1/B-09/1/KONV-2010-0005, TÁMOP-4.2.2/B-10/1-2010-0012, TÁMOP-4.2.2.A-11/1/KONV-2012-0035), Hungarian Scientific Research Fund (OTKA K79167), Hungary-Romania Cross-Border Co-operation Program 2007-2013 (HU-RO-TRANS-MED HURO/0901/137/2.2.2). Z.V.V. was supported by the European Union and the State of Hungary, co-financed by the European Social Fund in the framework of TÁMOP 4.2.4. A/-11-1-2012-0001 ‘National Excellence Program’.

I greatly acknowledge to Prof. László Dux for providing me the possibility to work at the prestigious Department of Biochemistry, and to Prof. Péter Ferdinandy who gave me opportunity to carry on research in the Cardiovascular Research Group and in the Pharmahungary Group. I am also thankful for his constant support and guideline he gave me.

I am indebted to my tutor, Tamás Csont for his scientific guidance, encouragement, patience and helpful suggestions he gave me during my graduate studies and during my PhD years. I am especially grateful to, Anikó Görbe and Krisztina Kupai for their altruistic help in our common work. I am also thankful to the members of our research group: Csaba Csonka, Péter Bencsik, Gergő Szűcs, Gabriella F. Kocsis, Veronika Fekete, Zoltán Giricz, Judit Pipis, János Pálóczi Renáta Gáspár, Márta Sárközy, Krisztina Kiss and all of the members of the Department of Biochemistry for their scientific support, and for the kind atmosphere. I am especially thankful to Szilvia Török, Erzsike Balázsházy, Zsuzsi Lajtos, Zita Felhő Makráné and Judit Kovács for their skillful technical assistance. I have to express my gratitude to my former undergraduate students Tímea Szegi, Tamás Baranyai and Márton Pipicz; their scientific success, enthusiasm and friendly support was always a positive reinforcement during my work. I am grateful to our collaborators: to the members of Functional Genomics Lab of the Biological Research Center (Nóra Faragó, Ágnes Zvara, and Professor László G. Puskás), to Zsolt Rázga and László Tiszlavicz (Department of Pathology, University of Szeged), and to Prof. Rainer Schulz and Kerstin Boengler (Justus Liebig Universität, Giessen, Germany).

Above all, I am greatly thankful for my wife, Ági for her love and belief, for my mother's preserving help and for my whole family's support. I also dedicate this work to my little daughter, Lenke.

11. References

- [1] Roger VL, Go AS, Lloyd-Jones DM, Benjamin EJ, Berry JD, Borden WB et al. Executive summary: heart disease and stroke statistics--2012 update: a report from the American Heart Association. *Circulation* 2012;125:188-97.
- [2] Ray KK, Seshasai SR, Wijesuriya S, Sivakumaran R, Nethercott S, Preiss D et al. Effect of intensive control of glucose on cardiovascular outcomes and death in patients with diabetes mellitus: a meta-analysis of randomised controlled trials. *Lancet* 2009;373:1765-72.
- [3] Glass CK, Witztum JL. Atherosclerosis. the road ahead. *Cell* 2001;104:503-16.
- [4] Wick G, Schett G, Amberger A, Kleindienst R, Xu Q. Is atherosclerosis an immunologically mediated disease? *Immunol Today* 1995;16:27-33.
- [5] Kleemann R, Zadelaar S, Kooistra T. Cytokines and atherosclerosis: a comprehensive review of studies in mice. *Cardiovasc Res* 2008;79:360-76.
- [6] Brown MS, Goldstein JL. A proteolytic pathway that controls the cholesterol content of membranes, cells, and blood *Proc Natl Acad Sci U S A* 1999;96:11041-8.
- [7] Repa JJ, Mangelsdorf DJ. The role of orphan nuclear receptors in the regulation of cholesterol homeostasis *Annu Rev Cell Dev Biol* 2000;16:459-81.
- [8] Shimano H. Sterol regulatory element-binding proteins (SREBPs): transcriptional regulators of lipid synthetic genes. *Prog Lipid Res* 2001;40:439-52.
- [9] Puskas LG, Nagy ZB, Giricz Z, Onody A, Csonka C, Kitajka K et al. Cholesterol diet-induced hyperlipidemia influences gene expression pattern of rat hearts: a DNA microarray study *FEBS Lett* 2004;562:99-104.
- [10] Bartel DP. MicroRNAs: genomics, biogenesis, mechanism, and function *Cell* 2004;116:281-97.
- [11] Doench JG, Sharp PA. Specificity of microRNA target selection in translational repression. *Genes Dev* 2004;18:504-11.
- [12] Stark A, Brennecke J, Bushati N, Russell RB, Cohen SM. Animal MicroRNAs confer robustness to gene expression and have a significant impact on 3'UTR evolution. *Cell* 2005;123:1133-46.
- [13] Thum T, Catalucci D, Bauersachs J. MicroRNAs: novel regulators in cardiac development and disease. *Cardiovasc Res* 2008;79:562-70.

- [14] Droge W. Free radicals in the physiological control of cell function. *Physiol Rev* 2002;82:47-95.
- [15] Griendling KK, Sorescu D, Ushio-Fukai M. NAD(P)H oxidase: role in cardiovascular biology and disease. *Circ Res* 2000;86:494-501.
- [16] Zalba G, San Jose G, Moreno MU, Fortuno MA, Fortuno A, Beaumont FJ et al. Oxidative stress in arterial hypertension: role of NAD(P)H oxidase. *Hypertension* 2001;38:1395-9.
- [17] Ceriello A, Motz E. Is oxidative stress the pathogenic mechanism underlying insulin resistance, diabetes, and cardiovascular disease? The common soil hypothesis revisited. *Arterioscler Thromb Vasc Biol* 2004;24:816-23.
- [18] Heitzer T, Schlinzig T, Krohn K, Meinertz T, Munzel T. Endothelial dysfunction, oxidative stress, and risk of cardiovascular events in patients with coronary artery disease. *Circulation* 2001;104:2673-8.
- [19] Giordano FJ. Oxygen, oxidative stress, hypoxia, and heart failure. *J Clin Invest* 2005;115:500-8.
- [20] Rodriguez-Porcel M, Lerman A, Best PJ, Krier JD, Napoli C, Lerman LO. Hypercholesterolemia impairs myocardial perfusion and permeability: role of oxidative stress and endogenous scavenging activity. *J Am Coll Cardiol* 2001;37:608-15.
- [21] Onody A, Csonka C, Giricz Z, Ferdinandy P. Hyperlipidemia induced by a cholesterol-rich diet leads to enhanced peroxynitrite formation in rat hearts *Cardiovasc Res* 2003;58:663-70.
- [22] Csont T, Bereczki E, Bencsik P, Fodor G, Gorbe A, Zvara A et al. Hypercholesterolemia increases myocardial oxidative and nitrosative stress thereby leading to cardiac dysfunction in apoB-100 transgenic mice *Cardiovasc Res* 2007;76:100-9.
- [23] Dalen H, Thorstensen A, Romundstad PR, Aase SA, Stoylen A, Vatten LJ. Cardiovascular risk factors and systolic and diastolic cardiac function: a tissue Doppler and speckle tracking echocardiographic study. *J Am Soc Echocardiogr* 2011;24:322.
- [24] Horio T, Miyazato J, Kamide K, Takiuchi S, Kawano Y. Influence of low high-density lipoprotein cholesterol on left ventricular hypertrophy and diastolic function in essential hypertension *Am J Hypertens* 2003;16:938-44.
- [25] Huang Y, Walker KE, Hanley F, Narula J, Houser SR, Tulenko TN. Cardiac systolic and diastolic dysfunction after a cholesterol-rich diet *Circulation* 2004;109:97-102.
- [26] Horwich TB, MacLellan WR, Fonarow GC. Statin therapy is associated with improved survival in ischemic and non-ischemic heart failure. *J Am Coll Cardiol* 2004;43:642-8.

- [27] Bastiaanse EM, Atsma DE, Kuijpers MM, Van der Laarse A. The effect of sarcolemmal cholesterol content on intracellular calcium ion concentration in cultured cardiomyocytes. *Arch Biochem Biophys* 1994;313:58-63.
- [28] Ferdinandy P, Szilvassy Z, Horvath LI, Csont T, Csonka C, Nagy E et al. Loss of pacing-induced preconditioning in rat hearts: role of nitric oxide and cholesterol-enriched diet *J Mol Cell Cardiol* 1997;29:3321-33.
- [29] Wang TD, Wu CC, Chen WJ, Lee CM, Chen MF, Liao CS et al. Dyslipidemias have a detrimental effect on left ventricular systolic function in patients with a first acute myocardial infarction *Am J Cardiol* 1998;81:531-7.
- [30] Wang TD, Lee CM, Wu CC, Lee TM, Chen WJ, Chen MF et al. The effects of dyslipidemia on left ventricular systolic function in patients with stable angina pectoris. *Atherosclerosis* 1999;146:117-24.
- [31] Gonzalez-Vilchez F, Ayuela J, Ares M, Pi J, Castillo L, Martin-Duran R. Oxidative stress and fibrosis in incipient myocardial dysfunction in type 2 diabetic patients. *Int J Cardiol* 2005;101:53-8.
- [32] Canton M, Menazza S, Sheeran FL, Polverino de Laureto P, Di Lisa F, Pepe S. Oxidation of myofibrillar proteins in human heart failure *J Am Coll Cardiol* 2011;57:300-9.
- [33] Osipov RM, Bianchi C, Feng J, Clements RT, Liu Y, Robich MP et al. Effect of hypercholesterolemia on myocardial necrosis and apoptosis in the setting of ischemia-reperfusion *Circulation* 2009;120:S22-30.
- [34] Golino P, Maroko PR, Carew TE. The effect of acute hypercholesterolemia on myocardial infarct size and the no-reflow phenomenon during coronary occlusion-reperfusion. *Circulation* 1987;75:292-8.
- [35] Tilton RG, Cole PA, Zions JD, Daugherty A, Larson KB, Sutera SP et al. Increased ischemia-reperfusion injury to the heart associated with short-term, diet-induced hypercholesterolemia in rabbits. *Circ Res* 1987;60:551-9.
- [36] Osborne JA, Lento PH, Siegfried MR, Stahl GL, Fusman B, Lefer AM. Cardiovascular effects of acute hypercholesterolemia in rabbits. Reversal with lovastatin treatment. *J Clin Invest* 1989;83:465-73.
- [37] Maczewski M, Maczewska J, Duda M. Hypercholesterolaemia exacerbates ventricular remodelling after myocardial infarction in the rat: role of angiotensin II type 1 receptors. *Br J Pharmacol* 2008;154:1640-8.
- [38] Pfeffer MA, Braunwald E. Ventricular remodeling after myocardial infarction. Experimental observations and clinical implications. *Circulation* 1990;81:1161-72.

- [39] Murry CE, Jennings RB, Reimer KA. Preconditioning with ischemia: a delay of lethal cell injury in ischemic myocardium. *Circulation* 1986;74:1124-36.
- [40] Ferdinandy P, Schulz R, Baxter GF. Interaction of cardiovascular risk factors with myocardial ischemia/reperfusion injury, preconditioning, and postconditioning *Pharmacol Rev* 2007;59:418-58.
- [41] Zhao ZQ, Corvera JS, Halkos ME, Kerendi F, Wang NP, Guyton RA et al. Inhibition of myocardial injury by ischemic postconditioning during reperfusion: comparison with ischemic preconditioning. *Am J Physiol Heart Circ Physiol* 2003;285:H579-88.
- [42] Kupai K, Csonka C, Fekete V, Odendaal L, van Rooyen J, Marais DW et al. Cholesterol Diet-Induced Hyperlipidemia Impairs the Cardioprotective Effect of Postconditioning: Role of Peroxynitrite. *Am J Physiol Heart Circ Physiol* 2009;297:H1729-35.
- [43] Ungi I, Ungi T, Ruzsa Z, Nagy E, Zimmermann Z, Csont T et al. Hypercholesterolemia attenuates the anti-ischemic effect of preconditioning during coronary angioplasty *Chest* 2005;128:1623-8.
- [44] Garcia-Dorado D, Rodriguez-Sinovas A, Ruiz-Meana M, Inserte J, Agullo L, Cabestrero A. The end-effectors of preconditioning protection against myocardial cell death secondary to ischemia-reperfusion. *Cardiovasc Res* 2006;70:274-85.
- [45] Garcia-Dorado D, Inserte J, Ruiz-Meana M, Gonzalez MA, Solares J, Julia M et al. Gap junction uncoupler heptanol prevents cell-to-cell progression of hypercontracture and limits necrosis during myocardial reperfusion. *Circulation* 1997;96:3579-86.
- [46] Li G, Whittaker P, Yao M, Kloner RA, Przyklenk K. The gap junction uncoupler heptanol abrogates infarct size reduction with preconditioning in mouse hearts. *Cardiovasc Pathol* 2002;11:158-65.
- [47] Schwanke U, Konietzka I, Duschin A, Li X, Schulz R, Heusch G. No ischemic preconditioning in heterozygous connexin43-deficient mice. *Am J Physiol Heart Circ Physiol* 2002;283:H1740-2.
- [48] Boengler K, Stahlhofen S, van de Sand A, Gres P, Ruiz-Meana M, Garcia-Dorado D et al. Presence of connexin 43 in subsarcolemmal, but not in interfibrillar cardiomyocyte mitochondria. *Basic Res Cardiol* 2009;104:141-7.
- [49] Miro-Casas E, Ruiz-Meana M, Agullo E, Stahlhofen S, Rodriguez-Sinovas A, Cabestrero A et al. Connexin43 in cardiomyocyte mitochondria contributes to mitochondrial potassium uptake. *Cardiovasc Res* 2009;83:747-56.
- [50] Rodriguez-Sinovas A, Boengler K, Cabestrero A, Gres P, Morente M, Ruiz-Meana M et al. Translocation of connexin 43 to the inner mitochondrial membrane of cardiomyocytes through

the heat shock protein 90-dependent TOM pathway and its importance for cardioprotection. *Circ Res* 2006;99:93-101.

[51] Basuroy S, Bhattacharya S, Leffler CW, Parfenova H. Nox4 NADPH oxidase mediates oxidative stress and apoptosis caused by TNF-alpha in cerebral vascular endothelial cells *Am J Physiol Cell Physiol* 2009;296:C422-32.

[52] Maalouf RM, Eid AA, Gorin YC, Block K, Escobar GP, Bailey S et al. Nox4-derived reactive oxygen species mediate cardiomyocyte injury in early type 1 diabetes. *Am J Physiol Cell Physiol* 2012;302:C597-604.

[53] Farago N, Zvara A, Varga Z, Ferdinandy P, Puskas LG. Purification of high-quality micro RNA from the heart tissue. *Acta Biol Hung* 2011;62:413-25.

[54] Lewis BP, Burge CB, Bartel DP. Conserved seed pairing, often flanked by adenosines, indicates that thousands of human genes are microRNA targets *Cell* 2005;120:15-20.

[55] Betel D, Koppal A, Agius P, Sander C, Leslie C. Comprehensive modeling of microRNA targets predicts functional non-conserved and non-canonical sites *Genome Biol* 2010;11:R90.

[56] Silvestri P, Di Russo C, Rigattieri S, Fedele S, Todaro D, Ferraiuolo G et al. MicroRNAs and ischemic heart disease: towards a better comprehension of pathogenesis, new diagnostic tools and new therapeutic targets *Recent Pat Cardiovasc Drug Discov* 2009;4:109-18.

[57] van Rooij E, Olson EN. MicroRNAs: powerful new regulators of heart disease and provocative therapeutic targets *J Clin Invest* 2007;117:2369-76.

[58] Rayner KJ, Suarez Y, Davalos A, Parathath S, Fitzgerald ML, Tamehiro N et al. MiR-33 contributes to the regulation of cholesterol homeostasis. *Science* 2010;328:1570-3.

[59] Marquart TJ, Allen RM, Ory DS, Baldan A. miR-33 links SREBP-2 induction to repression of sterol transporters. *Proc Natl Acad Sci U S A* 2010;107:12228-32.

[60] Cirera S, Birck M, Busk PK, Fredholm M. Expression profiles of miRNA-122 and its target CAT1 in minipigs (*Sus scrofa*) fed a high-cholesterol diet *Comp Med* 2010;60:136-41.

[61] Karere GM, Glenn JP, Vandeberg JL, Cox LA. Differential microRNA response to a high-cholesterol, high-fat diet in livers of low and high LDL-C baboons. *BMC Genomics* 2012;13:320.

[62] Chen KC, Liao YC, Hsieh IC, Wang YS, Hu CY, Juo SH. OxLDL causes both epigenetic modification and signaling regulation on the microRNA-29b gene: novel mechanisms for cardiovascular diseases *J Mol Cell Cardiol* 2012;52:587-95.

- [63] Dwinell MR, Worthey EA, Shimoyama M, Bakir-Gungor B, DePons J, Laulederkind S et al. The Rat Genome Database 2009: variation, ontologies and pathways *Nucleic Acids Res* 2009;37:D744-9.
- [64] Razumilava N, Bronk SF, Smoot RL, Fingas CD, Werneburg NW, Roberts LR et al. miR-25 targets TNF-related apoptosis inducing ligand (TRAIL) death receptor-4 and promotes apoptosis resistance in cholangiocarcinoma *Hepatology* 2012;55:465-75.
- [65] Xu X, Chen Z, Zhao X, Wang J, Ding D, Wang Z et al. MicroRNA-25 promotes cell migration and invasion in esophageal squamous cell carcinoma. *Biochem Biophys Res Commun* 2012;421:640-5.
- [66] Geiszt M, Kopp JB, Varnai P, Leto TL. Identification of renox, an NAD(P)H oxidase in kidney *Proc Natl Acad Sci U S A* 2000;97:8010-4.
- [67] Ago T, Kuroda J, Pain J, Fu C, Li H, Sadoshima J. Upregulation of Nox4 by hypertrophic stimuli promotes apoptosis and mitochondrial dysfunction in cardiac myocytes *Circ Res* 2010;106:1253-64.
- [68] Zhang L, Nguyen MV, Lardy B, Jesaitis AJ, Grichine A, Rousset F et al. New insight into the Nox4 subcellular localization in HEK293 cells: first monoclonal antibodies against Nox4 *Biochimie* 2011;93:457-68.
- [69] Anilkumar N, Jose GS, Sawyer I, Santos CX, Sand C, Brewer AC et al. A 28-kDa Splice Variant of NADPH Oxidase-4 Is Nuclear-Localized and Involved in Redox Signaling in Vascular Cells *Arterioscler Thromb Vasc Biol* 2013;33:e104-12.
- [70] Matsushima S, Kuroda J, Ago T, Zhai P, Park JY, Xie LH et al. Increased Oxidative Stress in the Nucleus Caused by Nox4 Mediates Oxidation of HDAC4 and Cardiac Hypertrophy *Circ Res* 2013;112:651-63.
- [71] Kuroda J, Ago T, Matsushima S, Zhai P, Schneider MD, Sadoshima J. NADPH oxidase 4 (Nox4) is a major source of oxidative stress in the failing heart *Proc Natl Acad Sci U S A* 2010;107:15565-70.
- [72] Zhang M, Brewer AC, Schroder K, Santos CX, Grieve DJ, Wang M et al. NADPH oxidase-4 mediates protection against chronic load-induced stress in mouse hearts by enhancing angiogenesis *Proc Natl Acad Sci U S A* 2010;107:18121-6.
- [73] Altenhofer S, Kleikers PW, Radermacher KA, Scheurer P, Rob Hermans JJ, Schiffers P et al. The NOX toolbox: validating the role of NADPH oxidases in physiology and disease *Cell Mol Life Sci* 2012;69:2327-43.
- [74] Kleinschnitz C, Grund H, Wingler K, Armitage ME, Jones E, Mittal M et al. Post-stroke inhibition of induced NADPH oxidase type 4 prevents oxidative stress and neurodegeneration. *PLoS Biol* 2010;8:e1000479.

- [75] Vilhardt F, van Deurs B. The phagocyte NADPH oxidase depends on cholesterol-enriched membrane microdomains for assembly EMBO J 2004;23:739-48.
- [76] Serrander L, Cartier L, Bedard K, Banfi B, Lardy B, Plastre O et al. NOX4 activity is determined by mRNA levels and reveals a unique pattern of ROS generation Biochem J 2007;406:105-14.
- [77] Fu Y, Zhang Y, Wang Z, Wang L, Wei X, Zhang B et al. Regulation of NADPH oxidase activity is associated with miRNA-25-mediated NOX4 expression in experimental diabetic nephropathy Am J Nephrol 2010;32:581-9.
- [78] Dhalla NS, Temsah RM, Netticadan T. Role of oxidative stress in cardiovascular diseases J Hypertens 2000;18:655-73.
- [79] Lin LC, Wu CC, Yeh HI, Lu LS, Liu YB, Lin SF et al. Downregulated myocardial connexin 43 and suppressed contractility in rabbits subjected to a cholesterol-enriched diet. Lab Invest 2005;85:1224-37.
- [80] Peters NS, Green CR, Poole-Wilson PA, Severs NJ. Reduced content of connexin43 gap junctions in ventricular myocardium from hypertrophied and ischemic human hearts Circulation 1993;88:864-75.
- [81] Spragg DD, Leclercq C, Loghmani M, Faris OP, Tunin RS, DiSilvestre D et al. Regional alterations in protein expression in the dyssynchronous failing heart Circulation 2003;108:929-32.
- [82] Li H, Brodsky S, Kumari S, Valiunas V, Brink P, Kaide J et al. Paradoxical overexpression and translocation of connexin43 in homocysteine-treated endothelial cells Am J Physiol Heart Circ Physiol 2002;282:H2124-33.
- [83] Boengler K, Heusch G, Schulz R. Connexin 43 and ischemic preconditioning: effects of age and disease. Exp Gerontol 2006;41:485-8.
- [84] Penna C, Perrelli MG, Raimondo S, Tullio F, Merlino A, Moro F et al. Postconditioning induces an anti-apoptotic effect and preserves mitochondrial integrity in isolated rat hearts. Biochim Biophys Acta 2009;1787:794-801.
- [85] Goubaeva F, Mikami M, Giardina S, Ding B, Abe J, Yang J. Cardiac mitochondrial connexin 43 regulates apoptosis. Biochem Biophys Res Commun 2007;352:97-103.

12. Annex

A HIPERKOLESZTERINÉMIA FUNKCIONÁLIS ÉS MOLEKULÁRIS HATÁSAI A SZÍVRE: A CONNEXIN-43 ÉS A MIKRORNA-25 SZEREPE

Tézis kivonat

Bevezetés

Az emelkedett koleszterinszint a kardiovaszkuláris megbetegedések kiemelt rizikófaktora. Oki szerepe tisztázott az érlemezés patomechanizmusában, azonban az utóbbi évek kutatásai rávilágítottak a magas koleszterinszint direkt szívizomra kifejtett hatásaira is.

A koleszterin maga képes direkt módon a génexpresszió befolyásolásra, mely folyamatban számos molekuláris faktor szerepe feltételezett, azonban részleteiben mindezt tisztázatlan (transzkripciós faktorok, poszttranszkripciós regulátorok, epigenetikus faktorok). A mikroRNA-függő poszttranszkripciós génreguláció egy jelentős mechanizmus a génexpresszió finom szabályozásában. A mikroRNA-ek szekvencia komplementaritás alapján a cél mRNA 3'UTR régiójához kötődnek és annak lebomlását/transzlációs blokkját okozzák. A mikroRNA-ek szerepe kiemelt a szív élettani és patológiai állapotaiban, azonban a hiperkoleszterinémias szívizomban betöltött szerepük még tisztázatlan.

A génexpressziós változások mellett a hiperkoleszterinémia sejt és szövet szintű hatásait részletesebben vizsgálták. Régóta ismert, hogy emelkedett oxidatív stressz jön létre számos sejttípusban magas koleszterinszint hatására, mely hozzájárulhat mind az érlemezés mind pedig a szívizom diszfunkció kialakulásához. A szívizom diszfunkció megnyilvánulása többféle: egyrészt kontraktilitási zavar tapasztalható (diasztolés diszfunkció), másrészt a szív endogén iszkémiás adaptációja (pre- és posztkondicionálás) gyengül/hatástalanná válik hiperkoleszterinémia hatására. Korábban kutatócsoportunk is kimutatta, hogy különféle hiperkoleszterinémias állatmodellekben (koleszterinnel etetett patkány és apoB100 transzgenikus egér) emelkedett oxidatív és nitratív stressz detektálható a szívben. Vizsgálatainkban azt is

kimutattuk, hogy a NADPH oxidáz enzimek emelkedett aktivitása kiemelt szereppel bírhat a hiperkoleszterinémia-indukált oxidatív stressz létrejöttében, továbbá az oxidatív/nitratív stressz farmakológiai mérséklése képes a kontraktilis diszfunkció helyreállítására. Azonban az oxidatív stressz kialakulásának molekuláris mechanizmusa még nem teljesen ismert.

Az endogén iszkémiás adaptációs mechanizmusok gyengülése/hatástalansága hiperkoleszterinémia során egy klinikailag jelentős, a valós klinikai felhasználhatóságot jelentősen limitáló megfigyelés. Azonban pontosan nem ismert, hogy milyen faktorok játszanak szerepet az anti-iszkémiás hatás létrejöttében, vagy éppen a hatás gyengülésében hiperkoleszterinémia során. Feltételezhető, számos mitokondriális faktor szerepe a citoprotektív hatás létrejöttében, mint amilyen a mitokondriális permeabilitási pórus (MPTP) vagy a connexin 43 (Cx43) csatorna. A Cx43 jelenlétét a mitokondriumban Boengler és munkacsoportja írta le, valamint igazolták, hogy prekondicionálás hatására szintje emelkedést mutat, mely oki szereppel bír az anti-iszkémiás hatás létrejöttében. Azonban, hogy ez a folyamat változik-e hiperkoleszterinémiában, még nem ismert.

2. Célkitűzések

Kísérleteink egyik fő célja a hiperkoleszterinémia-indukált oxidatív/nitratív stressz és a következményesen kialakult szívizom diszfunkció mechanizmusának vizsgálata volt.

Vizsgálataink tárgyát képezte a hiperkoleszterinémiás szívizomban:

- MikroRNS expresszió meghatározása.
- MikroRNS-ek szerepének vizsgálata az oxidatív/nitratív stressz létrejöttében.
- Potenciális fehérje célpontok azonosítása és validálása.

Kísérleteink másik fő célja a hiperkoleszterinémia kardioprotektív mechanizmusokra kifejtett hatásának vizsgálata volt. Ismert, hogy a mitokondriális Cx43 kiemelt szereppel bír az iszkémiás prekondicionálás kialakulásában, azonban a hiperkoleszterinémiás szívben szerepe még tisztázatlan. Célunk volt tehát teljes és mitokondriális Cx43 expresszió meghatározása normál és hiperkoleszterinémiás szívben, valamint annak vizsgálata, hogy a Cx43 szerepet játszik-e az iszkémiás prekondicionálás hatáscsökkenésében hiperkoleszterinémia során.

3. Anyagok és Módszerek

Kísérleteinkhez normál vagy koleszterinnel dúsított táppal etetett hím Wistar patkányokat használtunk. Vénás vérvételt követően meghatároztuk a szérum lipid paramétereit. A szívfunkciót ex vivo dolgozó szívperfúzió (Neely szerint) segítségével valamint in vivo nyomástérfigat katéterezéssel határoztuk meg. Külön kísérletekben kamrai szívizom szövetmintákat fagyasztottunk le további molekuláris analízisek elvégzése céljából (mikroRNS mikrocsip és QRT-PCR, NADPH oxidáz izoenzim QRT-PCR és western blot, nitro-tirozin ELISA, friss fagyasztott metszetek, fehérje karboniláció). A mitokondriális Cx43 prekondicionálásban betöltött szerepének vizsgálatára külön kísérletekben szívek Langendorff szerint kerültek perfundálásra. A szíveket prekondicionálási vagy kontroll iszkémia/reperfúziós protokolloknak tettük ki, infarktus méretet határoztunk meg trifenil-tetrazólium-klorid festéssel, valamint külön kísérletekben minták készültek hisztológiai vizsgálatokhoz, mitokondrium izoláláshoz, és western blot kísérletekhez.

MikroRNS célfehérje keresésre online predikciós adatbázisokat használtunk. Sejtkultúra kísérletekben mikroRNS transzfekció segítségével vizsgáltuk a mikroRNS-25-függő NADPH oxidáz 4 regulációt (western blot) valamint a következményes oxidatív stressz létrejöttét (dihidroethidium és DCF festés) fluoreszcens mikroplate leolvasóval valamint fluoreszcens mikroszkóppal. Luciferáz riporter plazmid segítségével a mikroRNS-25-NOX4 direkt kapcsolatot vizsgáltuk. Kontroll kísérletekben vizsgáltuk a transzfekció hatékonyságát (QRT-PCR, fluoreszcens mikroszkóp).

Statisztikai analízisre a SigmaPlot programot használtuk. Egy- és két-utas ANOVA vizsgálatot valamint T-próbát alkalmaztunk, kísérleti csoportjainkhoz igazodóan.

4. Eredmények

4.1 Koleszterin etetés hatására megnő a szérum koleszterin szint

12 hetes diéta hatására a koleszterinnel etetett állatok összkoleszterin szintje megemelkedett, a HDL frakció csökkenést mutatott, azonban a szérum triglicerid szint nem változott.

4.2 A hiperkoleszterinémia hatására enyhe diasztolés diszfunkció jön létre

A balkamrai végdiasztolés nyomás emelkedését tapasztaltuk hiperkoleszterinémia hatására (ex vivo és in vivo kísérletekben is), ami a szív enyhe diasztolés funkciózavarára utal.

4.3 Hiperkoleszterinémia hatására megemelkedik az oxidatív és nitratív stressz a szívizomban

Dihydroethidium hisztokémia segítségével emelkedett szuperoxid termelést detektáltunk a szívizomban. Az oxidatív módon módosult fehérjék (fehérje karboniláció) mennyisége hasonló emelkedést mutatott a diéta hatására, valamint a nitratív stressz marker 3-nitrotirozin szintje is szignifikánsan megemelkedett a diéta során.

A NADPH oxidáz enzimek szerepének vizsgálata során megállapítottuk, hogy transzkript szinten egyik izoenzim (NOX1, 2, és 4) sem mutat szignifikáns változást a szívben. Azonban fehérje szinten a három izoenzim közül a NOX 4 izoenzim szignifikáns expresszió fokozódását detektáltuk western blot segítségével. A NOX 4 immunhisztokémiai vizsgálata során diffúz szívizomsejt specifikus pozitív festődést találtunk mindkét diéta hatására.

4.4 Hiperkoleszterinémia hatására megváltozik a globális mikroRNS expresszió a szívben

A vizsgált 350 mikroRNS-ből, 120 expressziója volt detektálható mintáinkban. A legszembetűnőbb változást a mikroRNS-25 esetében detektáltuk (-1.13 log₂ változás), melyet további QRT-PCR vizsgálattal erősítettünk meg.

4.5 NOX 4, mint mikroRNS-25 célfehérje

On-line predikciós adatbázisok segítségével a NOX4 enzim valószínűsíthető mikroRNS-25 célfehérje (4 kötőhely azonosítható szekvencia komplementaritás alapján).

4.6 A mikroRNS-25 expresszió csökkenés NOX4 expresszió emelkedést és oxidatív stresszt okoz

Luciferáz riportter konstrukt segítségével igazoltuk a mikroRNS-25 kötődését a NOX4 3' UTR régióhoz.

A mikroRNS-25 transzfekció segítségével történő sejtbe juttatása csökkentette a celluláris oxidatív stresszt, míg expressziójának csökkentése antiszensz RNS-sel (mikroRNS-25 inhibitor)

növelte az oxidatív stressz mértékét. Az oxidatív stressz emelkedése felfüggeszthető volt a nem-szelektív NADPH oxidáz inhibitor, difenilén-jodonium (DPI) alkalmazásával. A mikroRNS-25 inhibitorral transzfektált sejtekben a NOX4 expressziója fehérje szinten is megnőtt.

4.7 Hiperkoleszterinémia felfüggeszti a prekondicionálás anti-iszkémiás hatását és a Cx43 intracelluláris redisztribúciójához vezet

Az iszkémiás prekondicionálás infarktus méret csökkentő hatása nem jött létre koleszterinnel etetett állatok szívében. A Cx43 teljes mennyisége nem változott a diéta során, azonban a Cx43 foszforiláció növekedést mutatott iszkémia hatására, míg prekondicionálás hatására ez nem jött létre. A rés kapcsolatokban elhelyezkedő Cx43 mennyisége szignifikánsan csökkent koleszterin etetés hatására, valamint a mitokondriális Cx43 frakció jelentős csökkenése volt detektálható a diéta hatására.

5. Következtetés

5.1 Új eredmények

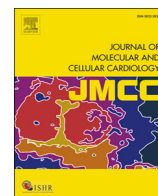
- 1. A szívizom mikroRNS expressziója megváltozik koleszterin-dús diéta hatására*
- 2. A mikroRNS-25 a NOX4 fehérje reguláló faktora a szívben*
- 3. NOX4 expresszió fokozódik hiperkoleszterinémia hatására a szívben*
- 4. Cx43 szerepet játszhat a prekondicionálás anti-iszkémiás hatásának elvesztésében hiperkoleszterinémia során*

Az emelkedett oxidatív/nitratív stressz központi szerepet játszik a hiperkoleszterinémiában észlelhető kardiális funkcionális zavarok létrejöttében. Jelen eredményeink igazolják, hogy a NADPH oxidáz enzimek (főként a NOX 4) az oxigén szabadgyökök fő forrásai a hiperkoleszterinémiás szívben, ezen felül pedig a NOX4 fehérje expresszióját egy mikroRNS-25 függő poszttranszkripcionális mechanizmus befolyásolja. Továbbá igazoltuk, hogy koleszterin-dús diéta hatására a Cx43 intracelluláris átrendeződése és a mitokondriális Cx43 szint változása következik be, ami szerepet játszhat a prekondicionálás hatásának elvesztésében hiperkoleszterinémiában.

Eredményeink hozzájárultak az oxidatív stressz forrásának (mikroRNS-25-NOX4) valamint a károsító hatás egy lehetséges célmechanizmusának (mitokondriális Cx43-prekondicionálás) pontosabb megismeréséhez a hiperkoleszterinémiás szívizomban.

I.

Varga ZV, Kupai K, Szűcs G, Gáspár R, Pálóczi J, Faragó N, Zvara A, Puskás LG, Rázga Z, Tiszlavicz L, Bencsik P, Görbe A, Csonka C, Ferdinandy P, Csont T.: MicroRNA-25-dependent up-regulation of NADPH oxidase 4 (NOX4) mediates hypercholesterolemia-induced oxidative/nitrative stress and subsequent dysfunction in the heart. *J Mol Cell Cardiol.* (2013) 62:111-21. [IF: 5.148]



Original article

MicroRNA-25-dependent up-regulation of NADPH oxidase 4 (NOX4) mediates hypercholesterolemia-induced oxidative/nitrative stress and subsequent dysfunction in the heart



Zoltán V. Varga^{a,b}, Krisztina Kupai^a, Gergő Szűcs^a, Renáta Gáspár^a, János Pálóczi^a, Nóra Faragó^c, Ágnes Zvara^c, László G. Puskás^c, Zsolt Rázga^d, László Tiszlavicz^d, Péter Bencsik^{a,e}, Anikó Görbe^{a,e}, Csaba Csonka^{a,e}, Péter Ferdinandy^{a,b,e}, Tamás Csont^{a,e,*}

^a Cardiovascular Research Group, Department of Biochemistry, University of Szeged, Szeged, Hungary

^b Department of Pharmacology and Pharmacotherapy, Semmelweis University, Budapest, Hungary

^c Institute of Genetics, Biological Research Center, Hungarian Academy of Sciences, Szeged, Hungary

^d Department of Pathology, University of Szeged, Szeged, Hungary

^e Pharmahungary Group, Szeged, Hungary

ARTICLE INFO

Article history:

Received 6 December 2012

Received in revised form 13 May 2013

Accepted 17 May 2013

Available online 27 May 2013

Keywords:

Hyperlipidemia

Peroxyntirite

Superoxide

Metabolic syndrome

Cholesterol

Nitrosative stress

ABSTRACT

Diet-induced hypercholesterolemia leads to oxidative/nitrative stress and subsequent myocardial dysfunction. However, the regulatory role of microRNAs in this phenomenon is unknown. We aimed to investigate, whether hypercholesterolemia-induced myocardial microRNA alterations play a role in the development of oxidative/nitrative stress and in subsequent cardiac dysfunction. Male Wistar rats were fed with 2% cholesterol/0.25% cholate-enriched or standard diet for 12 weeks. Serum and tissue cholesterol levels were significantly elevated by cholesterol-enriched diet. Left ventricular end-diastolic pressure was significantly increased in cholesterol-fed rats both in vivo and in isolated perfused hearts, indicating diastolic dysfunction. Myocardial expression of microRNAs was affected by cholesterol-enriched diet as assessed by microarray analysis. MicroRNA-25 showed a significant down-regulation as detected by microarray analysis and QRT-PCR. In silico target prediction revealed NADPH oxidase 4 (NOX4) as a putative target of microRNA-25. NOX4 protein showed significant up-regulation in the hearts of cholesterol-fed rats, while NOX1 and NOX2 remained unaffected. Cholesterol-feeding significantly increased myocardial oxidative/nitrative stress as assessed by dihydroethidium staining, protein oxidation assay, and nitro-tyrosine ELISA, respectively. Direct binding of microRNA-25 mimic to the 3' UTR region of NOX4 was demonstrated using a luciferase reporter assay. Transfection of a microRNA-25 mimic into primary cardiomyocytes decreased superoxide production, while a microRNA-25 inhibitor resulted in an up-regulation of NOX4 protein and an increase in oxidative stress that was attenuated by the NADPH oxidase inhibitor diphenyleneiodonium. Here we demonstrated for the first time that hypercholesterolemia affects myocardial microRNA expression, and by down-regulating microRNA-25 increases NOX4 expression and consequently oxidative/nitrative stress in the heart. We conclude that hypercholesterolemia-induced microRNA alterations play an important role in the regulation of oxidative/nitrative stress and in consequent myocardial dysfunction.

© 2013 Elsevier Ltd. All rights reserved.

1. Introduction

Incidence of metabolic diseases (including obesity, type II diabetes, high blood pressure, and dyslipidemia) leading to severe cardiovascular complications is constantly growing worldwide. The cost of this both in human lives and in dollars is overwhelming. According to the American Heart Association 2012 Heart Disease and Stroke

Statistics, elevated cholesterol level is still the leading risk factor for heart diseases. Almost 34 million people in the US have elevated total cholesterol level [1]. While metabolic diseases and especially hypercholesterolemia have been studied extensively for many years, the underlying genetic networks and molecular signaling pathways remain to be identified.

It is well known, that hypercholesterolemic patients have a much higher morbidity and mortality from cardiovascular diseases, considering the central role of elevated cholesterol levels in the development of atherosclerosis. However, several studies have shown that hypercholesterolemia exerts direct myocardial effects independent of the development of atherosclerosis both in humans [2–4] and

* Corresponding author at: Cardiovascular Research Group, Department of Biochemistry, University of Szeged, Dóm tér 9, Szeged, H-6720, Hungary. Tel.: +36 62 545 096; fax: +36 62 545 097.

E-mail address: csont.tamas@med.u-szeged.hu (T. Csont).

animal models [5–12]. Hypercholesterolemia negatively influences myocardial performance: impairs systolic as well as diastolic contractile function [5–7], aggravates the deleterious effects of ischemia/reperfusion injury [8], and interferes with the anti-ischemic effect of ischemic pre- [7,9,13] and postconditioning [10]. Moreover, it has been previously shown that hypercholesterolemia-induced myocardial oxidative/nitrative stress significantly contributes to the development of cardiac dysfunction [5,11,12]. However, the exact underlying molecular mechanisms in relation to hypercholesterolemia and oxidative stress are still not entirely clear.

Previous works from our group suggested the central role of NADPH oxidase enzymes in hypercholesterolemia-induced oxidative stress [11] as well as in pro-inflammatory cytokine-induced myocardial dysfunction [14]. Factors (epigenetic, transcriptional, posttranscriptional, and posttranslational) that may regulate NADPH oxidase expression and activity are not entirely known. Recently, microRNAs have emerged as powerful posttranscriptional regulators of gene expression [15]. MicroRNAs are known to play important roles in many physiological and pathological processes in the heart, including myocyte contractility, cardiac development, myocardial infarction, cardiac fibrosis, hypertrophic response, and arrhythmogenesis [16]. However, the role of cardiac microRNAs in metabolic disease states, especially in the myocardium in hypercholesterolemia is not known.

In the present study we aimed to investigate whether microRNAs are altered in the heart of hypercholesterolemic rats. We have demonstrated a decrease in the level of microRNA-25 in the heart of cholesterol-fed rats, and identified microRNA-25 as an important regulator of NADPH oxidase 4 expression and thereby cardiac oxidative/nitrative stress, which is known to be a major contributor of myocardial dysfunction induced by hypercholesterolemia.

2. Materials and methods

This investigation conforms to the Guide for the Care and Use of Laboratory Animals published by the US National Institutes of Health (NIH publication No. 85-23, revised 1996) and was approved by local animal ethics committee of the University of Szeged.

2.1. Experimental setup

Six-week-old male Wistar rats were fed normal or 2% cholesterol- and 0.25% cholate-enriched rat chow for 12 weeks. At the end of the diet period, venous blood was taken for determination of serum lipids. Hearts of anesthetized (sodium pentobarbital; 60 mg/kg i.p.) and heparinized (sodium heparin; 500 U/kg i.v.) rats were then isolated and perfused according to Langendorff with an oxygenated Krebs–Henseleit buffer at 37 °C for 10 min as described [17]. Tissue samples of the ventricular myocardium (n = 10–12 in each group) were rapidly frozen in liquid nitrogen for further biochemical analysis. Some of the hearts were fixed in 4% formaldehyde and were used for histological analysis. In a separate set of experiments, isolated hearts were perfused in a “working” mode according to Neely for 30 min following the 10-min Langendorff perfusion. Hemodynamic parameters including heart rate, coronary flow, aortic flow and ventricular pressure parameters were measured at the end of “working” perfusion, as described earlier [18]. Another set of animals was used for heart catheterization to record ventricular pressure in vivo.

2.2. In vivo heart catheterization

Rats were anesthetized with an intraperitoneal injection of pentobarbital sodium (60 mg/kg) and placed on a heated pad to maintain body temperature. To record left ventricular pressure curve, the right carotid artery was exposed, and a 1.6-Fr pressure catheter (Transonic Scisense Inc., London, ON, Canada) was inserted into the

left ventricle. Left ventricular pressure curves were evaluated using the LabScribe2 software.

2.3. Histology, immunohistochemistry, and transmission electron microscopy

Formaldehyde-fixed myocardial samples were embedded in paraffin, 4- μ m sections were placed on silanized slides and, after conventional methods of dewaxing and rehydration, the samples were either stained with hematoxylin–eosin (to determine the development of hypertrophy and number of infiltrating immune cells), stained for collagen (Masson's trichrome), or were subjected to immunohistochemical analysis for NOX4 protein. Rabbit polyclonal anti-NOX4 antibody (Novus Biologicals, Cambridge, UK) was used as primary antibody (1:100; 30 min). The Envision Flex System (DAKO, Denmark) with high pH was used as visualization system. The sections were counterstained with hematoxylin (for 1 min) and examined by two independent histologists by means of light microscopy at 40 \times magnification.

For transmission electron microscopy, the formalin-fixed, paraffin-embedded specimens were re-embedded to plastic (Embed812, EMS, USA). 70 nm-thick sections were cut and placed on oval slot copper grids, and were analyzed under a transmission electron microscope (Philips CM10, 100 KV).

2.4. Measurement of lipid parameters

At the end of the diet period, serum cholesterol and triacylglycerol levels were determined by colorimetric assays, as described earlier [11] (Diagnosticum, Budapest, Hungary). To analyze α (HDL), pre- β (VLDL), and β -lipoproteins (LDL) in the serum of rats fed cholesterol-enriched or normal diet, lipoproteins were separated on agarose gels, using Paragon Electrophoresis System Lipoprotein Electrophoresis Kit (Beckman Coulter, Fullerton, CA) according to the manufacturer's instructions. To determine the tissue cholesterol content of normal and cholesterol-fed myocardial samples a gas chromatographic–mass spectrometric analysis was carried out according to the method published by Luzon-Toro et al. [19] as previously described [9]. Amount of tissue cholesterol determined in each sample was normalized to tissue wet weight and expressed as μ g/mg tissue.

2.5. MicroRNA isolation

Heart samples (n = 6) from both diet groups were powdered in liquid nitrogen. Steps of microRNA isolation were done according to the protocol of the microRNA isolation kit (Roche, Germany) with modifications [20]. The quality and quantity were assessed spectrophotometrically (Nanodrop, USA) and with 2100 Bioanalyzer (Agilent, CA, USA). Random pairs of the RNA extracted from the 6 different samples in each group were pooled, and the obtained 3 samples/group were assayed on the microarrays.

2.6. Microarray analysis of microRNA expression

A total of 50 ng purified microRNA was labeled using Agilent's microRNA Complete Labeling and Hyb kit system (Agilent Technologies Palo Alto, CA, USA). The protocol was briefly the following: 25–25 ng of two parallel samples were pooled together in a final volume of 2 μ l and subjected to a dephosphorylation reaction using Calf Intestinal Alkaline Phosphatase (CIP) at 37 °C for 30 min in the final volume of 4 μ l. In the second step, 2.8 μ l of DMSO was added to each sample for denaturation at 100 °C for 5 min and placed on ice immediately. Following this step, a ligation reaction was carried out using T4 RNA Ligase and Cyanine3-pCp in a total volume of 11.3 μ l for 2 h at 16 °C to label the RNA samples. The labeled samples were completely vacuum dried on medium–high (45 °C) heat setting and hybridized onto the surface of Agilent 8 \times 15k Rat microRNA

Microarray (Agilent Technologies, Palo Alto, CA, USA). The microarray contained probes for 350 microRNAs from the Sanger database v 10.1. Dried and labeled samples were re-suspended in 18 μ l of nuclease-free water and denatured at 100 °C for 5 min in the presence of 1 \times Blocking Agent and 1 \times Hi-RPM Hybridization Buffer in a final volume of 45 μ l and immediately placed on ice. These mixes were used for the hybridization, which was done in microarray hybridization chambers (Agilent Technologies, Palo Alto, CA), as previously described [21]. After hybridization the slides were washed in Gene Expression Wash buffer 1 containing Triton X-100 from Agilent Technologies at room temperature for 1 min, then in Gene Expression Wash buffer 2 containing Triton X-100 at 37 °C for another 1 min before scanning. Each array was scanned as described earlier with an Agilent Scanner with 5 μ m resolution [21]. Output image analysis and feature extraction were done using Feature Extraction software of Agilent Technologies.

2.7. Validation of microarray data by QRT-PCR

To confirm microarray results, quantitative real-time PCR (QRT-PCR) was used. The reverse transcription reaction was performed with the TaqMan® MicroRNA Reverse Transcription Kit (Applied Biosystems, CA, USA). 350 ng from each sample was reverse transcribed in the presence of 5 \times RT TaqMan® MicroRNA Assays (Applied Biosystems, CA, USA). 8 μ l reaction mixture contained 0.2 μ l dNTPs, 1.5 μ l MultiScribe™ Reverse Transcriptase (50 U/ μ l), 0.8 μ l 10 \times RT Buffer, 0.9 μ l MgCl₂, 0.1 μ l RNase Inhibitor (20 U/ μ l), 1.5 μ l 5 \times RT primer and the template in a total volume of 3 μ l. Reverse Transcription was carried out with the following cycling parameters in a thermocycler (Bioneer, Daedong, Korea): 16 °C for 2 min, 42 °C for 1 min, 50 °C for 1 s, 45 cycles, then hold the samples on 85 °C for 5 min. After dilution with 64 μ l of water, 9 μ l of the diluted reaction mix was used as template in QRT-PCR. Reactions were performed on a RotorGene 3000 instrument (Corbett Research, Sydney, Australia) with the TaqMan protocol. 20 μ l reaction mixture contained 10 μ l TaqMan® Universal PCR Master Mix (Applied Biosystems), 1 μ l of the TaqMan® MicroRNA Assays and 9 μ l of the diluted cDNA.

2.8. MicroRNA target prediction

The microRNA databases and target prediction tools TargetScan (www.targetscan.org) [22] and microRNA.org (www.microrna.org) [23] were used to identify potential microRNA-25 targets.

2.9. Quantitative analysis of NOX mRNAs by QRT-PCR

QRT-PCR was performed on a RotorGene 3000 instrument (Corbett Research, Sydney, Australia) with gene-specific primers and SybrGreen protocol to monitor gene expression. 2 μ g of total RNA was reverse transcribed using the High-Capacity cDNA Archive Kit (Applied Biosystems Foster City, CA, USA) according to the manufacturer's instructions in a final volume of 30 μ l. The temperature profile of the reverse transcription was the following: 10 min at room temperature, 2 h at 37 °C, 5 min on ice and finally 10 min at 75 °C for enzyme inactivation. These steps were carried out in a Thermal Cycler machine (MJ Research Waltham, MA, USA). After dilution with 30 μ l of water, 1 μ l of the diluted reaction mix was used as template in the QRT-PCR. Reactions were done with FastStart SYBR Green Master mix (Roche Applied Science, Mannheim, Germany) according to the manufacturer's instructions at a final primer concentration of 250 nM under the following conditions: 15 min at 95 °C, 45 cycles of 95 °C for 15 s, 60 °C for 25 s and 72 °C for 25 s. The fluorescence intensity of SybrGreen dye was detected after each amplification step. Relative expressions were calculated as normalized ratios to the average Ct value of rat HPRT and Cyclophilin genes. The final relative gene expression ratios were calculated as delta-delta Ct values [21].

2.10. Measurement of NOX proteins by western immunoblotting

In order to investigate whether hypercholesterolemia or microRNA-25 inhibitor transfection leads to an increased expression of NOX4 at the protein level in the heart, western blot analysis was performed. Frozen heart samples were homogenized with NP-40 lysis buffer (150 mM NaCl, 50 mM Tris, 1% NP-40) or cultured cardiomyocytes were harvested by scraping and then homogenized and concentrated by centrifugation (7500 \times g, 20 min). Protein concentrations were determined by means of bicinchoninic acid method using bovine serum albumin as standard (Pierce, Rockford, USA). Forty (heart) or twenty (cells) μ g of protein was loaded from each sample onto 10% SDS-polyacrylamide gel. After separation by electrophoresis, proteins were transferred (wet transfer, 2.5 h) onto the nitrocellulose membrane (Amersham Biosciences, Piscataway, USA). Transfer was controlled by using Ponceau dye. The membrane was blocked with 5% non-fat dry milk in 0.1% TBS-T overnight at 4 °C. After the blocking step, the membrane was cut horizontally and the upper part was incubated with a primary antibody (dissolved in 1% non-fat dry milk-TBS-T, 1:1000 dilution) against either NOX4 (Novus Biologicals, Cambridge, United Kingdom) – reported to specifically recognize NOX4 protein [24–27] –, NOX2 (Merck-Millipore, Darmstadt, Germany), or NOX1 (Novus Biologicals, Cambridge, United Kingdom) for 2 h at room temperature, followed by washing with TBS-T (3 \times 10 min). After washing, the membrane was incubated with a secondary antibody (horseradish peroxidase-conjugated affinity purified goat anti-rabbit, 1/5000 dilution) in 1% non-fat dry milk in TBS-T for 1 h at room temperature. Then the membrane was washed again 3 times for 10 min. For detection of the bands, the membrane was incubated with ECL-plus reagent (Amersham Biosciences, Piscataway, USA) for 5 min and then visualized on X-ray films. Band densities were evaluated by using Quantity One software (Bio-Rad Imaging System, Hercules, USA). Loading control was done by determining the GAPDH content of each sample. Briefly, the bottom of the membrane was probed with a primary antibody that recognizes GAPDH (1/10,000 dilution) for 2 h at room temperature, followed by washing with TBS-T. Then the membrane was incubated with horseradish peroxidase-conjugated affinity purified goat anti-rabbit antibody (1/20,000 dilution) for 1 h at room temperature. The membrane was washed again and band visualization and evaluation of band densities were done as described above. There was no significant difference in GAPDH between the groups.

2.11. In situ detection of superoxide

In situ detection of superoxide was performed by fluorescent microscopy using the oxidative fluorescent dye dihydroethidium (DHE). DHE is freely permeable to cell membranes and reacts with superoxide anions forming a red fluorescent product which intercalates with DNA. Fresh frozen heart sections (30 μ m) were incubated with 10⁻⁶ mol/L DHE (Sigma) in PBS (pH 7.4; 37 °C; 30 min) in a dark humidified container. Fluorescence in heart sections was then detected by a fluorescent microscope (Nikon, Japan) with a 590-nm long-pass filter [11]. Images of sections treated with saline (negative control) were measured first. The fluorescence intensity was evaluated with ImageJ 1.44.

2.12. Measurement of protein carbonylation

Total myocardial protein carbonylation was measured using the Oxyblot protein oxidation detection kit (Merck-Millipore, Billerica, USA) according to the manufacturer's protocol. Briefly, carbonyl groups were derivatized with 2,4-dinitrophenylhydrazine for 15 min. Dinitrophenyl-derivatized proteins were resolved by sodium dodecylsulphate-polyacrylamide gel electrophoresis and transferred to nitrocellulose membrane. Membranes were incubated overnight with anti-dinitrophenyl primary antibodies and then with goat anti-rabbit/

horseradish peroxidase antibodies. Signals were visualized by chemiluminescence detection using X-ray films.

Myocardial nitrotyrosine was measured from cardiac tissue homogenates by ELISA, as described earlier [10].

2.13. Luciferase reporter assay

To investigate whether microRNA-25 directly regulates NOX4 expression, human NOX4 3' UTR sequence was inserted downstream of a Renilla luciferase open reading frame (GoClone System, SwitchGear Genomics, Menlo Park, CA). The luciferase construct was transfected into HEK293 reporter cells together with either a mimic of microRNA-25 or with an inhibitor of microRNA-25 or with a non-targeting sequence (mimic/inhibitor control), respectively, by using the Dharmafect Duo transfection reagent. In each case, 10 ng plasmid DNA and 100 nM microRNA were used. HEK293 cells were chosen for their high efficiency of transfection. Cells were cultured for 24 h and assayed with the Luciferase Assay Reagent of the manufacturer (SwitchGear Genomics, Menlo Park, CA).

2.14. Primary cardiomyocyte culture

To further confirm the direct link between microRNA-25 down-regulation and NOX4 expression followed by increased oxidative stress, neonatal rat cardiomyocyte cultures were prepared from newborn Wistar rats, as described earlier [28]. Cardiomyocytes were plated at a density of 3×10^4 cells/well onto 96-well plates and 5×10^5 cells/well onto 6-well plates. The culture was grown for 3 days before experimentation. Culture medium was changed the day after preparation. The cells were maintained at 37 °C (humidified atmosphere; 5% CO₂) in a standard CO₂ incubator (Sanyo, Japan).

2.15. MicroRNA-25 inhibitor or mimic transfection

To knock-down endogenous expression of microRNA-25, a microRNA-25 inhibitor was used, while to up-regulate microRNA-25, a synthetic microRNA-25 mimic was used (both from Dharmacon, Lafayette, USA). As a negative control, a microRNA inhibitor or mimic control (Dharmacon, Lafayette, USA) was transfected into rat neonatal cardiomyocytes, as recommended by the manufacturer. The transfection was carried out according to the recommendations of the manufacturer. Briefly, the microRNA-25 inhibitor or the inhibitor control was diluted in the medium at a final concentration of 100 nM. To confirm the efficiency of transfection, the same amount of Dy547-labeled positive control (Dharmacon, Lafayette, USA) was transfected in separate experiments. The 100 nM concentration of Dy547-labeled microRNA-inhibitor did not decrease cell viability as compared to 25 and 50 nM, however, it considerably increased efficacy of transfection (data not shown). The morphology and contractile ability of the transfected primary cardiomyocytes were not affected significantly by the transfection process as indicated by spontaneous beating 24 h after transfection (online video supplemental material, showing beating cardiomyocytes transfected with the fluorescent non-targeting negative control microRNA). Cells were incubated with microRNA-25 inhibitor or with the negative control microRNA inhibitor for 24 h and then used for NOX4 western blot analysis or for fluorescent oxidative stress measurement. Expression level of microRNA-25 following microRNA-25 mimic and inhibitor transfection was assessed by QRT-PCR, as described in Section 2.7.

2.16. Measurement of oxidative stress in microRNA-25 inhibitor or mimic transfected cells by fluorescent microplate reader

Transfected neonatal cardiomyocytes were loaded either with 2',7'-dichlorofluorescein-diacetate (DCF-DA) or dihydroethidium

(DHE). Briefly, the cells were washed twice with Dulbecco's PBS (D-PBS) and loaded with DCF-DA (10 μM) or DHE (10 μM) for 30 min in dark at room temperature. After loading the dyes were removed, and the cells were covered with D-PBS and each well was scanned in a fluorescent microplate reader (FluoStar Optima, BMG Labtech, Ortenberg, Germany) using 495 nm excitation/520 nm emission filter combination for DCF-DA, and 505 nm excitation/620 nm emission filter combination for DHE. To test the NADPH oxidase inhibitor diphenyleioidonium (DPI), the cells were pre-incubated with DPI for 4 h, before fluorescent staining.

2.17. Measurement of oxidative stress in microRNA-25 inhibitor or mimic transfected cells by fluorescent microscopy

Neonatal cardiomyocytes were plated on glass coverslips, and transfected with a microRNA-25 mimic or inhibitor, or with their corresponding controls. The transfected cells were loaded with dihydroethidium (DHE), as described above. The coverslips were mounted on glass microscope slides covered with a fluorescent mounting medium (Dako, Glostrup, Denmark), to reduce fading of the fluorescent dye. Fluorescence in the transfected cells was detected by a fluorescent microscope (Nikon, Japan) with a standard rhodamine filter, using the same settings (exposition time, ISO sensitivity, etc) on each sample.

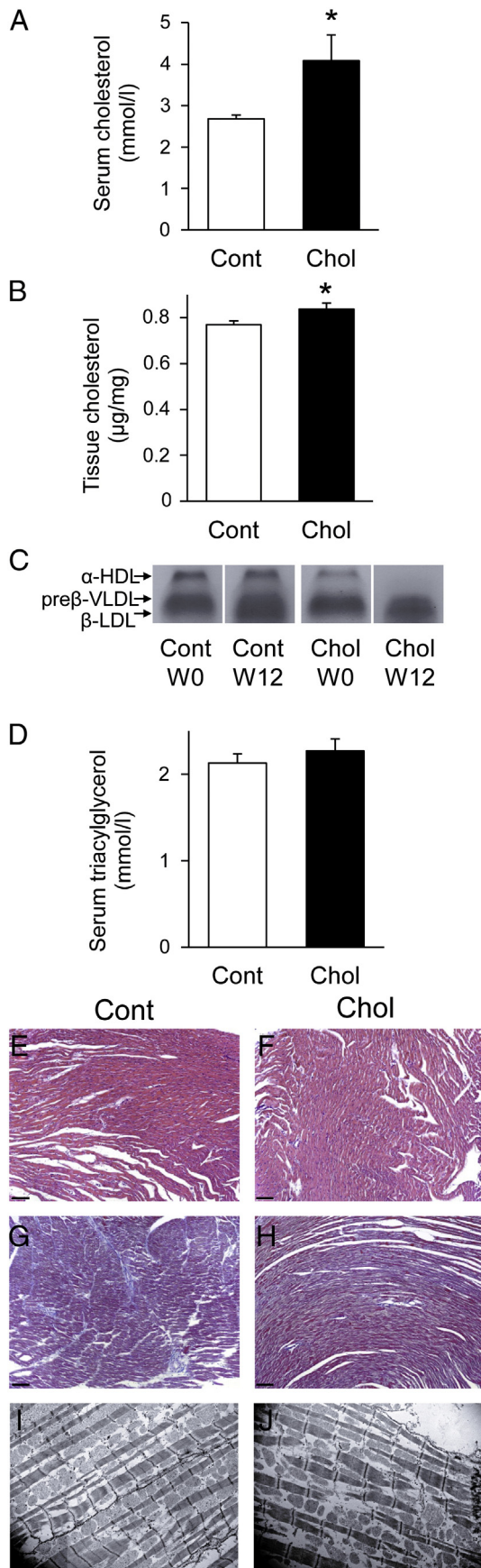
2.18. Statistical analysis

Values are expressed as mean ± SEM. One way analysis of variance (ANOVA) was used to evaluate differences in cell transfection experiments to determine differences in oxidative stress. Otherwise Student's T-test was used. Statistical analysis of microRNA microarrays was done as described earlier by using the Feature Extraction software of Agilent Technologies [29]. All the individual microRNAs were represented by 20 different probes on the array. A microRNA was considered as detected, if at least one probe from all the 20 probes was detected. Total gene signal is equal to the sum of the signals of the individual probes. Expressions of all the 350 microRNAs found in the Sanger miRBase (version 10.1) were checked. Six heart samples from each diet groups were analyzed by microRNA microarray. Two-two samples were pooled together and a total of 6 hybridization experiments were carried out to gain raw data for statistical analysis. Altogether 9 individual parallel gene activity comparisons were done to determine the average changes, standard deviations and p-values. Using two tailed two sample unequal variance Student t-test, the p-value was determined and used to find the significant gene expression changes. Gene expression ratio with p-value <0.05 and log₂ ratio <−0.6 or log₂ ratio >0.6 (~1.5 fold change) are considered as repression and overexpression, respectively. Changes in gene expression were plotted as log₂ ratios of signal intensity values. MicroRNAs having less than 4 individual parallel gene activity comparisons were excluded.

3. Results

3.1. Cholesterol-fed rats display elevated serum and tissue cholesterol levels

Cholesterol-enriched diet for 12 weeks caused a significant increase in cholesterol level in the serum (Fig. 1A) as well as in the myocardial tissue (Fig. 1B) which was accompanied by an altered lipoprotein pattern (Fig. 1C). The 12 week long diet induced a decrease in HDL-fraction. Cholesterol-enriched diet had no influence on serum triacylglycerol level (Fig. 1D).



3.2. Cholesterol-feeding leads to mild myocardial dysfunction without signs of histological alterations

Parameters of myocardial function measured both in vivo and in isolated perfused hearts are shown in Table 1. Left ventricular end-diastolic pressure (LVEDP) showed a significant increase in the cholesterol-fed group as assessed both in vivo and ex vivo, indicating impaired relaxation and diastolic dysfunction. In addition, there was a non-significant ($p = 0.096$) decrease in $+dP/dt_{max}$ in the ex vivo perfused hearts of cholesterol-fed rats. Other examined parameters (heart weight, heart weight/body weight ratio, coronary flow, cardiac output, left ventricular developed pressure, $-dP/dt_{max}$) did not change significantly due to the diet.

Cholesterol feeding had no apparent effect on myocardial histology (hematoxylin/eosin – Figs. 1E–F, Masson's trichrome – Figs. 1G–H) and subcellular ultrastructure (transmission electron microscopy – Figs. 1I–J).

3.3. MicroRNA-25 is down-regulated in hypercholesterolemic hearts

Myocardial microRNAs were isolated from the left ventricles of cholesterol-fed and control rats and were analyzed on a microRNA microarray. Among the assessed 350 microRNAs 120 showed detectable expression in both groups (Fig. 2A). One of the most pronounced and significant alteration with reasonable inter-sample variation was seen in the case of microRNA-25 ($-1.13 \log_2$ down-regulation). MicroRNA-29c* also showed a significant down-regulation ($-2.35 \log_2$ down-regulation), however, a marked inter-sample variation was seen in the case of this microRNA. The cholesterol-enriched diet-induced down-regulation of microRNA-25 was further confirmed by QRT-PCR (Fig. 2B).

3.4. In silico microRNA-25 target prediction reveals NOX4 as a putative target

To identify putative microRNA-25 targets, we have performed a bioinformatic analysis by searching for potential 3' UTR binding sites in two different databases (Table 2.). Several proteins were listed, which were previously shown to be involved in myocardial physiology and/or pathophysiology. Out of these hypothetical targets, NADPH oxidase 4 (NOX4) seemed to be a promising one, as it has 3 conserved and 1 poorly conserved 3' UTR sites (Fig. 2C). As we have previously proposed in our studies that NADPH oxidases might be involved in hypercholesterolemia-induced oxidative stress [11], in the present study we have examined, whether hypercholesterolemia leads to microRNA-25-dependent modulation of NOX4 expression. To exclude the role of other cardiac NOX isoforms, we also screened microRNA-25 binding sites for NOX1, NOX2, and p22 phox, however, neither of these were predicted to be a potential target of microRNA-25.

3.5. NOX4 is expressed in the heart and is up-regulated by cholesterol-enriched diet

To examine the presence of NOX4 in the heart of cholesterol-fed rats, the expression level of NOX4 protein was determined by western blot. Our analysis revealed the up-regulation of NOX4 after 12 weeks of cholesterol-enriched diet, suggesting its role in

Fig. 1. Effect of 12-week cholesterol-enriched diet on serum cholesterol (A), heart total tissue cholesterol (B), serum lipoprotein distribution (C), serum triacylglycerol (D), and microscopic morphology (representative images E–J). The cholesterol-fed group (Chol) displayed a decrease in HDL concentration as compared to the standard chow-fed group (Cont). There was no sign of any histological alteration as assessed by standard HE (E and F) and Masson's trichrome staining (G and H). Scale bar represents 100 µm. There was no sign of any subcellular ultrastructural alterations (sarcomere or mitochondrial disorganization) as assessed by transmission electron microscopy (magnification 25,000×, I and J). Results are expressed as mean \pm SEM; $n = 8-10$. * $p < 0.05$ vs. control.

Table 1
Hemodynamic parameters at the end of 12-week diet.

	Control	Cholesterol-fed
HW (mg)	1753 ± 52	1687 ± 25
HW/BW (%)	3.29 ± 0.08	3.32 ± 0.07
Ex vivo parameters:		
CF (ml/min)	34.4 ± 2.4	34.5 ± 3.1
CO (ml/min)	93.7 ± 5.6	93.2 ± 5.1
LVDP (kPa)	19.9 ± 1.25	19.6 ± 1.18
LVEDP (kPa)	1.41 ± 0.30	2.41 ± 0.35*
+dP/dt _{max} (kPa/s)	742.6 ± 43.6	624.6 ± 50.4
−dP/dt _{max} (kPa/s)	437.6 ± 12.4	417.2 ± 14.3
In vivo parameters:		
LVDP (mm Hg)	104.6 ± 8.0	104.1 ± 8.0
LVEDP (mm Hg)	2.93 ± 0.20	3.50 ± 0.14*
+dP/dt _{max} (mm Hg/s)	7958 ± 615	8233 ± 648
−dP/dt _{max} (mm Hg/s)	7740 ± 632	8712 ± 726

Data are presented as means ± SEM, *p < 0.05 vs. control, n = 8.

HW: heart weight; HW/BW: heart weight/body weight ratio; CF: coronary flow; CO: cardiac output; LVDP: left ventricular developed pressure; LVEDP: left ventricular end-diastolic pressure; +dP/dt_{max}: maximal rate of ventricular pressure rise; −dP/dt_{max}: maximal rate of ventricular pressure decline.

hypercholesterolemia-induced oxidative stress (Figs. 3A and D). To determine whether hypercholesterolemia induces expression alteration in other abundant cardiac NOX isoform, we also examined the expression of NOX1 and NOX2, however, there were no alterations in the protein level of cardiac NOX1 or NOX2 due to cholesterol-enriched diet (Figs. 3A, B, and C).

Immunostaining for NOX4 showed a diffuse positive staining in cardiomyocytes in both diet groups (Figs. 3E and F).

QRT-PCR analysis of myocardial samples obtained from cholesterol-fed and control animals showed no alterations in transcript levels of any of the NOX isoforms (NOX1, 2, and 4; Table 3.), suggesting that the up-regulation of NOX4 protein due to cholesterol-enriched diet may occur due to posttranscriptional gene regulation.

3.6. Increased myocardial oxidative and nitrative stress in cholesterol-fed rats

Myocardial oxidative stress was estimated by staining frozen myocardial sections with dihydroethidium. Increased nuclear red fluorescence was detectable in the hearts of cholesterol-fed rats as compared to control rats, indicating enhanced superoxide formation (Figs. 3G, H, and I).

The amount of oxidatively modified myocardial proteins was elevated in the cholesterol-fed group as assessed by dinitrophenylhydrazine assay (Oxyblot; Fig. 3J). The intensity of the band with a molecular weight corresponding to actin (42 kDa) was significantly increased (Figs. 3J and K), suggesting that oxidation of contractile proteins is likely involved in hypercholesterolemia-induced myocardial dysfunction.

The nitrative stress marker nitrotyrosine was also elevated in the heart due to cholesterol-enriched diet (Fig. 3L).

3.7. NOX4 is a direct target of microRNA-25

Luciferase reporter assay was carried out, in order to prove the direct binding of microRNA-25 to NOX4 3' UTR (Fig. 4A). Co-transfection of a mimic of microRNA-25 and the luciferase construct (consisting of the 3' UTR region of the NOX4 mRNA) resulted in a decrease in the luciferase signal, indicating a direct binding of microRNA-25 to NOX4 3' UTR. In addition, when the inhibitor of microRNA-25 was co-transfected with the luciferase construct, there was a non-significant increase in the luciferase signal (p = 0.062).

To further investigate, whether binding of microRNA-25 to NOX4 3' UTR affects oxidative stress, cardiomyocytes were transfected with a

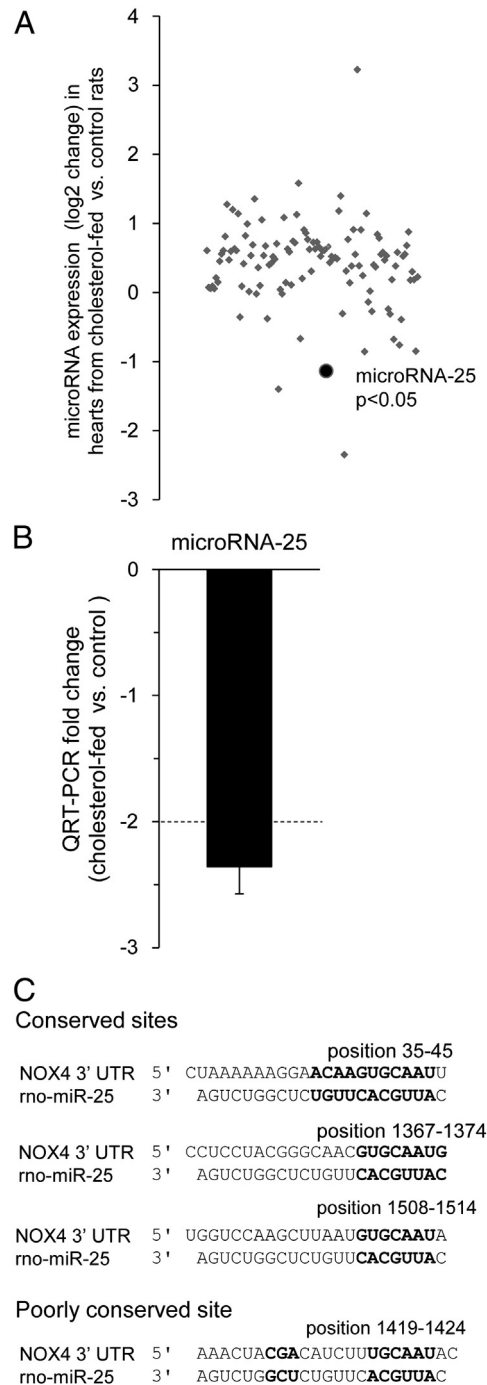


Fig. 2. Effects of 12-week cholesterol-enriched diet on global cardiac microRNA expression as assessed by microarray analysis (A), each data point represents a log₂ ratio of signal intensity values of a certain microRNA, showing myocardial expression alteration in response to cholesterol-enriched diet. The black circle represents, microRNA-25 showing a pronounced and significant down-regulation in the heart of cholesterol-fed rats. MicroRNA-25 expression was further validated by using QRT-PCR (B), results are expressed as mean ± SEM. Sequences of microRNA-25 binding sites in NOX4 3' UTR (C). Complementary nucleotide sequences are indicated by bold letters.

mimic of microRNA-25 resulting in an up-regulation of microRNA-25 (4.14 ± 1.22 log₂ expression alteration). Dihydroethidium staining showed a decrease in superoxide level (Fig. 4B), suggesting that the direct binding of microRNA-25 to NOX4 3' UTR likely results in decreased NOX4 activity.

Table 2
Predicted microRNA-25 target messenger RNAs selected on their relation to cardiovascular diseases.

Gene symbol	Gene name	Reference	Predicted target (TargetScan)	Predicted target (microRNA.org)	Seed match (TargetScan)
NOX4	NADPH oxidase 4	[43]	Yes	Yes	8mer
BGN	Biglycan	[28]	Yes	Yes	8mer
SMAD7	SMAD family member 7	[52]	Yes	Yes	7mer
GATA2	GATA binding protein 2	[53]	Yes	Yes	8mer
PRKCE	Protein kinase C, epsilon	[54]	Yes	No	7mer
AQP2	Aquaporin 2	[55]	Yes	Yes	7mer
COL1A2	Collagen, type I, alpha 2	[56]	Yes	Yes	8mer
MEF2D	Myocyte-specific enhancer factor 2D	[57]	Yes	No	8mer
IDH1	Isocitrate dehydrogenase	[58]	Yes	No	8mer

The microRNA target prediction tools microRNA.org (<http://www.microRNA.org>) and TargetScan (<http://www.targetscan.org>) were used to identify potential microRNA-25 targets.

3.8. Effects of microRNA-25 inhibitor on oxidative stress and NOX4 expression

To further investigate if the down-regulation of microRNA-25 – as seen in hypercholesterolemic hearts – is responsible for increased oxidative stress by modulation of NOX4, we have transfected neonatal rat cardiomyocytes with a synthetic microRNA-25 inhibitor which induces knock-down of endogenous microRNA-25 level (-6.96 ± 3.07 log₂ expression alteration). As a negative control, a non-targeting microRNA inhibitor control was used. Transfection efficiency was analyzed by transfecting Dy547-labeled positive control microRNA yielding in an efficient transfection (data not shown).

We have found that microRNA-25 knock-down significantly increased the fluorescence intensity of the hydrogen peroxide-sensitive dye dichlorofluorescein-diacetate (DCF-DA) (Fig. 4C) in cultured cardiomyocytes. Similarly, the fluorescence signal of the superoxide-specific dihydroethidium (DHE) was also increased significantly in cells transfected with microRNA-25 inhibitor (Fig. 4D). The non-selective NADPH oxidase inhibitor, diphenileniodonium (DPI), dose-dependently attenuated the microRNA-25 inhibitor-induced oxidative stress (Figs. 4C and D).

Transfection of cardiomyocytes with microRNA-25 inhibitor showed an increased fluorescent signal as assessed by DHE histochemistry, whereas, a reduced signal was detected in the microRNA-25 mimic transfected cells, as shown on representative images (Fig. 4E).

To confirm that the knock-down of microRNA-25 results in increased oxidative stress as a result of NOX4 up-regulation, NOX4 protein level was determined in transfected cells. MicroRNA-25 inhibitor significantly increased NOX4 protein level in primary cardiomyocytes (Fig. 4F).

4. Discussion

In the present study we have confirmed that hypercholesterolemia leads to cardiac oxidative/nitrative stress and myocardial dysfunction. We have demonstrated for the first time in the literature that hypercholesterolemia affects myocardial microRNA expression, moreover, hypercholesterolemia by down-regulating microRNA-25 increases NOX4 expression and consequently oxidative/nitrative stress in the heart, thereby leading to diastolic dysfunction (Fig. 5). Our present results show that microRNA-25 is an important regulator of cardiac NADPH oxidase 4 and thereby myocardial oxidative/nitrative stress.

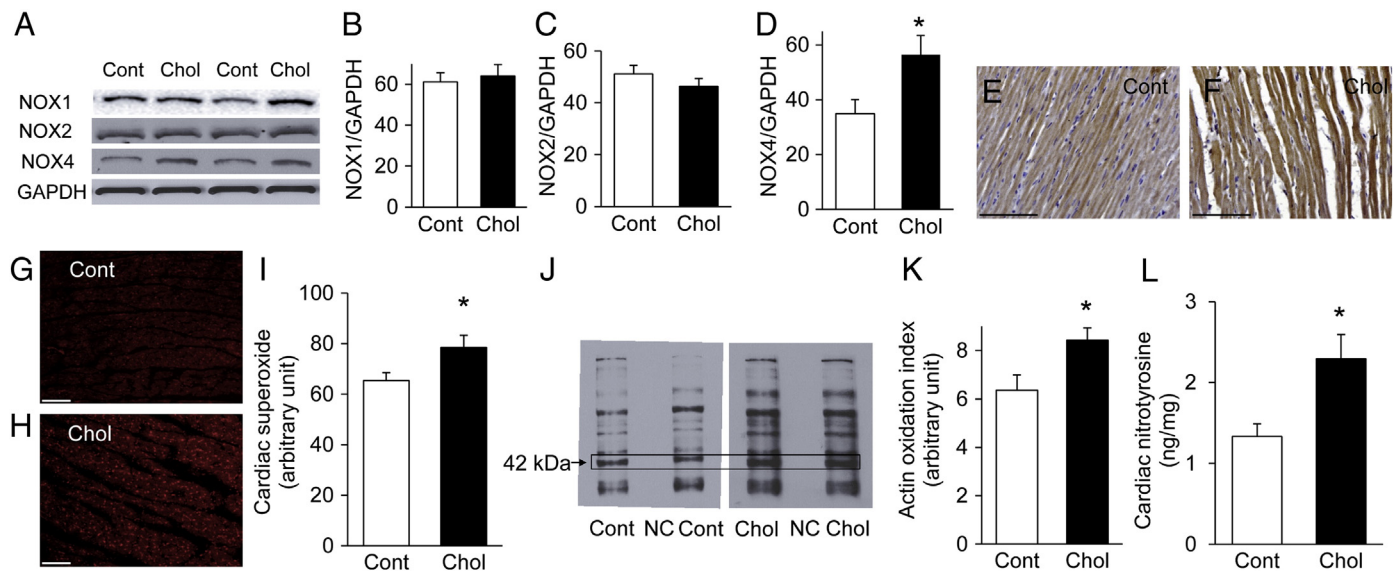


Fig. 3. Representative western blots of NOX1, NOX2, NOX4, and GAPDH from cardiac homogenates from cholesterol-fed (Chol) and control (Cont) animals (A). Quantification of western blot analysis of NOX1 (B), NOX2 (C), and NOX4 (D) proteins in hearts of normal and cholesterol-fed rats normalized to the GAPDH control. Data are mean \pm SEM; $n = 8-10$ in each group. * $p < 0.05$ vs. control rats. Representative ventricular sections from control (G) and cholesterol-fed rats (H) immunostained for NOX4 (scale bar represents 100 μ m). Representative ventricular sections from control (E) and cholesterol-fed rats (F) immunostained for NOX4 (scale bar represents 100 μ m). Representative images show the localization and intensity (red fluorescence) of superoxide in the nucleus (scale bar represents 100 μ m). Bar chart (I) shows quantification of dihydroethidium fluorescence of hearts from control and cholesterol-fed rats, representing myocardial oxidative stress. Values are mean \pm SEM; $n = 10$ in each group. * $p < 0.05$ vs. control group. Representative western blot of carbonylated myocardial proteins (J) from cardiac homogenates from cholesterol-fed (Chol) and control (Cont) animals (NC represents negative control lane). The 42 kDa band corresponds to actin. Quantification of the intensity of the carbonylated 42 kDa bands (K) from cholesterol-fed (Chol) and control (Cont) animals. Values are mean \pm SEM; $n = 5$ in each group. * $p < 0.05$ vs. control group. Quantification of cardiac 3-nitrotyrosine content, a marker of endogenous peroxynitrite-induced nitrative stress (L). Free 3-nitrotyrosine was assayed by enzyme-linked immunosorbent assay (ELISA). Values are mean \pm SEM; $n = 10-12$. * $p < 0.05$ vs. control. (For interpretation of the references to color in this figure legend, the reader is referred to the web version of this article.)

Table 3
QRT-PCR analysis of NOX isoenzyme (NOX1, NOX2, and NOX4) transcript levels.

Gene	Accession number	Forward primer	Reverse primer	Log2 change	SEM	Fold change
NOX1	NM_053683	ggcatccctttactctgacct	tgctgctcgaatatgaatgg	-0.25	0.33	-1.19
NOX2	NM_023965	gctgggattggagtcacg	gcacagccagtagaagtagatcttt	-0.001	0.24	-1.001
NOX4	NM_053524	gaaccaagtccaagctca	gcacaaaggtccagaatcc	-0.123	0.16	-1.09

Here we report for the first time in the literature that diet-induced hypercholesterolemia affects myocardial microRNA expression pattern, indicating a possible role of these posttranscriptional regulators

in the hearts of hypercholesterolemic rats. Cholesterol-induced gene regulation is still an enigmatic research area. Cholesterol may regulate gene expression at both transcriptional and posttranscriptional

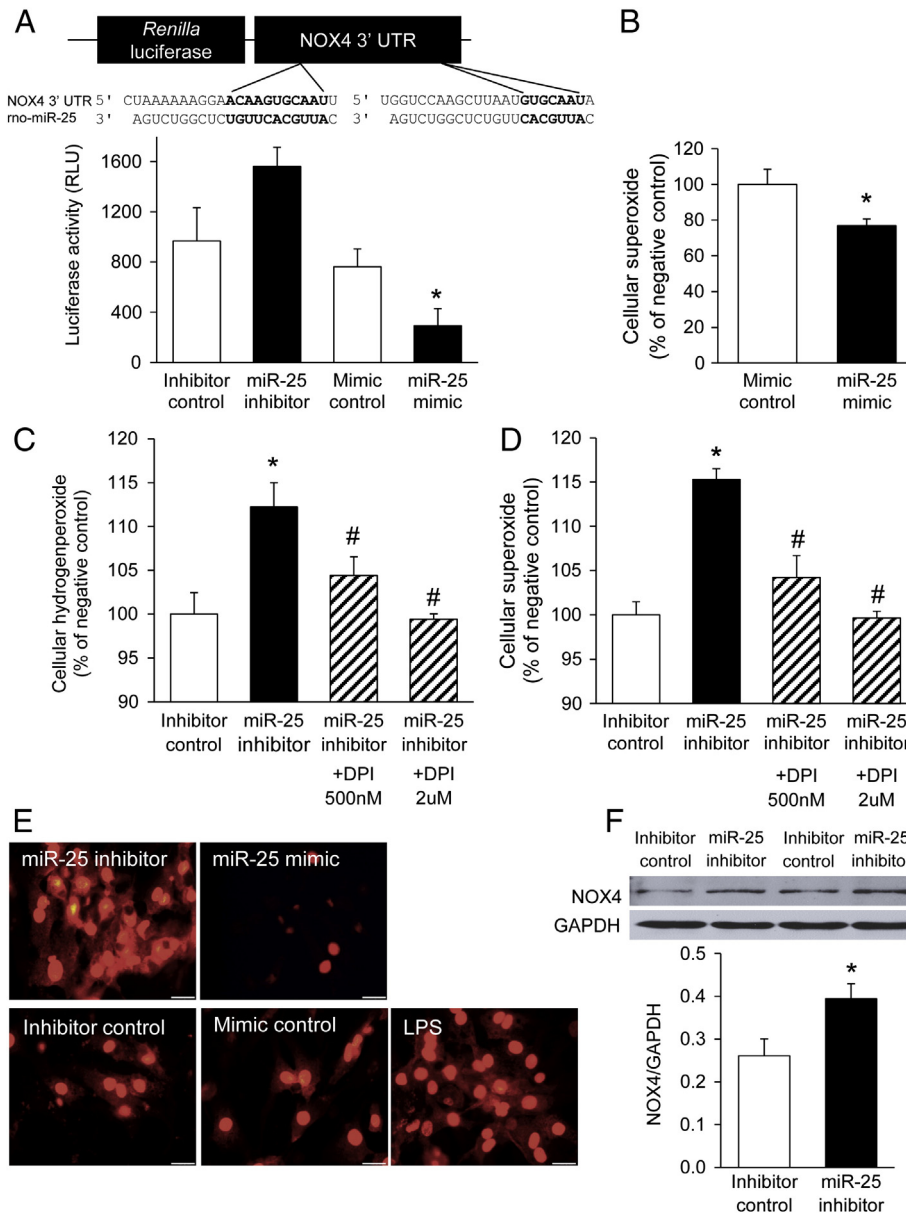


Fig. 4. Demonstration of the direct binding of rat microRNA-25 to human NOX4 3' UTR (A) using HEK293 cells. Values are mean ± SEM; n = 3. *p < 0.05 vs. corresponding control. Quantification of cellular oxidative stress by the superoxide-specific dihydroethidium in microRNA-25 mimic transfected primary rat cardiomyocytes (B). Values are mean ± SEM; n = 4. *p < 0.05 vs. control. Quantification of cellular oxidative stress by the hydrogen peroxide-sensitive dye dichlorofluorescein-diacetate (DCF-DA) and by the superoxide-specific dihydroethidium (DHE), analyzed by a fluorescent microplate reader (C and D). Neonatal cardiac myocytes were treated with a microRNA-25 inhibitor or a non-targeting microRNA inhibitor control in the presence or absence of 500 nM or 2 μM diphenyleneiodonium (DPI), a non-specific NOX inhibitor (C and D). MicroRNA-25 inhibitor significantly increased the amount of ROS level while DPI abolished both hydrogen peroxide (C) and superoxide (D) generations in a dose-dependent manner. Values are mean ± SEM; n = 5–6. *p < 0.05 vs. control. Representative microscopic images showing the relative amount of superoxide in primary cardiomyocytes transfected with the inhibitor control, mimic control, and inhibitor control treated with LPS (10 μg/ml) or with microRNA-25 inhibitor, and microRNA-25 mimic (E). Scale bar represents 20 μm. Regulation of NOX4 protein expression by microRNA-25 in neonatal cardiac myocytes transfected with microRNA-25 inhibitor or microRNA inhibitor control (F). Representative NOX4 and GAPDH western blots as well as quantified NOX4/GAPDH ratios show increased NOX4 expression in neonatal cardiac myocytes transfected with microRNA-25 inhibitor (F). Values are mean ± SEM; n = 5–6. *p < 0.05 vs. control.

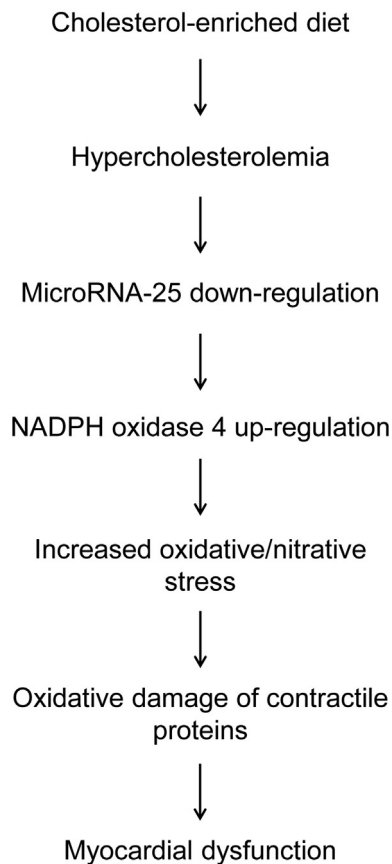


Fig. 5. Hypothetical model for the role of microRNA-25-dependent NOX4 up-regulation in hypercholesterolemia-mediated myocardial dysfunction. Cholesterol feeding induces hypercholesterolemia, which results in the down-regulation of myocardial microRNA-25. MicroRNA-25 targets NOX4, which is up-regulated in the absence of its feedback regulator microRNA-25. NOX4 produces reactive oxygen species which negatively affects myocardial contractile performance likely due to oxidation of contractile proteins.

levels, and in the former, two key transcription factors have been implicated so far, sterol-regulatory element binding protein (SREBP) and the liver X receptor (LXR) [30,31]. There are only a few reports showing that cholesterol affects microRNA expression, however, these studies were carried out on the liver in cholesterol fed pigs [32] and baboons [33]. Interestingly, a recent report showed an epigenetic regulation of microRNA-29b expression by oxidized-LDL [34], raising the possibility that serum cholesterol may also control microRNA-25 level by epigenetic regulation.

In our present study, cardiac microRNA-25 showed a pronounced down-regulation due to cholesterol-enriched diet. MicroRNA-25 is encoded in an intronic region of the mini-chromosome maintenance helixase 7. Interestingly, this region has been previously associated with a serum cholesterol QTL (quantitative trait locus) in rats [35]. To date, mainly cancer related reports were published showing the involvement of microRNA-25 in apoptotic signaling [36] and in cell invasion and migration [37]. Here we used bioinformatic analyses to characterize microRNA-25 mRNA targets (targetome) and a luciferase reporter assay to validate the direct binding of microRNA-25 to the 3' UTR region of the most putative target, NOX4. We have identified and validated NOX4 as a major microRNA-25 target that is responsible for oxidative/nitrative stress in hearts of hypercholesterolemic rats. However, several additional targets may be involved in the action of microRNA-25, especially in other cardiovascular disease conditions, considering the relevance of the identified hypothetical targets in cardiovascular diseases (Table 2.).

One of the most interesting finding in this study was to show that hypercholesterolemia-induced myocardial dysfunction is mediated

by a microRNA-dependent regulation of NADPH oxidase activity. The NADPH oxidase 4 isoenzyme (NOX4, first described as Renox [38]) is highly expressed in the heart [39] including cardiomyocytes (Figs. 3E and F) and localized in different intracellular organelles (e.g. mitochondria [39], ER [40], nucleus [41,42]). In addition, its increased expression has been shown to be involved in myocardial dysfunction in heart failure after transverse aortic constriction [43]. Nevertheless, some reports showed opposite results, i.e. NOX4 may be protective against pressure overload-induced heart failure [44]. This discrepancy may be due to the use of different knock-out animal models, allowing the expression of active splice variants [45]. However, there is increasing evidence showing that NOX4 is involved in many pathological cardiac and vascular processes, including diabetic cardiomyopathy [24], TNF alpha-induced endothelial cell apoptosis [25], and stroke associated neurodegeneration by increasing the production of reactive oxygen species [46]. Our present study also suggests that the reactive oxygen species produced by NOX4 may contribute to myocardial dysfunction induced by cholesterol-feeding.

Despite its definite role in the myocardium, the molecular mechanisms, which mediate up-regulation of cardiac NOX4 were not identified so far. It has been previously hypothesized, that increased cellular cholesterol level increases NADPH oxidase activity by acting on membrane microdomain assembly to recruit and organize the cytosolic NADPH oxidase subunits to form the active NADPH oxidase [47]. This can be true especially for the NOX2 isoenzyme, having several cytosolic and membrane-associated subunits. However, in case of NOX4, cytosolic regulatory subunits are not required for activation [48]. Moreover, the NOX4 mRNA and protein have a very rapid turnover (1–2 h is needed for induction and 4–8 h for degradation) in strike contrast to NOX2 (persists for several days) suggesting that NOX4 is likely regulated at the posttranscriptional level [48]. In a recent report, Fu et al. analyzed the potential role of microRNAs in the regulation of NOX4 in renal mesangial cells. They found, that at least five different microRNAs (microRNA-363, -92-a, 92-b, -32 and -25) have a predicted binding site to the rat NOX4 3' UTR [49]. This further suggests that microRNA-25 may act as an endogenous regulator of NOX4 by fine-tuning its expression in physiologic and pathologic conditions as well, which was now confirmed in our present study in the hearts of hypercholesterolemic rats as well as in primary cardiomyocyte cultures.

Our present results show, that the microRNA-25 dependent up-regulation of NOX4 is likely a major contributor of increased oxidative/nitrative stress. Oxidative as well as nitrative stress has been shown to play a central role in several cardiovascular diseases, including hyperlipidemia-induced cardiovascular pathologies [50]. Previous studies from our research group showed that diet-induced hyperlipidemia increases cardiac oxidative and nitrative stress and contributes to myocardial dysfunction [5,11]. In addition, recently Canton et al. has reported that oxidation of myocardial contractile proteins (e.g. actin, tropomyosin) in human samples correlates with decreased ejection fraction in heart failure [51]. In line with these reports we have confirmed in our current model that oxidation of myocardial proteins may contribute to hypercholesterolemia-induced cardiac dysfunction. The present study confirms our previous reports, and reveals a previously unknown molecular regulatory pathway (i.e. hypercholesterolemia–microRNA-25–NOX4–oxidative stress–oxidized contractile protein–dysfunction axis, see Fig. 5), providing more insight into the mechanism of hypercholesterolemia-induced myocardial dysfunction.

Although in the present study the link between microRNA-25, NOX4, oxidative stress, and myocardial dysfunction has been proven by several lines of evidence, further studies would be necessary to confirm our findings *in vivo*. This would require treatment of experimental animals with microRNA-25 antagomiR and/or mimomiR *in vivo*. In these extensive studies the administration routes of the exogenous microRNA modulators and their dosing schedule would require

further thorough experimentations. Another limitation of our study is that unspecific oxidation of the superoxide- and H₂O₂-sensitive fluorescent dyes in transfected cardiomyocytes cannot be excluded.

5. Conclusion

In conclusion, we have demonstrated that microRNA-25 is an important regulator in the context of hypercholesterolemia-induced oxidative stress by targeting NADPH oxidase 4. Loss of microRNA-25 expression induced by hypercholesterolemia in the heart may have a pathogenic role in the impaired diastolic function, which is mediated by a microRNA-25-dependent NOX4 up-regulation. The findings of this study highlight important clinical implications of microRNA-25 and NOX4 in hypercholesterolemia-associated cardiac complications.

Supplementary data to this article can be found online at <http://dx.doi.org/10.1016/j.yjmcc.2013.05.009>.

Sources of funding

This work was supported by the following grants: National Development Agency (BAROSS-DA07-DA-TECH-07-2008-0041; MED_FOOD), New Hungary Development Plan (TÁMOP-4.2.2-08/1/2008-0013, TÁMOP-4.2.1/B-09/1/KONV-2010-0005, TÁMOP-4.2.2/B-10/1-2010-0012, TÁMOP-4.2.2.A-11/1/KONV-2012-0035), Hungarian Scientific Research Fund (OTKA K79167), and Hungary–Romania Cross-Border Co-operation Program 2007–2013 (HU-RO-TRANS-MED HURO/0901/137/2.2.2). T.C., A.G. and A.Z. hold a “János Bolyai Fellowship” from the Hungarian Academy of Sciences. Z.V.V. was supported by the National Program of Excellence (TÁMOP 4.2.4.A/1-11-1-2012-0001).

Conflict of interest statement

No competing financial interest exists.

Acknowledgment

We thank Dr. Miklós Geiszt (Semmelweis University) for his scientific advices and we are indebted to Szilvia Török and Tamás Baranyai (University of Szeged) for their skillful technical assistance.

References

- [1] Roger VL, Go AS, Lloyd-Jones DM, Benjamin EJ, Berry JD, Borden WB, et al. Executive summary: heart disease and stroke statistics—2012 update: a report from the American Heart Association. *Circulation* 2012;125:188–97.
- [2] Dalen H, Thorstensen A, Romundstad PR, Aase SA, Stoylen A, Vatten LJ. Cardiovascular risk factors and systolic and diastolic cardiac function: a tissue Doppler and speckle tracking echocardiographic study. *J Am Soc Echocardiogr* 2011;24:322–32.
- [3] Horio T, Miyazato J, Kamide K, Takiuchi S, Kawano Y. Influence of low high-density lipoprotein cholesterol on left ventricular hypertrophy and diastolic function in essential hypertension. *Am J Hypertens* 2003;16:938–44.
- [4] Wang TD, Wu CC, Chen WJ, Lee CM, Chen MF, Liao CS, et al. Dyslipidemias have a detrimental effect on left ventricular systolic function in patients with a first acute myocardial infarction. *Am J Cardiol* 1998;81:531–7.
- [5] Onody A, Csonka C, Giricz Z, Ferdinandy P. Hyperlipidemia induced by a cholesterol-rich diet leads to enhanced peroxynitrite formation in rat hearts. *Cardiovasc Res* 2003;58:663–70.
- [6] Huang Y, Walker KE, Hanley F, Narula J, Houser SR, Tulenko TN. Cardiac systolic and diastolic dysfunction after a cholesterol-rich diet. *Circulation* 2004;109:97–102.
- [7] Ferdinandy P, Szilvassy Z, Horvath LI, Csont T, Csonka C, Nagy E, et al. Loss of pacing-induced preconditioning in rat hearts: role of nitric oxide and cholesterol-enriched diet. *J Mol Cell Cardiol* 1997;29:3321–33.
- [8] Osipov RM, Bianchi C, Feng J, Clements RT, Liu Y, Robich MP, et al. Effect of hypercholesterolemia on myocardial necrosis and apoptosis in the setting of ischemia-reperfusion. *Circulation* 2009;120:S22–30.
- [9] Gorbe A, Varga ZV, Kupai K, Bencsik P, Kocsis GF, Csont T, et al. Cholesterol diet leads to attenuation of ischemic preconditioning-induced cardiac protection: the role of connexin 43. *Am J Physiol Heart Circ Physiol* 2011;300:H1907–13.
- [10] Kupai K, Csonka C, Fekete V, Odendaal L, van Rooyen J, Marais de W, et al. Cholesterol diet-induced hyperlipidemia impairs the cardioprotective effect of postconditioning: role of peroxynitrite. *Am J Physiol Heart Circ Physiol* 2009;297:H1729–35.

- [11] Csont T, Bereczki E, Bencsik P, Fodor G, Gorbe A, Zvara A, et al. Hypercholesterolemia increases myocardial oxidative and nitrosative stress thereby leading to cardiac dysfunction in apoB-100 transgenic mice. *Cardiovasc Res* 2007;76:100–9.
- [12] Chu LM, Lassaletta AD, Robich MP, Liu Y, Burgess T, Laham RJ, et al. Effects of red wine and vodka on collateral-dependent perfusion and cardiovascular function in hypercholesterolemic swine. *Circulation* 2012;126:S65–72.
- [13] Ungi I, Ungi T, Ruzsa Z, Nagy E, Zimmermann Z, Csont T, et al. Hypercholesterolemia attenuates the anti-ischemic effect of preconditioning during coronary angioplasty. *Chest* 2005;128:1623–8.
- [14] Csont T, Viappiani S, Sawicka J, Slee S, Altarejos JY, Batinic-Haberle I, et al. The involvement of superoxide and iNOS-derived NO in cardiac dysfunction induced by pro-inflammatory cytokines. *J Mol Cell Cardiol* 2005;39:833–40.
- [15] Bartel DP. MicroRNAs: genomics, biogenesis, mechanism, and function. *Cell* 2004;116:281–97.
- [16] Thum T, Catalucci D, Bauersachs J. MicroRNAs: novel regulators in cardiac development and disease. *Cardiovasc Res* 2008;79:562–70.
- [17] Csonka C, Kupai K, Kocsis GF, Novak G, Fekete V, Bencsik P, et al. Measurement of myocardial infarct size in preclinical studies. *J Pharmacol Toxicol Methods* 2010;61:163–70.
- [18] Csonka C, Szilvassy Z, Fulop F, Pali T, Blasig IE, Tosaki A, et al. Classic preconditioning decreases the harmful accumulation of nitric oxide during ischemia and reperfusion in rat hearts. *Circulation* 1999;100:2260–6.
- [19] Luzon-Toro B, Zafrá-Gomez A, Ballesteros O. Gas chromatographic–mass spectrometric determination of brain levels of alpha-cholest-8-en-3beta-ol (lathosterol). *J Chromatogr B Analyt Technol Biomed Life Sci* 2007;850:177–82.
- [20] Farago N, Zvara A, Varga Z, Ferdinandy P, Puskas LG. Purification of high-quality micro RNA from the heart tissue. *Acta Biol Hung* 2011;62:413–25.
- [21] Farago N, Kocsis GF, Feher LZ, Csont T, Hackler Jr L, Varga-Orvos Z, et al. Gene and protein expression changes in response to normoxic perfusion in mouse hearts. *J Pharmacol Toxicol Methods* 2008;57:145–54.
- [22] Lewis BP, Burge CB, Bartel DP. Conserved seed pairing, often flanked by adenosines, indicates that thousands of human genes are microRNA targets. *Cell* 2005;120:15–20.
- [23] Betel D, Koppal A, Agius P, Sander C, Leslie C. Comprehensive modeling of microRNA targets predicts functional non-conserved and non-canonical sites. *Genome Biol* 2010;11:R90.
- [24] Maalouf RM, Eid AA, Gorin YC, Block K, Escobar GP, Bailey S, et al. Nox4-derived reactive oxygen species mediate cardiomyocyte injury in early type 1 diabetes. *Am J Physiol Cell Physiol* 2012;302:C597–604.
- [25] Basuroy S, Bhattacharya S, Leffler CW, Parfenova H. Nox4 NADPH oxidase mediates oxidative stress and apoptosis caused by TNF-alpha in cerebral vascular endothelial cells. *Am J Physiol Cell Physiol* 2009;296:C422–32.
- [26] Kim SM, Kim YG, Jeong KH, Lee SH, Lee TW, Ihm CG, et al. Angiotensin II-induced mitochondrial Nox4 is a major endogenous source of oxidative stress in kidney tubular cells. *PLoS One* 2012;7:e39739.
- [27] Siuda D, Zechner U, El Hajj N, Prawitt D, Langer D, Xia N. Transcriptional regulation of Nox4 by histone deacetylases in human endothelial cells. *Basic Res Cardiol* 2012;107 [283,012-0283-3. Epub 2012 Jul 13].
- [28] Csont T, Gorbe A, Bereczki E, Szunyog A, Aypar E, Toth ME, et al. Biglycan protects cardiomyocytes against hypoxia/reoxygenation injury: role of nitric oxide. *J Mol Cell Cardiol* 2010;48:649–52.
- [29] Feher LZ, Kalman J, Puskas LG, Gyulveszi G, Kitajka K, Penke B, et al. Impact of haloperidol and risperidone on gene expression profile in the rat cortex. *Neurochem Int* 2005;47:271–80.
- [30] Brown MS, Goldstein JL. A proteolytic pathway that controls the cholesterol content of membranes, cells, and blood. *Proc Natl Acad Sci U S A* 1999;96:11041–8.
- [31] Repa JJ, Mangelsdorf DJ. The role of orphan nuclear receptors in the regulation of cholesterol homeostasis. *Annu Rev Cell Dev Biol* 2000;16:459–81.
- [32] Cirera S, Birck M, Busk PK, Fredholm M. Expression profiles of miRNA-122 and its target CAT1 in minipigs (*Sus scrofa*) fed a high-cholesterol diet. *Comp Med* 2010;60:136–41.
- [33] Karere GM, Glenn JP, Vandeberg JL, Cox LA. Differential microRNA response to a high-cholesterol, high-fat diet in livers of low and high LDL-C baboons. *BMC Genomics* 2012;13:320.
- [34] Chen KC, Liao YC, Hsieh IC, Wang YS, Hu CY, Juo SH. OxLDL causes both epigenetic modification and signaling regulation on the microRNA-29b gene: novel mechanisms for cardiovascular diseases. *J Mol Cell Cardiol* 2012;52:587–95.
- [35] Dwinell MR, Worthey EA, Shimoyama M, Bakir-Gungor B, DePons J, Laulederkind S, et al. The Rat Genome Database 2009: variation, ontologies and pathways. *Nucleic Acids Res* 2009;37:D744–9.
- [36] Razumilava N, Bronk SF, Smoot RL, Fingas CD, Werneburg NW, Roberts LR. miR-25 targets TNF-related apoptosis inducing ligand (TRAIL) death receptor-4 and promotes apoptosis resistance in cholangiocarcinoma. *Hepatology* 2012;55:465–75.
- [37] Xu X, Chen Z, Zhao X, Wang J, Ding D, Wang Z, et al. MicroRNA-25 promotes cell migration and invasion in esophageal squamous cell carcinoma. *Biochem Biophys Res Commun* 2012;421:640–5.
- [38] Geiszt M, Kopp JB, Varnai P, Leto TL. Identification of renox, an NAD(P)H oxidase in kidney. *Proc Natl Acad Sci U S A* 2000;97:8010–4.
- [39] Ago T, Kuroda J, Pain J, Fu C, Li H, Sadoshima J. Upregulation of Nox4 by hypertrophic stimuli promotes apoptosis and mitochondrial dysfunction in cardiac myocytes. *Circ Res* 2010;106:1253–64.
- [40] Zhang L, Nguyen MV, Lardy B, Jesaitis AJ, Grichine A, Rousset F, et al. New insight into the Nox4 subcellular localization in HEK293 cells: first monoclonal antibodies against Nox4. *Biochimie* 2011;93:457–68.
- [41] Anilkumar N, Jose GS, Sawyer I, Santos CX, Sand C, Brewer AC, et al. A 28-kDa splice variant of NADPH oxidase-4 is nuclear-localized and involved in redox signaling in vascular cells. *Arterioscler Thromb Vasc Biol* 2013;33:e104–12.

- [42] Matsushima S, Kuroda J, Ago T, Zhai P, Park JY, Xie LH, et al. Increased oxidative stress in the nucleus caused by Nox4 mediates oxidation of HDAC4 and cardiac hypertrophy. *Circ Res* 2013;112:651–63.
- [43] Kuroda J, Ago T, Matsushima S, Zhai P, Schneider MD, Sadoshima J. NADPH oxidase 4 (Nox4) is a major source of oxidative stress in the failing heart. *Proc Natl Acad Sci U S A* 2010;107:15565–70.
- [44] Zhang M, Brewer AC, Schroder K, Santos CX, Grieve DJ, Wang M, et al. NADPH oxidase-4 mediates protection against chronic load-induced stress in mouse hearts by enhancing angiogenesis. *Proc Natl Acad Sci U S A* 2010;107:18121–6.
- [45] Altenhofer S, Kleikers PW, Radermacher KA, Scheurer P, Rob Hermans JJ, Schiffers P, et al. The NOX toolbox: validating the role of NADPH oxidases in physiology and disease. *Cell Mol Life Sci* 2012;69:2327–43.
- [46] Kleinschnitz C, Grund H, Wingler K, Armitage ME, Jones E, Mittal M, et al. Post-stroke inhibition of induced NADPH oxidase type 4 prevents oxidative stress and neurodegeneration. *PLoS Biol* 2010;8:e1000479.
- [47] Vilhardt F, van Deurs B. The phagocyte NADPH oxidase depends on cholesterol-enriched membrane microdomains for assembly. *EMBO J* 2004;23:739–48.
- [48] Serrander L, Cartier L, Bedard K, Banfi B, Lardy B, Plastre O, et al. NOX4 activity is determined by mRNA levels and reveals a unique pattern of ROS generation. *Biochem J* 2007;406:105–14.
- [49] Fu Y, Zhang Y, Wang Z, Wang L, Wei X, Zhang B, et al. Regulation of NADPH oxidase activity is associated with miRNA-25-mediated NOX4 expression in experimental diabetic nephropathy. *Am J Nephrol* 2010;32:581–9.
- [50] Dhalla NS, Temsah RM, Netticadan T. Role of oxidative stress in cardiovascular diseases. *J Hypertens* 2000;18:655–73.
- [51] Canton M, Menazza S, Sheeran FL, Polverino de Laureto P, Di Lisa F, Pepe S. Oxidation of myofibrillar proteins in human heart failure. *J Am Coll Cardiol* 2011;57:300–9.
- [52] Wang B, Hao J, Jones SC, Yee MS, Roth JC, Dixon IM. Decreased Smad 7 expression contributes to cardiac fibrosis in the infarcted rat heart. *Am J Physiol Heart Circ Physiol* 2002;282:H1685–96.
- [53] Fiedler J, Jazbutyte V, Kirchmaier BC, Gupta SK, Lorenzen J, Hartmann D, et al. MicroRNA-24 regulates vascularity after myocardial infarction. *Circulation* 2011;124:720–30.
- [54] Bogoyevitch MA, Parker PJ, Sugden PH. Characterization of protein kinase C isotype expression in adult rat heart. Protein kinase C-epsilon is a major isotype present, and it is activated by phorbol esters, epinephrine, and endothelin. *Circ Res* 1993;72:757–67.
- [55] Xu DL, Martin PY, Ohara M, St John J, Pattison T, Meng X, et al. Upregulation of aquaporin-2 water channel expression in chronic heart failure rat. *J Clin Invest* 1997;99:1500–5.
- [56] Manabe I, Shindo T, Nagai R. Gene expression in fibroblasts and fibrosis: involvement in cardiac hypertrophy. *Circ Res* 2002;91:1103–13.
- [57] Kim Y, Phan D, van Rooij E, Wang DZ, McAnally J, Qi X, et al. The MEF2D transcription factor mediates stress-dependent cardiac remodeling in mice. *J Clin Invest* 2008;118:124–32.
- [58] Cruz-Topete D, List EO, Okada S, Kelder B, Kopchick JJ. Proteomic changes in the heart of diet-induced pre-diabetic mice. *J Proteomics* 2011;74:716–27.

Glossary

- CF: coronary flow
 CO: cardiac output
 DCF-DA: 2',7'-dichlorofluorescein-diacetate
 DHE: dihydroethidium
 DMSO: dimethyl sulfoxide
 $+dP/dt_{max}$: maximal rate of ventricular pressure rise
 $-dP/dt_{max}$: maximal rate of ventricular pressure decline
 DPI: diphenyleonium
 ELISA: enzyme-linked immunosorbent assay
 GAPDH: glyceraldehyde 3-phosphate dehydrogenase
 HDL: high density lipoprotein
 HW: heart weight
 HW/BW: heart weight/body weight ratio
 LDL: low density lipoprotein
 LVDP: left ventricular developed pressure
 LVEDP: left ventricular end-diastolic pressure
 LXR: liver X receptor
 NOX1: NADPH oxidase isoenzyme 1
 NOX2: NADPH oxidase isoenzyme 2
 NOX4: NADPH oxidase isoenzyme 4
 PBS: phosphate buffered saline
 QRT-PCR: quantitative reverse transcription polymerase chain reaction
 rno-miR: *Rattus norvegicus* microRNA
 ROS: reactive oxygen species
 SREBP: sterol-regulatory element binding protein
 TBS: Tris-buffered saline
 3' UTR: three prime untranslated region
 VLDL: very low density lipoprotein

II.

Görbe A, **Varga ZV**, Kupai K, Bencsik P, Kocsis GF, Csont T, Boengler K, Schulz R, Ferdinandy P.: Cholesterol diet leads to attenuation of ischemic preconditioning-induced cardiac protection: the role of connexin 43. *Am J Physiol Heart Circ Physiol.* (2011) 300:H1907-13. [IF: 3.708]

Cholesterol diet leads to attenuation of ischemic preconditioning-induced cardiac protection: the role of connexin 43

Anikó Görbe, Zoltán V. Varga, Krisztina Kupai, Péter Bencsik, Gabriella F. Kocsis, Tamás Csont, Kerstin Boengler, Rainer Schulz and Péter Ferdinandy

Am J Physiol Heart Circ Physiol 300:H1907-H1913, 2011. First published 11 March 2011;
doi:10.1152/ajpheart.01242.2010

You might find this additional info useful...

This article cites 41 articles, 22 of which can be accessed free at:

<http://ajpheart.physiology.org/content/300/5/H1907.full.html#ref-list-1>

Updated information and services including high resolution figures, can be found at:

<http://ajpheart.physiology.org/content/300/5/H1907.full.html>

Additional material and information about *AJP - Heart and Circulatory Physiology* can be found at:

<http://www.the-aps.org/publications/ajpheart>

This information is current as of August 2, 2011.

Cholesterol diet leads to attenuation of ischemic preconditioning-induced cardiac protection: the role of connexin 43

Anikó Görbe,^{1,2} Zoltán V. Varga,¹ Krisztina Kupai,^{1,2} Péter Bencsik,² Gabriella F. Kocsis,^{1,2} Tamás Csont,^{1,2} Kerstin Boengler,³ Rainer Schulz,⁴ and Péter Ferdinandy^{1,2}

¹Cardiovascular Research Group, Department of Biochemistry, University of Szeged, and ²Pharmahungary Group, Szeged, Hungary; ³Institut für Pathophysiologie, Zentrum für Innere Medizin, Universitätsklinikum Essen, Essen; and ⁴Institut für Physiologie, Justus-Liebig Universität Giessen, Giessen, Germany

Submitted 7 December 2010; accepted in final form 7 February 2011

Görbe A, Varga ZV, Kupai K, Bencsik P, Kocsis GF, Csont T, Boengler K, Schulz R, Ferdinandy P. Cholesterol diet leads to attenuation of ischemic preconditioning-induced cardiac protection: the role of connexin 43. *Am J Physiol Heart Circ Physiol* 300: H1907–H1913, 2011. First published March 11, 2010; doi:10.1152/ajpheart.01242.2010.—Cardioprotection by ischemic preconditioning (IP) was abolished in connexin 43 (Cx43)-deficient mice due to loss of Cx43 located in mitochondria rather than at the sarcolemma. IP is lost in hyperlipidemic rat hearts as well. Since changes in mitochondrial Cx43 in hyperlipidemia have not yet been analyzed, we determined total and mitochondrial Cx43 levels in male Wistar rats fed a laboratory chow enriched with 2% cholesterol or normal chow for 12 wk. Hearts were isolated and perfused according to Langendorff. After a 10-min perfusion, myocardial tissue cholesterol, superoxide, and nitrotyrosine contents were measured and Cx43 content in whole heart homogenate and a mitochondrial fraction determined. In the cholesterol-fed group, tissue cholesterol and superoxide formation was increased ($P < 0.05$), while total Cx43 content remained unchanged. Mitochondrial total and dephosphorylated Cx43 content decreased. Hearts were subjected to an IP protocol (3 × 5 min ischemia-reperfusion) or time-matched aerobic perfusion followed by 30-min global ischemia and 5-min reperfusion. IP reduced infarct size in normal but not in cholesterol-fed rats. At 5-min reperfusion following 30-min global ischemia, the total and dephosphorylated mitochondrial Cx43 content was increased, which was abolished by IP in both normal and high-cholesterol diet. In conclusion, loss of cardioprotection by IP in hyperlipidemia is associated with a redistribution of both sarcolemmal and mitochondrial Cx43.

mitochondria; superoxide

HYPERLIPIDEMIA IS A WELL-KNOWN risk factor in development of cardiovascular diseases, as it contributes to the formation of atherosclerotic plaques in coronary vessels (1, 16). Many studies suggested that cardiovascular risk factors such as diabetes, aging, hypertension, and hyperlipidemia (11) attenuate the protective action of preconditioning (10, 15, 19) and postconditioning (11, 21, 29) in the heart independently from coronary atherosclerosis. However, the underlying molecular alterations in hyperlipidemia attenuating the adaptation of the ischemic heart remain unknown.

Among the six connexin types found in the heart, connexin 43 (Cx43) is the dominant one in the ventricles, taking part in gap junction formation and thus in electrical and chemical coupling of cardiomyocytes. Under physiological conditions,

most of the Cx43 in cardiomyocytes is in the phosphorylated state (37). Hyperlipidemia is associated with enhanced oxidative-nitrosative stress (9, 28). Increased oxidative stress under pathophysiological conditions alters Cx43 lateralization (39). Indeed, a high-fat diet increased the lateralization of Cx43 in female rats resulting in an increased incidence of ventricular arrhythmias (2), and total myocardial Cx43 content was decreased in rabbits subjected to cholesterol-enriched diet (23).

Loss of myocardial Cx43 in heterozygous Cx43-deficient mice abolished the cardioprotection achieved by ischemic or pharmacological preconditioning (18, 38). The loss of protection was, however, dependent on Cx43 being located in mitochondria (5, 36) rather than the sarcolemma (35).

Since changes in cardiac mitochondrial Cx43 in hyperlipidemia have not yet been analyzed, we determined total and mitochondrial Cx43 levels in rats fed a cholesterol-rich diet. Furthermore, ischemic and preconditioned rat hearts were examined whether changes in mitochondrial Cx43 might be involved in attenuated cardioprotection in hyperlipidemia.

MATERIALS AND METHODS

Experimental Design

The investigation conforms with the *Guide for the Care and Use of Laboratory Animals* published by the U.S. National Institutes of Health (National Institutes of Health publication 85-23, revised 1996), and it was approved by a local animal ethics committee of the University of Szeged.

Male Wistar rats (250 g) were fed normal ($n = 18$) or 2% cholesterol-enriched rat chow ($n = 18$) for 12 wk. High-cholesterol diet induced moderate hyperlipidemia without substantial atherosclerosis in this species (12). At the end of the diet, animals were anesthetized with diethylether and given 500 U/kg heparin.

Cx43 content before ischemia-reperfusion. Hearts were isolated and perfused according to Langendorff with Krebs-Henseleit buffer. Hearts from normal ($n = 6$) and cholesterol-fed rats ($n = 6$) were perfused for 10 min at first part of experiment.

Cx43 content following ischemia-reperfusion. Then following hearts in both diet-groups were subjected to a no-flow ischemia-induced preconditioning protocol (3 × 5-min ischemia and 5-min reperfusion) or a time-matched nonpreconditioning protocol each followed by test ischemia-reperfusion (30-min global normothermic ischemia followed by 5-min or 120-min reperfusion, respectively) $n = 6$ in each group (Fig. 1).

Measurement of Tissue Cholesterol Level

To determine the tissue cholesterol content of normal and cholesterol-fed myocardial samples a gas chromatographic-mass spectrometric measurement was carried out according to the method published by Luzon-Toro et al. (26).

Address for reprint requests and other correspondence: P. Ferdinandy, Cardiovascular Research Group, Dept. of Biochemistry, Univ. of Szeged, Dóm tér 9, Szeged, H-6720, Hungary (e-mail: peter.ferdinandy@pharmahungary.com).

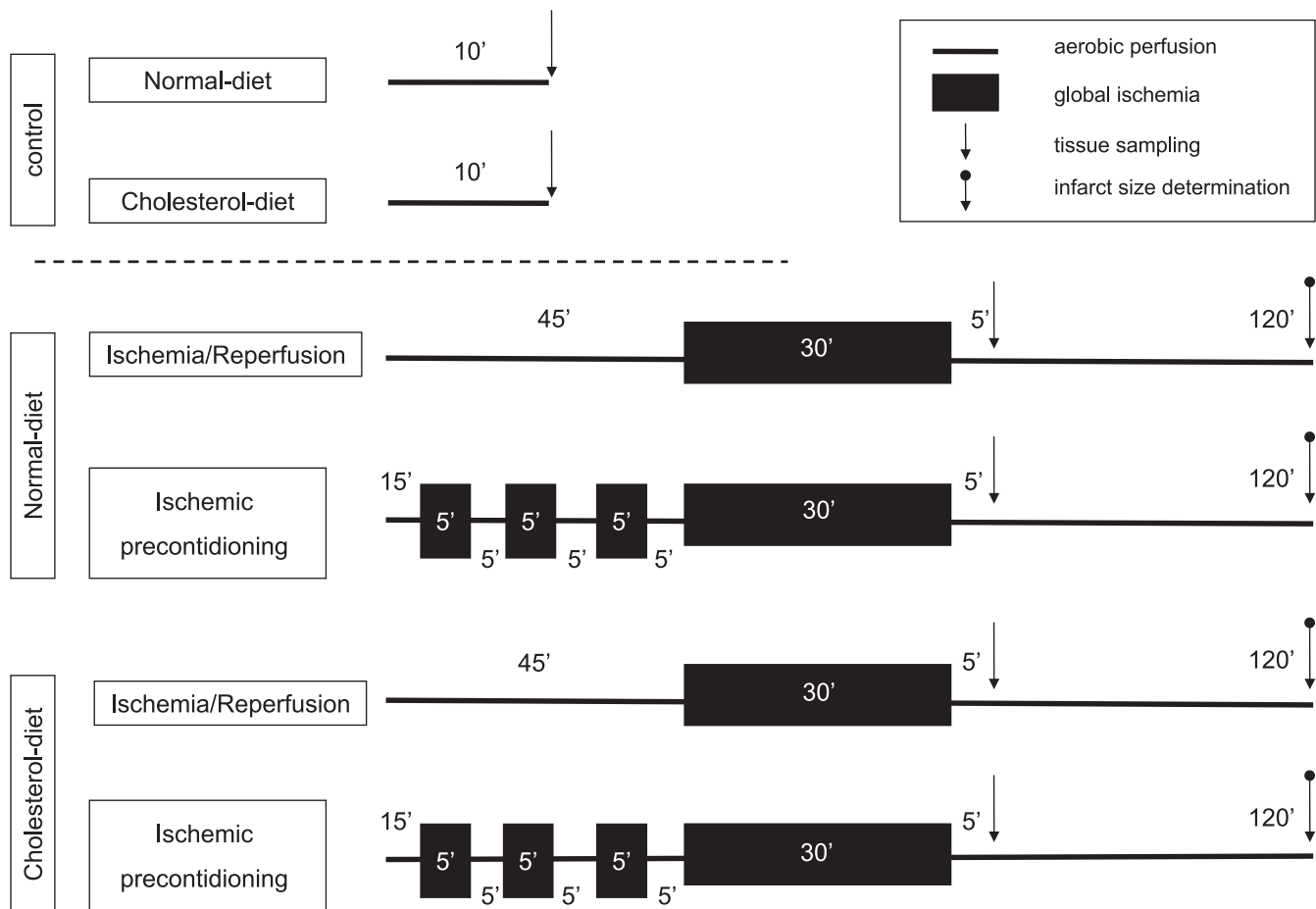


Fig. 1. Experimental protocol in ex vivo Langendorff-perfused rat hearts.

The sample extraction based on the method of Bligh and Dyer (4). Approximately 50 mg frozen rat heart powder were weighted into a capped glass tube, and then immediately 2 ml dilution solution (HPLC grade chloroform and ULS/MS grade methanol, 1:2) and the internal standard solution (100 μ l, 100 μ g/ml stigmasterol) were added and vortexed to extract the lipids. After that the crude extract was mixed with chloroform and subsequently with distilled water. The sample solution was centrifuged at 1,000 RPM for 5 min at room temperature to give a two-phase system (aqueous top, organic bottom). The bottom phase was recovered and evaporated to dryness under slight nitrogen stream. The lipid extract was derivatized with freshly prepared 50 μ l *N*-methyl-*N*-(trimethylsilyl)-trifluoroacetamide in 100 μ l acetonitrile. Samples were then incubated at 60 °C for 30 min.

The GC-MS measurement was carried out on HP-5 (5% phenyl-95% dimethylpolysiloxan) column with helium carrier gas. During the initial chromatographic run, the retention and fragmentation pattern of the standard compounds were determined. The applied chromatographic setup gave a retention time for cholesterol and the stigmasterol of 15.58 and 17.99 min, respectively. The quantitation was carried out in target ion mode and the qualification was made by three selected characteristic fragment ions. In the case of cholesterol, the target ion was m/z 129 and the quality ions were the m/z 329, 368, and 353; in the ratio of 73.9, 57.4, and 32.1, respectively, to the target ion. In the case of stigmasterol, the target ion was m/z 83 and the quality ions were the m/z 129, 255, and 394; in the ratio of 66.7, 45, and 36, respectively, to the target ion.

The GC-MS system was controlled and the acquired data were evaluated by the MSD Chemstation E.01.01 335 software and the NIST Mass Search Program v.2.0 with the NIST Mass Spectral Library v.05.

Indicators of Oxidative and Nitrosative Stress

Cardiac superoxide production in freshly minced ventricles was assessed by lucigenin-enhanced chemiluminescence in normal and cholesterol-fed groups. Approximately 100 mg of the apex of the heart were placed in 1 ml air-equilibrated Krebs-Henseleit solution containing 10 mmol/l HEPES (pH 7.4) and 5 μ mol/l lucigenin. Chemiluminescence was measured at room temperature in a liquid scintillation counter using a single active photomultiplier positioned in out-of-coincidence mode in the presence or absence of the superoxide scavenger nitroblue tetrazolium (NBT; 200 μ mol/l). NBT-inhibitable chemiluminescence was considered an index of myocardial superoxide generation. It should be noted that NBT, like other superoxide scavengers, is not entirely specific for superoxide.

Cardiac free 3-nitrotyrosine level was measured by ELISA (Cayman Chemical) from normal and cholesterol-fed heart tissue samples. Briefly, supernatants of ventricular tissue homogenate were incubated overnight with anti-nitrotyrosine rabbit IgG specific to free 3-nitrotyrosine and nitrotyrosine acetylcholinesterase tracer in precoated (mouse anti-rabbit IgG) microplates followed by development with Ellman's reagent. Free nitrotyrosine content was normalized to protein content of cardiac homogenate and expressed as nanograms per milligram protein.

Isolation of Mitochondria Samples

Mitochondrial isolation procedure was performed according to Boengler et al. (5). Briefly, fresh heart tissue were minced with scissors in ice-cold isolation buffer (250 mM sucrose, 10 mM HEPES, and 1 mM EGTA pH 7.4). The blood was washed out with buffer, and heart tissues samples were homogenized by ultraturax homogenizator

Table 1. Effects of cholesterol diet on oxidative/nitrosative stress

	Normal Diet	Cholesterol Diet
Tissue cholesterol content, $\mu\text{g}/\text{mg}$ wet weight	0.77 ± 0.01	$0.82 \pm 0.01^*$
Cardiac superoxide production (lucigenin chemiluminescence), cpm/mg wet weight	187 ± 27	$331 \pm 41^*$
Tissue nitrotyrosine content, ng/ml	1.78 ± 0.33	2.06 ± 0.47

Values are means \pm SE. * $P < 0.05$.

for 3×5 s. The homogenate was centrifuged at 480 g for 10 min, and the supernatant was filtered through a nylon filter (250- μm pore size) and then centrifuged again at 10,780 g for 10 min. The pellet containing mitochondria was resuspended in isolation buffer and then centrifuged again at 7,650 g for 20 min. Then, the pellet was resuspended in 50- μl isolation buffer and layered onto 30% Percoll solution and ultracentrifuged at 35,000 g for 30 min. The lower band reflecting intact mitochondria was collected and washed in isolation buffer by centrifugation at 8,000 g for 5 min.

Infarct Size Determination

At the end of the perfusion protocols, hearts were frozen, sliced, and incubated at 37°C in 1% triphenyltetrazolium chloride to delineate infarcted tissue. Slices were then fixed and quantified by planimetry using Infarctsize 1.0 software (Pharmahungary, Szeged, Hungary) as previously described by Csonka et al. (8).

Measurement of Cx43

The Cx43 level in heart samples and in isolated mitochondria was determined by Western blotting. Heart powder samples were homogenized by ultrasonic homogenizer at maximum power, 90% sonication time for 2×20 s. The protein concentrations of total heart and mitochondria fractions were determined by the bicinchoninic acid assay (Pierce). Twenty-microgram samples were loaded on SDS-PAGE (10%) followed by the transfer of proteins onto a nitrocellulose membrane (400 mA, 1 h). Membranes were then blocked overnight at 4°C in TBS-T (0.1% Tween-20) and 5% skimmed milk powder. Membranes were incubated either with rabbit polyclonal anti-rat Cx43 (Zymed) or mouse monoclonal anti-succinate dehydrogenase (Molecular Probes), rabbit polyclonal anti Na-K-ATPase α -1 (Upstate), and mouse monoclonal anti-actin (BD Biosciences) antibodies for 1.5 h at room temperature and horseradish peroxidase-conjugated rabbit anti-mouse or goat anti-rabbit secondary antibody (Dako) for 40 min. Membranes were then developed with an enhanced chemiluminescence kit (GE HealthCare), exposed to X-ray (Kodak) film and scanned. Band density was calculated by integrating the area (in pixels \times intensity, expressed in arbitrary units).

Cx43 level of intercalated discs were detected by immunohistochemistry. Fresh frozen sections (10 μm) of hearts were fixed in fresh acetone for 5 min. After being allowed to dry at room temperature for 30 min, the sections were blocked with 5% BSA (Sigma) in TBS for 15 min. Incubation with the primary antibody [monoclonal mouse anti-Cx43 (GAP1, 1:100; Refs. 3, 41)] was carried out at room temperature for 1.5 h in a humidified chamber. The sections were washed 3×5 min in TBS and incubated in secondary antibody (FITC-conjugated anti-mouse) (Dako) diluted in TBS (1:300) for 40 min. Sections were mounted on a slide in Faramount mounting medium (Dako). Images of immunostained sections were captured using a fluorescent microscope (Nikon, Labophot 2). At least eight random images were collected on each heart muscle sample stained for Cx43. Digital single channel images were transformed into 8-bit black-and-white format and were analyzed using the ImageJ 1.29x software (Wayne Rasband, NIH). At standard threshold settings,

which ensured that only specific signals were considered and the background was excluded, the area fraction of Cx43 immunofluorescent dots and plaques was measured on each image. Then, immunofluorescent plaques (size ≥ 50 pixels) were measured separately representing the intercalated disc fraction. The ratio of intercalated disc intensity and total intensity in each group was summarized in graphs.

Statistical Analysis

Results are expressed as means \pm SE. Student's *t*-test or two-way ANOVA followed by least significant difference post hoc tests was used to evaluate differences in mean values between groups. Differences were considered significant at $P < 0.05$.

RESULTS

Effects of Cholesterol Diet on Oxidative/Nitrosative Stress

Tissue cholesterol and cardiac superoxide contents were significantly higher in the myocardium after a 12-wk cholesterol-enriched diet (Table 1). In contrast, tissue nitrotyrosine (ELISA), indicative of reactive nitrogen species formation, was not significantly different between normal and cholesterol-fed rat hearts.

Effects of Cholesterol Diet on Total and Mitochondrial Cx43

Total myocardial Cx43 content remained unchanged following 12 wk of cholesterol-rich diet (Western blot; Fig. 2). Cx43 localized at the intercalated discs was significantly decreased by hyperlipidemia (Fig. 3, A and B).

In mitochondrial fractions (succinate dehydrogenase enriched) not contaminated with sarcolemma (no signal for Na-K-ATPase, Fig. 4A), Cx43 content was also decreased approximately by 50% in cholesterol-fed compared with normal-fed rats (Fig. 4B).

Cx43 Expression in Preconditioned Hearts

Neither ischemia-reperfusion nor ischemic preconditioning influenced the total cardiac Cx43 level (sum P_0 , P_1 , P_2 signal intensities) in normal and cholesterol-fed rats (Fig. 2). However, there was an increase in P_0 with ischemia that was

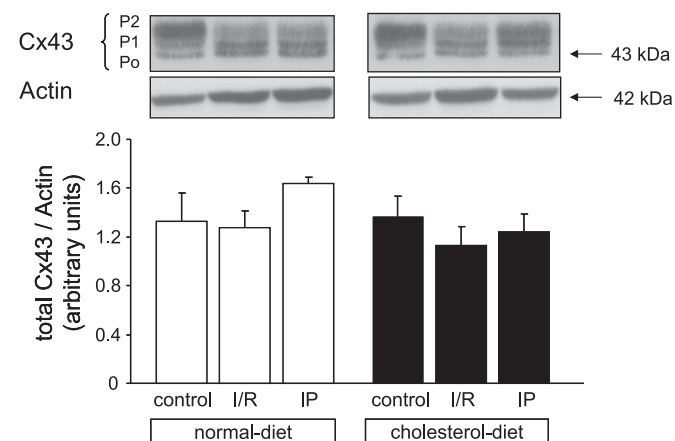
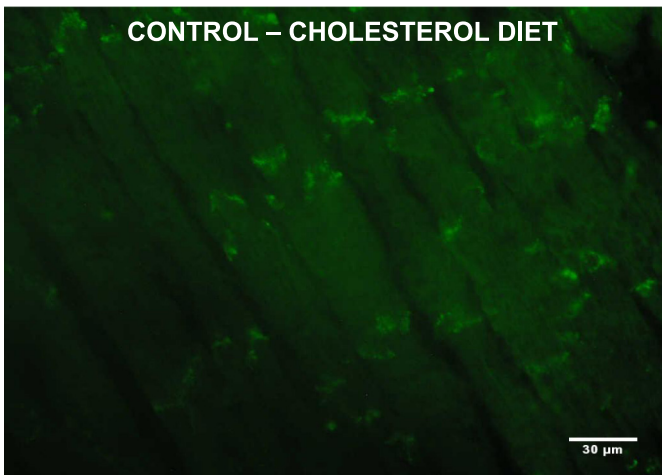
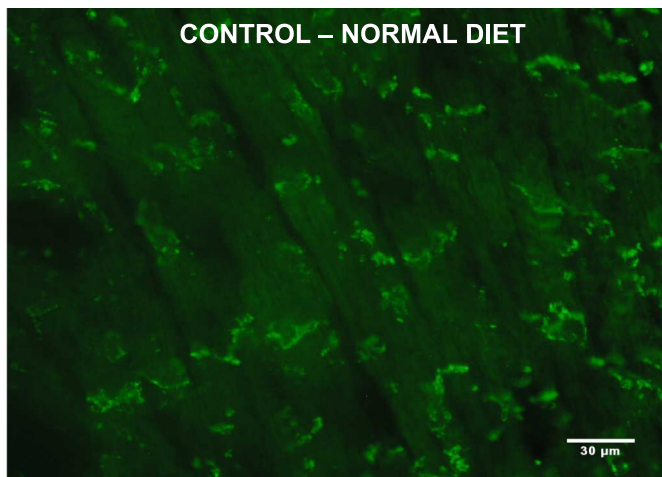


Fig. 2. Total connexin 43 (Cx43)/actin in control, ischemic-reperused (I/R), and ischemic preconditioned (IP) rat hearts. Western blot analysis of the Cx43 (P_0 , P_1 , P_2) and actin protein level in hearts of normal and cholesterol-fed rats. Representative images for normal and cholesterol-fed groups were spliced from 2 different regions of the same blot. Bar graphs represent the total Cx43-to-actin ratio in all groups. Data are means \pm SE; $n = 6$ in each group.

A



B

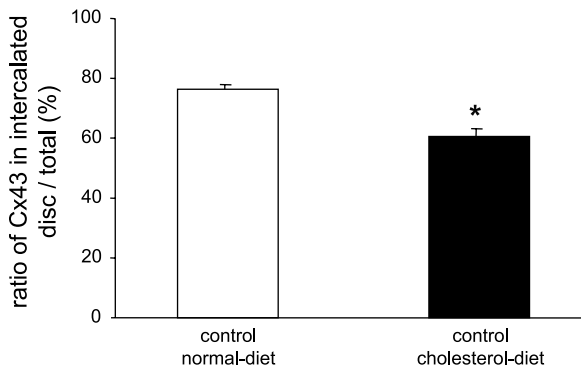


Fig. 3. Morphometric analysis of Cx43 in intercalated discs of rat hearts. *A*: immunofluorescent staining of Cx43 in longitudinal sections of myocardium in normal and cholesterol-fed control hearts. *B*: quantification in a bar diagram shows the ratio of intercalated disc and total Cx43 content in those groups. Data are means \pm SE. * $P < 0.05$, Student's *t*-test; $n = 6$ in both groups.

partially reversed by preconditioning in both cholesterol and normal-fed rats.

At 5-min reperfusion following 30-min global ischemia, the total and dephosphorylated mitochondrial Cx43 content was increased, which was significantly decreased by ischemic pre-

conditioning in case of both normal and high-cholesterol diet (Fig. 4*B*).

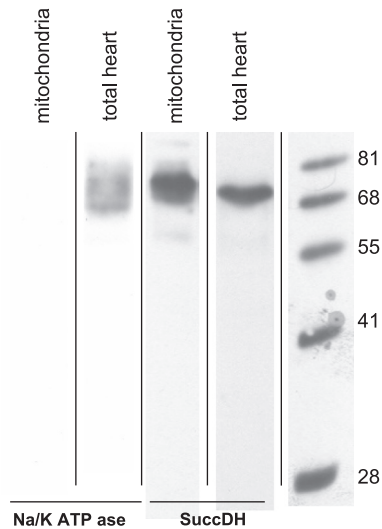
Infarct Size

Infarct size was $29 \pm 2\%$ in normal ischemic/reperfused heart, whereas it was significantly reduced to $9 \pm 2\%$ following ischemic preconditioning. The protective effect of ischemic preconditioning was abolished in cholesterol-fed rats (Fig. 5).

DISCUSSION

The present study demonstrated the intracellular redistribution of Cx43 in hyperlipidemia. Here we showed that cholesterol feeding did not affect the total expression of Cx43, while the mitochondrial total content and dephosphorylated Cx43 content as well as gap junctional Cx43 were

A



B

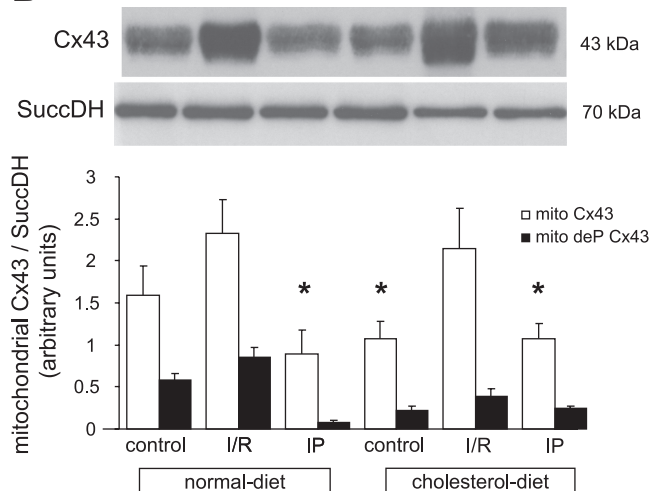


Fig. 4. Mitochondrial Cx43 in control, I/R, and IP rat hearts. *A*: Western blot analysis of the isolated mitochondria and total heart samples for anti-Na-K-ATPase (specific for plasma membrane) and anti-succinate-dehydrogenase (specific for mitochondria). *B*: Cx43 and succinate-dehydrogenase protein level in mitochondria isolated from all groups. Bar graphs represent the mitochondrial Cx43/succinate-dehydrogenase (SuccDH) level in all groups. Data are means \pm SE. * $P < 0.05$ vs. normal-diet control, two-way ANOVA; $n = 6$ in each group.

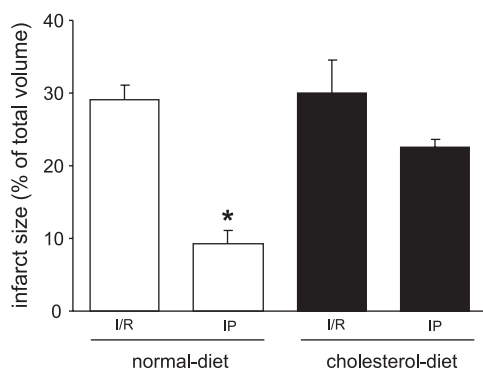


Fig. 5. Infarct size in rat hearts. Ratio of infarcted zone to total left ventricle in normal and cholesterol-fed I/R and IP rat hearts. Data are means \pm SE. * $P < 0.05$ vs. ischemia-reperfusion, two-way ANOVA; $n = 5$ each group.

decreased concomitantly with a significant increase in cardiac superoxide levels. Protective effect of preconditioning was found to be lost in hyperlipidemia. Both total fraction and dephosphorylated fraction of mitochondrial Cx43 were increased by ischemia-reperfusion and reduced by preconditioning in case of both normal and cholesterol diets.

Hyperlipidemia and Cx43 Content and Distribution

In this rat model, a 12-wk cholesterol-enriched diet induced mild hyperlipidemia independently from atherosclerosis (34). In the present study, mild hyperlipidemia did not alter total myocardial Cx43 protein expression. In contrast, strong hyperlipidemia, which can be induced by a 12-wk cholesterol-enriched diet in rabbits, caused downregulation of total myocardial Cx43 protein and also its redistribution (23). In the present study, intracellular Cx43 distribution was altered as the gap junctional Cx43 content was decreased in cholesterol-fed rats. The present results in male rats confirmed previously published data in cholesterol-fed female rats in which hyperlipidemia resulted in lateralization of Cx43 at the sarcolemma (2). Altered Cx43 protein levels, Cx43 phosphorylation, and/or Cx43 lateralization were already detected under a variety of pathophysiological conditions of the heart (20, 33, 40). The mechanism by which hyperlipidemia may influence Cx43 localization and content is not known in detail.

Sarcolemmal and mitochondrial membrane composition is influenced by high-cholesterol diet (10). Biphasic effects of cholesterol for membrane associated connexin channel activity were already shown (24): direct association of cholesterol with membrane proteins opened, while indirect action of cholesterol via alterations in membrane thickening closed and inactivated, the channels. Furthermore, hyperlipidemia could have an indirect effect on Cx43 expression and Cx43-formed channel activity. In endothelial cells, Cx43 trafficking was altered by oxidative stress (22). Accordingly, in the present study enhanced superoxide levels were detected in cholesterol-fed rat hearts, offering an explanation why Cx43 content was reduced in myocardial intercalated discs and mitochondria of cholesterol-fed rats. However, increased superoxide did not result in an increased cardiac nitrotyrosine level in cholesterol-fed rats in the present study. This is probably due to a decrease in cardiac NO content in hyperlipidemia as shown by our previous studies (12, 13).

Cx43 in Ischemia-Reperfusion and Preconditioning

Cx43 is present at the inner membrane of subsarcolemmal mitochondria (5, 7), increasing potassium influx into the mitochondrial matrix (27) through ATP-dependent potassium channels (36). Furthermore, mitochondrial Cx43 increases cardiomyocyte ROS formation during ischemia-reperfusion (18). Genetic deficiency of Cx43 (38) or decreased mitochondrial import of Cx43 (35) to $<50\%$ of normal attenuates the infarct size reduction by ischemic or diazoxide-induced preconditioning in mice and rat hearts (35, 38).

In the present study, mitochondrial Cx43 content in hyperlipidemic rat hearts was reduced to $\sim 50\%$ of the content measured in mitochondria obtained from rats fed a normal diet, and this decrease in mitochondrial Cx43 content was associated with the loss of ischemic preconditioning's cardioprotection. A similar association between a reduced mitochondrial Cx43 content and a loss of infarct size reduction by ischemic preconditioning was seen in aged hearts (6). Mitochondrial Cx43 content was slightly higher following the prolonged ischemic period in pig myocardium (5). In our present study, a similar tendency towards an increase in mitochondrial Cx43 at 5-min reperfusion following the prolonged ischemic period was seen in both normal and hyperlipidemic rats, thereby extending the previous observation (7) towards early reperfusion.

Ischemic preconditioning increased mitochondrial Cx43 content before (35) and at the end of the sustained ischemic period (5); however, in contrast to the previous studies, ischemic preconditioning reduced mitochondrial Cx43 content at 5-min reperfusion following the prolonged ischemic period in normal and hyperlipidemic rats. Similarly, ischemic postconditioning limited the migration of phospho-Cx43 to mitochondria following the prolonged ischemic period in isolated rat hearts (31). Such a decrease in mitochondrial Cx43 following ischemia-reperfusion in pre- and postconditioned hearts could contribute to protection, since mitochondrial Cx43 was proposed as a regulator of apoptosis in neonatal myocytes after simulated ischemia and reoxygenation (17).

Study Limitations

The present study describes an association between loss of mitochondrial Cx43 and the loss of cardioprotection by ischemic preconditioning but does not finally prove any cause-effect relationship. The loss of preconditioning in hyperlipidemia might also be due to changes in signal transduction cascades not related to Cx43. Increased oxidative stress, decreased myocardial NO content, inhibition of the mevalonate pathway, disruption of the cGMP-PKG due to increased PKG dimerization, and alteration in a variety of gene expression in the myocardium might all contribute to the loss of preconditioning in hyperlipidemia (10–12, 14). Moreover, hyperlipidemia and atherosclerosis are known to be associated by increased cardiovascular oxidative and nitrosative stress, which may also alter important proapoptotic and cell survival signaling pathways potentially being involved in the mechanism of preconditioning (25, 30, 32).

Our immunohistochemical analysis was performed with a different source of Cx43 antibody compared with the one used for Western blot. Immunostaining of heart sections was performed with the antibody GAP1 recognizing the cytoplasmic

loop of Cx43 (epitopes 131–142). This site contains a Tyr phosphorylation site, and its phosphorylation state could influence the staining intensity of the immunohistochemical sections.

In conclusion, the majority of preclinical and clinical studies shows that hyperlipidemia, independently of the development of coronary atherosclerosis, worsens the outcome of ischemia-reperfusion injury and attenuates the cardioprotective effect of pre- and postconditioning (11). While the mechanisms for the loss of protection still remain elusive, the present study offers a potential explanation in that hyperlipidemia caused an alteration in one of the main signal transduction element, i.e., a redistribution of the intracellular localization of Cx43 in the heart.

ACKNOWLEDGMENTS

The GAPI Cx4 antibody was a kind gift from David Becker (Department of Anatomy and Developmental Biology, University College London, London, UK). We are indebted to Zsuzsa Lajtos (University of Szeged) for skilful technical assistance.

GRANTS

This work was supported by grants from the National Office for Research and Technology (Jedlik-Medfood, TÁMOP-4.2.2-08/1/2008-0013, Baross-DA07-DATech-07-2008-0041). T. Csont holds a “János Bolyai Fellowship” from the Hungarian Academy of Sciences. R. Schultz was supported by the German Research Foundation (Schu843/7-2).

DISCLOSURES

No conflicts of interest, financial or otherwise, are declared by the author(s).

REFERENCES

- Anitschkow N, Chalataw S. Classics in arteriosclerosis research: on experimental cholesterol steatosis and its significance in the origin of some pathological processes by N. Anitschkow and S Chalataw, translated by Mary Z Pelias, 1913. *Arteriosclerosis* 3: 178–182, 1983.
- Aubin MC, Cardin S, Comtois P, Clement R, Gosselin H, Gillis MA, Le Quang K, Nattel S, Perrault LP, Calderone A. A high-fat diet increases risk of ventricular arrhythmia in female rats: enhanced arrhythmic risk in the absence of obesity or hyperlipidemia. *J Appl Physiol* 108: 933–940, 2010.
- Becker DL, Evans WH, Green CR, Warner A. Functional analysis of amino acid sequences in connexin43 involved in intercellular communication through gap junctions. *J Cell Sci* 108: 1455–1467, 1995.
- Bligh EG, Dyer WJ. A rapid method of total lipid extraction and purification. *Can J Biochem Physiol* 37: 911–917, 1959.
- Boengler K, Dodoni G, Rodriguez-Sinovas A, Cabestrero A, Ruiz-Meana M, Gres P, Konietzka I, Lopez-Iglesias C, Garcia-Dorado D, Di Lisa F, Heusch G, Schulz R. Connexin 43 in cardiomyocyte mitochondria and its increase by ischemic preconditioning. *Cardiovasc Res* 67: 234–244, 2005.
- Boengler K, Konietzka I, Buechert A, Heinen Y, Garcia-Dorado D, Heusch G, Schulz R. Loss of ischemic preconditioning's cardioprotection in aged mouse hearts is associated with reduced gap junctional and mitochondrial levels of connexin 43. *Am J Physiol Heart Circ Physiol* 292: H1764–H1769, 2007.
- Boengler K, Stahlhofen S, van de Sand A, Gres P, Ruiz-Meana M, Garcia-Dorado D, Heusch G, Schulz R. Presence of connexin 43 in subsarcolemmal, but not in interfibrillar cardiomyocyte mitochondria. *Basic Res Cardiol* 104: 141–147, 2009.
- Csonka C, Kupai K, Kocsis GF, Novak G, Fekete V, Bencsik P, Csont T, Ferdinandy P. Measurement of myocardial infarct size in preclinical studies. *J Pharmacol Toxicol Methods* 61: 163–170, 2010.
- Csont T, Bereczki E, Bencsik P, Fodor G, Gorbe A, Zvara A, Csonka C, Puskas LG, Santha M, Ferdinandy P. Hypercholesterolemia increases myocardial oxidative and nitrosative stress thereby leading to cardiac dysfunction in apoB-100 transgenic mice. *Cardiovasc Res* 76: 100–109, 2007.
- Ferdinandy P. Myocardial ischaemia/reperfusion injury and preconditioning: effects of hypercholesterolaemia/hyperlipidaemia. *Br J Pharmacol* 138: 283–285, 2003.
- Ferdinandy P, Schulz R, Baxter GF. Interaction of cardiovascular risk factors with myocardial ischemia/reperfusion injury, preconditioning, and postconditioning. *Pharmacol Rev* 59: 418–458, 2007.
- Ferdinandy P, Szilvassy Z, Horvath LI, Csont T, Csonka C, Nagy E, Szentgyorgyi R, Nagy I, Koltai M, Dux L. Loss of pacing-induced preconditioning in rat hearts: role of nitric oxide and cholesterol-enriched diet. *J Mol Cell Cardiol* 29: 3321–3333, 1997.
- Giricz Z, Csonka C, Onody A, Csont T, Ferdinandy P. Role of cholesterol-enriched diet and the mevalonate pathway in cardiac nitric oxide synthesis. *Basic Res Cardiol* 98: 304–310, 2003.
- Giricz Z, Gorbe A, Pipis J, Burley DS, Ferdinandy P, Baxter GF. Hyperlipidaemia induced by a high-cholesterol diet leads to the deterioration of guanosine-3',5'-cyclic monophosphate/protein kinase G-dependent cardioprotection in rats. *Br J Pharmacol* 158: 1495–1502, 2009.
- Giricz Z, Lalu MM, Csonka C, Bencsik P, Schulz R, Ferdinandy P. Hyperlipidemia attenuates the infarct size-limiting effect of ischemic preconditioning: role of matrix metalloproteinase-2 inhibition. *J Pharmacol Exp Ther* 316: 154–161, 2006.
- Goldstein JL, Hazzard WR, Schrott HG, Bierman EL, Motulsky AG. Hyperlipidemia in coronary heart disease. I. Lipid levels in 500 survivors of myocardial infarction. *J Clin Invest* 52: 1533–1543, 1973.
- Goubaeva F, Mikami M, Giardina S, Ding B, Abe J, Yang J. Cardiac mitochondrial connexin 43 regulates apoptosis. *Biochem Biophys Res Commun* 352: 97–103, 2007.
- Heinzel FR, Luo Y, Li X, Boengler K, Buechert A, Garcia-Dorado D, Di Lisa F, Schulz R, Heusch G. Impairment of diazoxide-induced formation of reactive oxygen species and loss of cardioprotection in connexin 43 deficient mice. *Circ Res* 97: 583–586, 2005.
- Juhász B, Der P, Turoczy T, Bacskay I, Varga E, Tosaki A. Preconditioning in intact and previously diseased myocardium: laboratory or clinical dilemma? *Antioxid Redox Signal* 6: 325–333, 2004.
- Kostin S, Rieger M, Dammer S, Hein S, Richter M, Klovekorn WP, Bauer EP, Schaper J. Gap junction remodeling and altered connexin43 expression in the failing human heart. *Mol Cell Biochem* 242: 135–144, 2003.
- Kupai K, Csonka C, Fekete V, Odendaal L, van Rooyen J, Marais DW, Csont T, Ferdinandy P. Cholesterol diet-induced hyperlipidemia impairs the cardioprotective effect of postconditioning: role of peroxynitrite. *Am J Physiol Heart Circ Physiol* 297: H1729–H1735, 2009.
- Li H, Brodsky S, Kumari S, Valiunas V, Brink P, Kaide J, Nasjletti A, Goligorsky MS. Paradoxical overexpression and translocation of connexin 43 in homocysteine-treated endothelial cells. *Am J Physiol Heart Circ Physiol* 282: H2124–H2133, 2002.
- Lin LC, Wu CC, Yeh HI, Lu LS, Liu YB, Lin SF, Lee YT. Down-regulated myocardial connexin 43 and suppressed contractility in rabbits subjected to a cholesterol-enriched diet. *Lab Invest* 85: 1224–1237, 2005.
- Locke D, Harris AL. Connexin channels and phospholipids: association and modulation. *BMC Biol* 7: 52, 2009.
- Loukili N, Rosenblatt-Velin N, Rolli J, Levrant S, Feihl F, Waerber B, Pacher P, Liaudet L. Oxidants positively or negatively regulate nuclear factor kappaB in a context-dependent manner. *J Biol Chem* 285: 15746–15752, 2010.
- Luzon-Toro B, Zafra-Gomez A, Ballesteros O. Gas chromatographic-mass spectrometric determination of brain levels of alpha-cholest-8-en-3beta-ol (lathosterol). *J Chromatogr B Analyt Technol Biomed Life Sci* 850: 177–182, 2007.
- Miro-Casas E, Ruiz-Meana M, Agullo E, Stahlhofen S, Rodriguez-Sinovas A, Cabestrero A, Jorge I, Torre I, Vazquez J, Boengler K, Schulz R, Heusch G, Garcia-Dorado D. Connexin43 in cardiomyocyte mitochondria contributes to mitochondrial potassium uptake. *Cardiovasc Res* 83: 747–756, 2009.
- Onody A, Csonka C, Giricz Z, Ferdinandy P. Hyperlipidemia induced by a cholesterol-rich diet leads to enhanced peroxynitrite formation in rat hearts. *Cardiovasc Res* 58: 663–670, 2003.
- Ovize M, Baxter GF, Di Lisa F, Ferdinandy P, Garcia-Dorado D, Hausenloy DJ, Heusch G, Vinten-Johansen J, Yellon DM, Schulz R; Working Group of Cellular Biology of Heart of European Society of Cardiology. Postconditioning and protection from reperfusion injury: where do we stand? Position paper from the Working Group of Cellular Biology of the Heart of the European Society of Cardiology. *Cardiovasc Res* 87: 406–423, 2010.

30. Pacher P, Beckman JS, Liaudet L. Nitric oxide and peroxynitrite in health and disease. *Physiol Rev* 87: 315–424, 2007.
31. Penna C, Perrelli MG, Raimondo S, Tullio F, Merlino A, Moro F, Geuna S, Mancardi D, Pagliaro P. Postconditioning induces an anti-apoptotic effect and preserves mitochondrial integrity in isolated rat hearts. *Biochim Biophys Acta* 1787: 794–801, 2009.
32. Pesse B, Levrant S, Feihl F, Waeber B, Gavillet B, Pacher P, Liaudet L. Peroxynitrite activates ERK via Raf-1 and MEK, independently from EGF receptor and p21Ras in H9C2 cardiomyocytes. *J Mol Cell Cardiol* 38: 765–775, 2005.
33. Peters NS, Green CR, Poole-Wilson PA, Severs NJ. Reduced content of connexin43 gap junctions in ventricular myocardium from hypertrophied and ischemic human hearts. *Circulation* 88: 864–875, 1993.
34. Roach PD, Balasubramaniam S, Hirata F, Abbey M, Szanto A, Simons LA, Nestel PJ. The low-density lipoprotein receptor and cholesterol synthesis are affected differently by dietary cholesterol in the rat. *Biochim Biophys Acta* 1170: 165–172, 1993.
35. Rodriguez-Sinovas A, Boengler K, Cabestrero A, Gres P, Morente M, Ruiz-Meana M, Konietzka I, Miro E, Totzeck A, Heusch G, Schulz R, Garcia-Dorado D. Translocation of connexin 43 to the inner mitochondrial membrane of cardiomyocytes through the heat shock protein 90-dependent TOM pathway and its importance for cardioprotection. *Circ Res* 99: 93–101, 2006.
36. Rottlaender D, Boengler K, Wolny M, Michels G, Endres-Becker J, Motloch LJ, Schwaiger A, Buechert A, Schulz R, Heusch G, Hoppe UC. Connexin 43 acts as a cytoprotective mediator of signal transduction by stimulating mitochondrial KATP channels in mouse cardiomyocytes. *J Clin Invest* 120: 1441–1453, 2010.
37. Schulz R, Boengler K, Totzeck A, Luo Y, Garcia-Dorado D, Heusch G. Connexin 43 in ischemic pre- and postconditioning. *Heart Fail Rev* 12: 261–266, 2007.
38. Schwanke U, Konietzka I, Duschin A, Li X, Schulz R, Heusch G. No ischemic preconditioning in heterozygous connexin43-deficient mice. *Am J Physiol Heart Circ Physiol* 283: H1740–H1742, 2002.
39. Severs NJ, Bruce AF, Dupont E, Rothery S. Remodelling of gap junctions and connexin expression in diseased myocardium. *Cardiovasc Res* 80: 9–19, 2008.
40. Spragg DD, Leclercq C, Loghmani M, Faris OP, Tunin RS, DiSilvestre D, McVeigh ER, Tomaselli GF, Kass DA. Regional alterations in protein expression in the dyssynchronous failing heart. *Circulation* 108: 929–932, 2003.
41. Wright CS, Becker DL, Lin JS, Warner AE, Hardy K. Stage-specific and differential expression of gap junctions in the mouse ovary: connexin-specific roles in follicular regulation. *Reproduction* 121: 77–88, 2001.

